Journal of Human Evolution 132 (2019) 137–173

Contents lists available at ScienceDirect

Journal of Human Evolution

journal homepage: www.elsevier.com/locate/jhevol

Internal nasal morphology of the Eocene primate *Rooneyia viejaensis* and extant Euarchonta: Using μCT scan data to understand and infer patterns of nasal fossa evolution in primates

Ingrid K. Lundeen [a, *], E. Christopher Kirk [a, b]

[a] Department of Anthropology, University of Texas at Austin, SAC 4.102, 2201 Speedway Stop C3200, Austin, TX 78712, USA
[b] Jackson School Museum of Earth History, University of Texas at Austin, J. J. Pickle Research Campus, 10100 Burnet Road, PRC 6-VPL, R7600, Austin, TX 78758, USA

ARTICLE INFO

Article history:
Received 27 October 2018
Accepted 19 April 2019
Available online 28 May 2019

Keywords:
Olfaction
Turbinal
Turbinate
Nasal cavity
Sensory system
Omomyid

ABSTRACT

Primates have historically been viewed as having a diminished sense of smell compared to other mammals. In haplorhines, olfactory reduction has been inferred partly based on the complexity of the bony turbinals within the nasal cavity. Some turbinals are covered in olfactory epithelium, which contains olfactory receptor neurons that detect odorants. Accordingly, turbinal number and complexity has been used as a rough anatomical proxy for the relative importance of olfactory cues for an animal's behavioral ecology. Unfortunately, turbinals are delicate and rarely preserved in fossil specimens, limiting opportunities to make direct observations of the olfactory periphery in extinct primates. Here we describe the turbinal morphology of *Rooneyia viejaensis,* a late middle Eocene primate of uncertain phylogenetic affinities from the Tornillo Basin of West Texas. This species is currently the oldest fossil primate for which turbinals are preserved with minimal damage or distortion. Microcomputed tomography (μCT) reveals that *Rooneyia* possessed 1 nasoturbinal, 4 bullar ethmoturbinals, 1 frontoturbinal, 1 interturbinal, and an olfactory recess. This pattern is broadly similar to the condition seen in some extant strepsirrhine primates but differs substantially from the condition seen in extant haplorhines. Crown haplorhines possess only two ethmoturbinals and lack frontoturbinals, interturbinals, and an olfactory recess. Additionally, crown anthropoids have ethmoturbinals that are non-bullar. These observations reinforce the conclusion that *Rooneyia* is not a stem tarsiiform or stem anthropoid. However, estimated olfactory turbinal surface area in *Rooneyia* is greater than that of similar-sized haplorhines but smaller than that of similar-sized lemuriforms and lorisiforms. This finding suggests that although *Rooneyia* was broadly plesiomorphic in retaining a large complement of olfactory turbinals as in living strepsirrhines, *Rooneyia* may have evolved somewhat diminished olfactory abilities as in living haplorhines.

1. Introduction

During nasal inhalation, air passes through the nares and into the nasal cavity before reaching the pharynx. Inspired air is brought into contact with mucosal epithelia lining the internal surfaces of the mammalian nasal cavity. Nasal mucosae are typically classified as either 'respiratory' or 'olfactory' according to their function (Rowe et al., 2005; Smith and Rossie, 2006; Macrini, 2014; Van Valkenburgh et al., 2014b). Respiratory epithelium (RE) aids respiration by warming and moistening inhaled air and by recovering heat and moisture from exhaled air (Van Valkenburgh et al., 2014). Olfactory epithelium (OE) differs from RE in containing specialized olfactory receptor neurons that are responsible for detecting olfactory stimuli (odorants; Purves et al., 2001). To be detected by the main olfactory system, odorant molecules must diffuse into the mucus layer of the OE and bind with receptor proteins expressed by olfactory receptor neurons (Tegoni et al., 2000; Adipietro et al., 2012; Persuy et al., 2015). Binding of odorant molecules with the appropriate receptor proteins initiates a transduction cascade that ultimately leads to depolarization of the receptor cell and generation of action potentials. Axons of olfactory receptor neurons travel from the OE through foramina in the cribriform plate of the

* Corresponding author.
E-mail address: ilundeen@utexas.edu (I.K. Lundeen).

https://doi.org/10.1016/j.jhevol.2019.04.009
0047-2484/

ethmoid to terminate within the brain's main olfactory bulb (Smith and Bhatnagar, 2004; Bird et al., 2014; Smith et al., 2015).

In most parts of the mammalian nasal cavity, the substrate underlying the nasal mucosae is bony. The nasal cavity itself is delimited by a complex mosaic of bony elements in therian mammals, including the premaxillae, maxillae, palatines, vomer, nasals, ethmoid, sphenoid, and frontals (Smith and Rossie, 2006; Van Valkenburgh et al., 2014b; Smith et al., 2015). A nasal septum (formed primarily by the septal cartilage anteriorly, the perpendicular plate of the ethmoid posterosuperiorly, and the vomer posteroinferiorly) runs in the midsagittal plane and divides the nasal cavity into right and left nasal fossae. Each nasal fossa is further divided into routes of airflow by thin bony elements sheathed in nasal mucosa called turbinals (Von Haller, 1756; Paulli, 1900a,b,c; Van Valkenburgh et al., 2014b; Smith et al., 2015). Larger turbinals are named for the bones to which they attach or from which they arise during ontogeny (i.e., maxilla: maxilloturbinal; nasal: nasoturbinal; ethmoid: ethmoturbinal; frontal: frontoturbinal; Table 1).[1] Turbinal morphology varies widely across mammals, but turbinal cross-sectional shape is often characterized by scrolling, branching, or other complex patterns of folding (Negus, 1956; Macrini, 2014; Van Valkenburgh et al., 2014b). Turbinals may also be hollow and enclosed anteriorly while opening to the nasal fossa posteriorly, referred to as a 'bullar' shape. This complex cross-sectional geometry increases the surface area of the mucosa supported by the turbinal, thus improving the efficiency of water and heat exchange and/or odorant capture within the nasal cavity.

Maxilloturbinals are typically the most inferiorly and anteriorly located turbinals (except in cases where the first ethmoturbinal is unusually elongate), and are also the only turbinals entirely covered in RE (Loo and Kanagasuntheram, 1971; Craven et al., 2010; Van Valkenburgh et al., 2014a; Smith et al., 2015). RE may extend posteriorly onto the ethmoturbinals, nasoturbinals, or frontoturbinals, but this pattern varies between taxa and individuals (Smith et al., 2011, 2016; DeLeon et al., 2014). Dorsal and posterior to the maxilloturbinals are turbinals covered to varying degrees in OE that are collectively referred to as 'olfactory turbinals' (Rowe et al., 2005; Smith et al., 2007a,b, 2011, 2016; Van Valkenburgh et al., 2014a). The olfactory turbinals include the nasoturbinals, frontoturbinals, and the 'ethmoturbinal complex' composed of ethmoturbinals and interturbinals (Smith et al., 2015).

The nasoturbinal (Table 1) is located superiorly and laterally within the nasal fossa, and usually has an anterior edge that contacts the nasal bone (Dieulafé, 1906; Wible, 2011). The nasoturbinal often arises as a dorsoventrally broad lamina along the lateral wall of the anterior nasal fossa, but typically forms a dorsoventrally narrower single scroll in the posterior nasal fossa as it approaches the cribriform plate (Smith and Rossie, 2008; Ruf, 2014). The nasoturbinal tends to have tube-like morphology that directs air to the more posteriorly positioned olfactory turbinals (Craven et al., 2007, 2010; Van Valkenburgh et al., 2014b).

Posterior to the nasoturbinal, the horizontal lamina[2] is a sheet of bone that arises from the lateral wall of the nasal fossa and extends medially into the nasal fossa (Maier and Ruf, 2014; Ruf, 2014; Ruf et al., 2015). The horizontal lamina demarcates the frontal recess superiorly from the maxillary recess inferiorly. The horizontal lamina also forms the primary contact between one or more turbinals and the lateral wall of the nasal fossa (Ruf et al., 2015). The first ethmoturbinal (ET I) is the only turbinal that consistently arises from the horizontal lamina, and the two structures are closely associated during the early ontogeny of the mammalian nasal capsule (Maier, 1993; Rossie, 2006; Smith and Rossie, 2008; Maier and Ruf, 2014). Ethmoturbinals may also have independent basal (= 'primary') laminae that directly contact the lateral wall of the nasal fossa, as is commonly the case for ethmoturbinals within the olfactory recess. Additionally, the second ethmoturbinal (ET II) commonly arises from the medial surface of ET I, and may then be indirectly linked to the lateral wall of the nasal fossa via the horizontal lamina. All ethmoturbinals typically extend posteriorly to directly contact the cribriform plate (Smith et al., 2007c). ET I is the anteriormost ethmoturbinal, and it is typically much larger than the more posterior ethmoturbinals. ET I also typically has a tube-like morphology, which among primates supports relatively large amounts of respiratory epithelium (Smith et al., 2007b), and in many euarchontan taxa the anterior margin of ET I is closed to form a bulla (Ruf, 2014; Smith et al., 2016). Within the frontal recess, the lateral wall of the nasal fossa is usually composed of the frontal bone. Accordingly, turbinals that arise from the lateral wall of the nasal fossa within the frontal recess are referred to as frontoturbinals (Smith et al., 2015). Frontoturbinals have often been characterized as 'ectoturbinals' because they do not extend as close to the midsagittal plane as ethmoturbinals (Paulli, 1900a,c; Moore, 1981). Nevertheless, in some euarchontan species the frontoturbinals are comparable to ethmoturbinals in size and complexity, and may therefore comprise a substantial portion of total olfactory turbinal surface area (e.g., *Galeopterus*, *Daubentonia*; see below).

The maxilloturbinal, nasoturbinal, and ethmoturbinals may be collectively referred to as 'endoturbinals' because their medial-most extent lies in close proximity to the nasal septum (Negus, 1958; Cave, 1973; Smith et al., 2007c). For clearly defining these different structures (Table 1), turbinals arising inferiorly or medially relative to the horizontal lamina and ET I will be referred to as 'ethmoturbinals' if they are directly lateral to the bony nasal septum and 'interturbinals' if they are not laterally adjacent to the bony nasal septum.[3] If turbinals are found in the frontal recess superior and lateral to the horizontal lamina and ET I, then they will be referred to as 'frontoturbinals' (Maier, 1993; Smith and Rossie, 2008).

In the posterior nasal cavity of most mammals, a horizontal sheet of bone (the 'transverse lamina') lies ventral to the posterior olfactory turbinals. The transverse lamina separates the 'olfactory recess,' a cul-de-sac lined with olfactory epithelium and containing the posterior ethmoturbinals, from the 'nasopharyngeal meatus,' the more ventrally located main airway (Negus, 1956; Smith et al., 2007c; Van Valkenburgh et al., 2014b). Using computational simulations of nasal airflow, Craven et al. (2010) have suggested that a large olfactory recess is characteristic of mammals with a well-developed sense of smell. This suggestion is based on the idea that a larger olfactory recess will slow airflow around the olfactory mucosa (Eiting et al., 2014b) and increase the residence time of odorants, thereby increasing the chances of binding with olfactory receptor proteins in the OE (Eiting et al., 2014a).

[1] Turbinal names, definitions, and synonyms can be found in Table 1 and follow Smith and Rossie (2008) unless otherwise noted.

[2] Our use of this term explicitly follows that of Ruf et al. (2015), but it should be noted the terms 'horizontal lamina' and 'frontomaxillary septum' (and their Latin equivalents) appear to be used synonymously in some previous publications (e.g., Maier, 1993; Maier and Ruf, 2014). Furthermore, some authors (e.g., Smith and Rossie, 2008) used these terms to refer only to structures within (or derived from) the fetal lateral recess (contained within the pars intermedia).

[3] Some descriptions further divide the ethmoturbinal complex into ethmoturbinals, interturbinals, and 'epiturbinals,' or accessory scrolls of ethmoturbinals (Maier, 1993; Smith and Rossie, 2008) but this terminology is not adopted here.

Table 1
Definitions, characteristics, and synonyms of anatomical terms used here.[a]

Term used here	Definition and characteristics	Synonyms	Source
Ethmoturbinal I	Anterior-most ethmoturbinal. Arises from the horizontal lamina or lateral wall of the nasal fossa. Usually terminates posteriorly at the cribriform plate. Typically much larger than other ethmoturbinals. Anterior surface often bullar in morphology (with the exception of the derived condition in anthropoids). Medial surface in close proximity to bony nasal septum	Middle nasal concha Concha media Ethmoturbinal II Endoturbinal II Upper lamella Endoturbinal I	Human anatomy ICVGAN (2017) Martin (1990) Paulli (1900a,b,c) Moore (1981) Allen (1882)
Ethmoturbinal II	Posterior to ethmoturbinal I. May arise from the horizontal lamina or lateral wall of the nasal fossa. Usually terminates posteriorly at the cribriform plate. Anterior surface typically bullar in morphology. Medial surface in close proximity to bony nasal septum	Superior nasal concha Concha ethmoidalis Ethmoturbinal III Endoturbinal II Lower lamella	Human anatomy ICVGAN (2017) Martin (1990) Paulli (1990a,b,c) Moore (1981)
Ethmoturbinal III	Posterior to ethmoturbinal II. May arise from the horizontal lamina or lateral wall of the nasal fossa. Terminates posteriorly at the cribriform plate. Anterior surface typically bullar in morphology. Medial surface in close proximity to bony nasal septum	Concha ethmoidalis Ethmoturbinal IV Endoturbinal II	ICVGAN (2017) Martin (1990) Paulli (1990a,b,c), Moore (1981)
Ethmoturbinal IV	Posterior to ethmoturbinal III. May arise from the horizontal lamina or lateral wall of the nasal fossa. Terminates posteriorly at the cribriform plate. Anterior surface typically bullar in morphology. Medial surface in close proximity to bony nasal septum. Typically contained primarily within the olfactory recess	Concha ethmoidalis Ethmoturbinal V Endoturbinal III	ICVGAN (2017) Martin (1990) Moore (1981)
Ethmoturbinal V	Posterior to ethmoturbinal IV. Arises from the lateral wall of the nasal fossa. Terminates posteriorly at the cribriform plate. Anterior surface typically bullar in morphology. Medial surface in close proximity to bony nasal septum. Typically contained primarily within the olfactory recess		Smith and Rossie (2008)
Frontal recess	Space dorsal to horizontal lamina and dorsolateral to the lateral root of ethmoturbinal I. May contain frontoturbinals	Superior maxillary recess	Negus (1958)
Frontoturbinal	Arises from the lateral wall or the horizontal lamina in the frontal recess. Terminates posteriorly at the cribriform plate. Typically more laterally positioned than adjacent ethmoturbinals. Medial surface not adjacent to the bony nasal septum	Concha frontalis Ectoturbinal Interturbinals	Pedziwiatr (1972) Moore (1981), Le Gros Clark (1959) Maier and Ruf (2014)
Horizontal lamina (sensu Maier and Ruf, 2014)	Lamina arising from the lateral wall and extending medially into the nasal cavity. Forms the primary lamina of ethmoturbinal I and (variably) additional turbinals. Variably contacts the transverse lamina posteriorly	Frontomaxillary septum Anterior root of ethmoturbinal I	Smith and Rossie (2008) de Beer (1937)
Interturbinal	Posterior to anterior portion of ethmoturbinal I. Arises from the lateral wall of the nasal fossa or the horizontal lamina. Terminates posteriorly at the cribriform plate. Typically more laterally positioned than adjacent ethmoturbinals. Medial surface not adjacent to the bony nasal septum	Ectoturbinal Accessory turbinal	Paulli (1900a, c) Dieulafé (1906)
Maxilloturbinal	Anterior portion arises ventrally from the maxilla. Terminates anterior to the nasopharyngeal meatus. Typically the most ventrally projecting turbinal	Inferior nasal concha Concha ventralis	Human anatomy ICVGAN (2017)
Nasoturbinal	Anterior portion arises from the nasal bone. Terminates posteriorly at the cribriform plate. Typically the most dorsally projecting turbinal	Pars caudalis Endoturbinal I Lamina semicircularis	ICVGAN (2017) Martin (1990) Ruf (2014)
Olfactory recess	Space dorsal to the transverse lamina. Typically contains the posterior ethmoturbinals	Sphenoethmoidal recess/ethmoturbinal recess Sphenoidal recess	Maier (1993) Loo (1973)
Transverse lamina	Lamina extending from the lateral walls of the nasal cavity to the bony nasal septum. Divides the olfactory recess from the nasopharyngeal meatus	Lamina terminalis	Kollman and Papin (1925), Hill (1953)

Abbreviations: ICVGAN = International Committee on Veterinary Gross Anatomical Nomenclature.
[a] Terms used here are from Smith and Rossie (2008) unless otherwise noted.

1.1. Olfactory reduction in primates

Many early attempts to characterize the adaptations of living primates claimed that some degree of olfactory reduction is characteristic of the order (Elliot Smith, 1927; Le Gros Clark, 1959). However, evidence that extant strepsirrhines exhibit reduced olfactory functionality compared to other mammals is currently limited. Like many other mammals, strepsirrhines have a complex nasal cavity with an olfactory recess, four or more ethmoturbinals, and a variable number of additional olfactory turbinals (Smith et al., 2007c, 2013, 2015, 2016; Smith and Rossie, 2008; Pihlström, 2012). These anatomical features presumably provide a large surface area for OE in the strepsirrhine nasal cavity, which in turn may facilitate relatively high sensitivity to volatile odorants (Smith and

Bhatnagar, 2004; Smith et al., 2007b). Living strepsirrhines further exhibit well-developed accessory olfactory systems for detecting non-volatile odorants (Smith et al., 2007a; Garrett et al., 2013). Notably, all strepsirrhines possess a rhinarium that surrounds the nares (Beard, 1988; Rossie and Smith, 2007; Smith et al., 2007c). The moist, hairless surface of the rhinarium facilitates non-volatile odorant capture and transport to the vomeronasal organ. Rhinarial moisture is produced partly by lacrimal fluid carried within subhorizontally oriented nasolacrimal ducts that have outlets just inside the nares (Rossie and Smith, 2007; Rossie et al., 2018). This generally plesiomorphic anatomy of the strepsirrhine olfactory periphery is consistent with field observations that olfaction plays a major role in strepsirrhine ecology and social behavior (e.g., Lewis, 2005; Irwin et al., 2007; Kappel et al., 2011; Morelli et al., 2013; Valenta et al., 2013).

At present, the best evidence suggesting that strepsirrhines exhibit any diminution in olfactory functionality compared to the ancestral condition for crown placentals is provided by comparative genomic studies of olfactory receptor gene repertoires (Buck and Axel, 1991). Though limited in taxonomic scope, the available sequence data indicate that strepsirrhines have fewer functional olfactory receptor genes than most non-primate mammals (Niimura, 2012; Mason et al., 2016; Niimura et al., 2018). Within euarchontans, strepsirrhines have fewer functional olfactory receptor genes than treeshrews, but data for colugos are ambiguous due to the uncertain functional role played by truncated genes (Niimura et al., 2018). Because any decrease in the number of functional olfactory receptor genes is expected to decrease the number of distinct odorant molecules that can be detected by the main olfactory system (Nei et al., 2008; Niimura, 2012), these genomic data suggest that strepsirrhines should be able to detect and discriminate between a smaller number of volatile odorants than treeshrews and most non-euarchontan mammals. These findings are generally consistent with the fact that most strepsirrhines have relatively small main olfactory bulbs compared to scandentians, glirans, afrosoricids, and eulipotyphlans (Baron et al., 1983; Silcox et al., 2010). As the first site of synapse linking the olfactory periphery with the rest of the brain (Shepherd, 1972), the size of the main olfactory bulb may be expected to vary with changes in amount of afferent input from olfactory receptor neurons in the OE. In particular, all olfactory receptor cells expressing a specific olfactory receptor gene have axons that terminate within a single glomerulus in each olfactory bulb (Lancet et al., 1982; Schoppa and Westbrook, 2001). Accordingly, the fact that strepsirrhines have relatively small olfactory bulbs may partly reflect a smaller number of glomeruli associated with a diminished olfactory receptor gene complement.

Although the anatomy of the strepsirrhine main and accessory olfactory systems is generally plesiomorphic, extant haplorhines share numerous derived reductions in olfactory anatomy. Haplorhines lack many of the olfactory turbinals seen in other euarchontans, and typically retain only two ethmoturbinals and a nasoturbinal (Smith and Rossie, 2006). Furthermore, the nasoturbinals of haplorhines are reported to be less complex than those of strepsirrhines (Smith et al., 2007c). Haplorhines are also reported to lack a transverse lamina and olfactory recess, and have a smaller proportion of their nasal cavity covered in olfactory epithelium compared to strepsirrhines (Smith and Rossie, 2008; Smith et al., 2014a). For example, olfactory epithelium lines the inner surface of about 31% of the nasal fossa of *Microcebus* but only about 15% of the nasal fossa of *Cebuella* (Smith et al., 2014a). These reductions in the number, size, and complexity of olfactory structures in the haplorhine nasal cavity are matched by corresponding reductions in relative olfactory bulb size (Baron et al., 1983; Kay et al., 2004a; Smith and Bhatnagar, 2004; Silcox et al., 2009; Heritage, 2014) and the number of intact olfactory receptor genes (Niimura et al., 2018). Additionally, while tarsiers and platyrrhines retain a functional vomeronasal organ, all haplorhines lack rhinaria and have vertically-oriented nasolacrimal canals with outlets well inside the nasal fossa under the maxilloturbinal (Maier, 1980; Keverne, 1999; Rossie and Smith, 2007; Garrett et al., 2013; Rossie et al., 2018). Although olfaction still plays an important role in the behavioral ecology of extant haplorhines (e.g., Bicca-Marques and Garber, 2004; Hiramatsu et al., 2009), these reductions in the anatomy of the olfactory periphery suggest that olfactory sensitivity is probably diminished in haplorhines compared with other euarchontans.

1.2. *Nasal cavity of* Rooneyia

Given the substantial differences between extant haplorhines and strepsirrhines in the bony morphology and functional anatomy of the nasal cavity, this anatomical region provides a potential wealth of information regarding the phylogenetic affinities and olfactory ecology of fossil primates (Barton et al., 1995; Silcox et al., 2010). The current widespread use of μCT scanning to study fossil crania has permitted non-destructive visualization of the nasal cavity in fossil specimens (Rossie et al., 2006, 2018; Tabuce et al., 2009; Kirk et al., 2014), but unfortunately turbinals are rarely preserved intact during fossilization (authors' pers. obs.). One exception to this generalization is provided by the holotype and only known specimen of *Rooneyia viejaensis* (TMM 40688-7), an unusually well-preserved cranium from the Duchesnean Chambers Tuff of the Sierra Vieja in West Texas (Wilson, 1966, 1986; Hofer and Wilson, 1967; Robinson et al., 2004; Kirk et al., 2014). Following a preliminary report by Seiffert et al. (1999), Kirk et al. (2014) used μCT data to describe the nasal cavity of *Rooneyia*. Although the resolution of the scan used by Kirk et al. (2014) was insufficient to visualize turbinals in their entirety, these authors documented a number of key internal nasal structures, including the presence of a transverse lamina and olfactory recess, an obliquely oriented (i.e., non-vertical) nasolacrimal canal, and multiple turbinal basal laminae. These visible basal laminae were used to infer the presence of one maxilloturbinal, one nasoturbinal, and four ethmoturbinals in each nasal fossa. In addition to basal laminae, more medially positioned portions of some turbinals (e.g., the maxilloturbinal and ethmoturbinal I) were also visible but were not described in detail (see Kirk et al., 2014:Figs. 7 and 8). Furthermore, Kirk et al. (2014) were unable to determine the number and disposition of frontoturbinals and interturbinals in *Rooneyia* based on the configuration of the preserved basal laminae.

Resolving outstanding questions regarding the turbinal number and morphology in *Rooneyia* is of particular interest because this specimen is currently the oldest known primate cranium with turbinals that are largely intact. Additionally, the phylogenetic affinities of *Rooneyia* have proven difficult to resolve, with different authors suggesting that the taxon is a stem strepsirrhine (Kay et al., 2004b), a stem haplorhine (Ross, 1994; Ross et al., 1998), a stem tarsiiform (Szalay and Delson, 1979; Seiffert et al., 2010; Ni et al., 2013, 2016), or a stem anthropoid (Rosenberger, 2006; Rosenberger et al., 2008). Based on a lack of derived features seen in the nasal cavities of crown haplorhines, Kirk et al. (2014) concluded that *Rooneyia* is unlikely to be either a stem anthropoid or stem tarsiiform. Additional information regarding the detailed morphology of the nasal cavity in *Rooneyia* may provide further evidence bearing on the phylogenetic affinities of this taxon, particularly if evaluated within the appropriate comparative context. Indeed, nasal cavity morphology is poorly documented for most living euarchontan species, leading to uncertainty regarding the most likely morphology of the nasal cavity in the last common

ancestors of the primate, strepsirrhine, and haplorhine crown groups.

Here we take advantage of improvements in μCT scanning resolution to re-examine the morphology of the nasal cavity in *Rooneyia*. Based on a more recent scan of substantially greater resolution than those examined by prior authors, we provide the first detailed description of *Rooneyia*'s nasal cavity, including turbinal number and morphology. In order to better understand the potential phylogenetic implications of our observations for *Rooneyia* we also characterize turbinal anatomy in a broad comparative sample of extant euarchontans, including scandentians, dermopterans, strepsirrhines, and haplorhines. We then use these data to reconstruct the most parsimonious scenario for changes in both turbinal number and morphology within Euarchonta. We also use these comparative data to quantify the surface areas of both the olfactory turbinals and the maxilloturbinal. Our goal in this analysis is thus two-fold. First, we seek to document the detailed anatomy of the nasal cavity in *Rooneyia* in order to provide the first comprehensive description of this anatomical region in an Eocene primate with intact turbinals. Second, we seek to better understand the phylogenetic and ecological significance of these observations for *Rooneyia* by providing a comparative framework for evaluating nasal cavity character evolution in Euarchonta.

2. Materials and methods

The nasal region of the *R. viejaensis* holotype (TMM 40688-7; which is housed in the Jackson School Museum of Earth History at the University of Texas at Austin) was scanned at the University of Texas High Resolution X-Ray Computed Tomography Scanning Facility (UTCT) in Austin, Texas. The scan was made using the ultra-high-resolution subsystem of a North Star Imaging scanner with a FeinFocus microfocal X-ray source a at 200 kV and 0.27 mA. The resulting scan has 2536 total slices and isometric voxels of 9.52 μm on each side. This scan improves on two earlier μCT scans of the entire cranium of *Rooneyia*, which had an in-plane resolution of 36 μm and an inter-slice spacing 120 μm (Seiffert et al., 1999) and an in-plane resolution of 39.1 μm and an inter-slice spacing of 86.7 μm (Kirk et al., 2014). 16-bit TIFF image stacks of the *Rooneyia* nasal scan and additional information about scan parameters are available for download at https://www.morphosource.org/. Comparative taxa ($n = 33$) were scanned at UTCT or downloaded from Morphosource (Morphosource object identifiers provided in Supplementary Online Material [SOM] Table S1). This comparative sample includes single specimens of 3 scandentian, 2 dermopteran, 7 lorisiform, 9 lemuriform, 1 tarsiid, 6 platyrrhine, and 5 catarrhine species. Species, museum specimen number, sex, and scanning facility information for each included specimen are listed in Table 2. Data sets for each cranium were rendered as 3D volumes in Avizo 8.1 (Visualization Sciences Group, Berlin). Turbinals of *Rooneyia* were manually segmented in each slice using the brush tool. Bony nasal structures in extant taxa were segmented using the brush tool to select the approximate nasal cavity space occupied by the structure and then the thresholding tool to select only the grayscale values representing bone. When possible, turbinals were segmented from the lateral wall of the nasal fossa at the point where the turbinal's basal lamina contacts the lateral wall (Fig. 1). Although the horizontal lamina may form the basal lamina by which more than one distinct turbinal ultimately contacts the lateral wall of the nasal fossa, for our olfactory turbinal surface area measurements and in our cross-sectional figures the horizontal lamina was segmented in most taxa as part of ET I. Note that this segmentation includes only those portions of the horizontal lamina that act as a basal lamina for ET I and does not include anterior portions of the horizontal lamina that have a free medial margin in coronal cross-section. Exceptions included *Daubentonia* and *Eulemur*, in which the horizontal lamina is continuous with the transverse lamina. Because we could identify no clear point of demarcation between the horizontal lamina and transverse laminae in these taxa, the horizontal lamina was not segmented as part of ET I. Surfaces were rendered in Avizo using minimal smoothing (1–2) to preserve maximum anatomical detail. To facilitate comparison with *Rooneyia*, in which turbinals are best preserved in the right nasal fossa, one nasal fossa was segmented in each extant taxon and mirrored if necessary in Adobe® Photoshop® CS6 (v. 13). All data and surface models of segmented turbinals are in a Morphosource project (P608), available for download at https://www.morphosource.org/Detail/ProjectDetail/Show/project_id/608.

Definitions of turbinals follow Smith and Rossie (2008) unless otherwise noted (Fig. 1; Table 1). Turbinals are described in an anterior to posterior sequence as they appear in coronal view. By convention ethmoturbinals are numbered using Roman numerals from anterior to posterior; here we follow the same convention for frontoturbinals and interturbinals. Ethmoturbinals typically have at least partly independent origins from the horizontal lamina or lateral wall of the nasal fossa. By definition, the medial surface of each ethmoturbinal approaches the midline of the nasal cavity. Ethmoturbinals typically also have bullar anterior morphology (e.g., strepsirrhines, dermopterans, tarsiers) and contact the cribriform plate posteriorly, but some taxa (e.g., anthropoids; see below) diverge from this pattern. As noted by Smith and Rossie (2008), ethmoturbinal I (ET I) and ethmoturbinal II (ET II) are often closely interconnected, and are treated by some authors as parts of a single complex turbinal (Ruf, 2014; Ruf et al., 2015). Interturbinals also typically arise from the lateral wall of the nasal fossa or the horizontal lamina and extend to the cribriform plate, but they do not lie directly adjacent to the bony nasal septum like ethmoturbinals. Frontoturbinals also do not lie in close proximity to the bony nasal septum but they occur in the frontal recess.

Terms used to describe turbinal shape in coronal cross-section include: 'single-scrolled' (1 distinct scroll extending from the basal lamina), 'double-scrolled' (2 distinct scrolls extending from the basal lamina, with each scroll coiling in opposite directions), 'bullar' (hollow internally, with a closed anterior margin), 'laminar' (a flat or curved plate), or 'arborized' (branching).

The lumen of the nasolacrimal canal was segmented using the magic wand tool in Avizo. Viewing the segmented nasolacrimal canal in lateral view, the orientation of each canal was classified as 'horizontal' (nearly parallel to the hard palate), 'oblique' (inclined 15–75° relative to the hard palate), or 'vertical' (nearly perpendicular to the hard palate). Structures in this study are described in the singular because one nasal fossa was described per extant taxon.

The rostrocaudal lengths of individual turbinals and other anatomical features were measured in *Rooneyia* by counting the number of coronal slices in which they appeared and multiplying by interslice thickness. Turbinal surface areas were measured using the surface area tool in Avizo. To facilitate comparison of turbinal surface areas across a range of body and head sizes, cranial size was calculated as the geometric mean of cranial length and width following Muchlinski (2010). Cranial length and width were measured on volume renderings of each skull using the 3D distance tool in Avizo. Surface areas of the maxilloturbinal and olfactory turbinals (i.e., nasoturbinal, ethmoturbinals, frontoturbinals, and interturbinals) were analyzed separately using bivariate plots of log turbinal surface area (y-axis) versus log cranial size (x-axis). In each of the two bivariate plots, minimum convex polygons were calculated to show the

Table 2
Specimen details.

Family	Species	Collection #	Sex	Scanning facility
Cynocephalidae	*Galeopterus variegatus*	private specimen		UTCT
Cynocephalidae	*Cynocephalus volans*	AMNH-M-187861	M	MIF
Tupaiidae	*Tupaia glis*	TMM-2256	M	UTCT
Tupaiidae	*Tupaia belangeri*	USNM-320680	M	SMiF
Ptilocercidae	*Ptilocercus lowii*	USNM-481107	F	SMiF
Cheirogaleidae	*Mirza coquereli*	DPC-1139	F	SMiF
Lepilemuridae	*Lepilemur mustelinus*	AMNH-M-170568	F	SMiF
Lemuridae	*Varecia rubra*	DPC-O50	F	SMiF
Lemuridae	*Eulemur collaris*	MCZ-44896	F	CNS
Lemuridae	*Hapalemur griseus griseus*	MCZ-44913	F	CNS
Indriidae	*Avahi laniger*	MCZ-44879		CNS
Indriidae	*Propithecus verreauxi verreauxi*	MCZ-16375	M	CNS
Indriidae	*Indri indri*	AMNH-M-100506	F	MIF
Daubentoniidae	*Daubentonia madagascariensis*	AMNH-M-100632	M	MIF
Galagidae	*Otolemur crassicaudatus*	DPC-O16		SMiF
Galagidae	*Euoticus elegantulus elegantulus*	MCZ-14657	M	CNS
Galagidae	*Galago moholi*	MCZ-44132	M	CNS
Galagidae	*Galago senegalensis*	DPC-O07		SMiF
Lorisidae	*Perodicticus potto potto*	MCZ-25831	M	CNS
Lorisidae	*Nycticebus coucang*	MCZ-BOM-5118		CNS
Lorisidae	*Loris tardigradus*	BAA-0006		SMiF
Tarsiidae	*Carlito syrichta syrichta*	DPC-045		SMiF
Aotidae	*Aotus griseimembra*	MCZ-19802	M	CNS
Atelidae	*Alouatta palliata palliata*	MCZ-BOM-5329		CNS
Atelidae	*Ateles geoffroyi geoffroyi*	MCZ-BOM-5336		CNS
Pitheciidae	*Callicebus discolor*	MCZ-26922		CNS
Callitrichidae	*Callithrix argentata*	MCZ-30582	M	CNS
Cebidae	*Saimiri oerstedii oerstedii*	MCZ-10131	M	CNS
Cercopithecidae	*Procolobus badius*	MCZ-24080	M	CNS
Cercopithecidae	*Mandrillus leucophaeus*	MCZ-19986	M	CNS
Cercopithecidae	*Miopithecus talapoin*	MCZ-23196	M	CNS
Cercopithecidae	*Presbytis hosei hosei*	MCZ-37371	M	CNS
Hylobatidae	*Hylobates lar lar*	MCZ-41463	M	CNS

Abbreviations: AMNH = American Museum of Natural History, New York City, New York, USA; BAA = Department of Evolutionary Anthropology, Duke University, Durham, North Carolina, USA; CNS = Center for Nanoscale Systems, Harvard University, Cambridge, Massachusetts, USA; DPC = Duke Primate Center, Durham, North Carolina, USA; MCZ = Museum of Comparative Zoology, Harvard University, Cambridge, Massachusetts, USA; MIF = Microscopy and Imaging Facility, American Museum of Natural History, New York City, New York, USA; SMiF = Shared Materials Instrumentation Facility, Duke University, Durham, North Carolina, USA; TMM = Jackson School Museum of Earth History, University of Texas at Austin, Austin, Texas, USA; USNM = Smithsonian National Museum of Natural History, Washington, District of Columbia, USA; UTCT = The University of Texas High-Resolution CT Facility, Austin, Texas, USA.

range of morphometric variation for scandentians, dermopterans, strepsirrhines, and haplorhines. Minimum convex polygons were calculated using the ggConvexHull package (Martin, 2017) in RStudio version 1.0.153 (RStudio Team, 2015).

A molecularly-resolved phylogeny (Perelman et al., 2011) was used to reconstruct ancestral states. Within Euarchonta, dermopterans are treated as the sister taxon to primates following Mason et al. (2016). In Mesquite 3.2 (Maddison and Maddison, 2017), nasoturbinal absence or presence, ethmoturbinal number, frontoturbinal number, and interturbinal number for extant taxa were used to reconstruct turbinal numbers at ancestral nodes. The most parsimonious ancestral states were reconstructed using the 'Trace All Characters' tool, which uses maximum parsimony to estimate characters at each node in a given tree. The character state changes were plotted onto the tree in Adobe® Illustrator® CS6 (v. 16.0.1).

3. Results

The turbinal numbers for each extant taxon examined here are listed in Table 3. For consistency, descriptions of turbinal morphology primarily follow an anterior to posterior sequence based on successive coronal μCT slices.

3.1. Rooneyia

The right nasal fossa of *Rooneyia* is well preserved, with all major turbinals at least partly intact (see below). By contrast, the left nasal fossa is less well preserved, and parts of the left maxilloturbinal, left ET I, and left nasoturbinal are comminuted. Both nasal fossae contain free-floating fragments of damaged turbinals that cannot be identified with confidence. Here we focus our description of the portions of turbinals that can be identified according to their cross-sectional morphology, relative position within the nasal fossa, and the nature of their contact with lateral wall of the nasal fossa and/or adjacent turbinals. We have not, however, segmented any of the detached turbinal fragments of uncertain identity, and will not describe these fragments here.

The left and right nasal fossae of *Rooneyia* are subdivided for most of their length by an intact bony nasal septum. The anterior margin of the vomer is first visible about 4.6 mm posterior to the piriform aperture, immediately superior to the nasal crests of the left and right maxillae. Moving posteriorly, the vomer acquires the classic U-shaped cross-sectional anatomy where it would have received the cartilaginous anterior portion of the nasal septum in life. The bony nasal septum completely subdivides the nasal cavity from about 8.9 mm posterior to the piriform aperture to the posterior margin of the olfactory recess. At its anterior end, the complete bony nasal septum is formed by the maxillae at its base, the vomer inferiorly, and the perpendicular plate of the ethmoid superiorly. The midsection of the anterior septum is thickened at the vomer-perpendicular plate articulation, and the superior ~2/3 of the anterior perpendicular plate is divided into separate left and right laminae with an intervening space. These

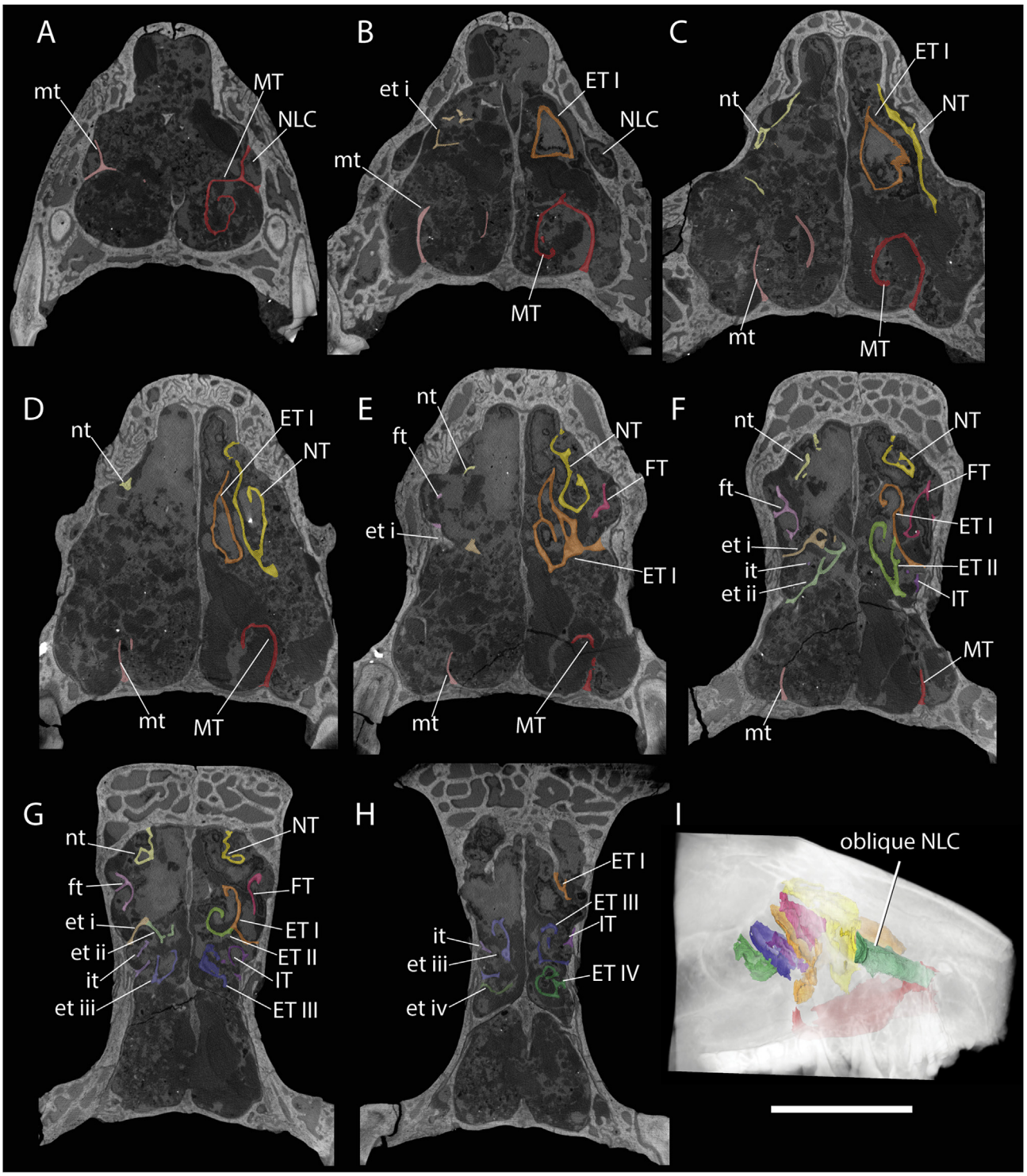

Figure 1. *Rooneyia viejaensis* high resolution CT scans through the nasal fossa of the holotype (TMM 40688-7). A–H) slices along the coronal plane showing preservation of left and right nasal fossa: 1865 (A), 1595 (B), 1338 (C), 1177 (D), 1087 (E), 967 (F), 886 (G), and 732 (H) of 2535 total slices. I) Lateral view of the nasolacrimal canal orientation. Right (uppercase abbreviations) and left (lowercase abbreviations) sides in cross-section can be compared with turbinal surface views in Figure 2. Scale bar = 10 mm.

left and right laminae of the perpendicular plate articulate with the nasal bones immediately lateral to the internasal suture. Though the space between the left and right laminae narrows as the perpendicular plate approaches the olfactory recess, at least part of the perpendicular plate remains subdivided for most of its length.

About 13.5 mm posterior to the piriform aperture, laterally directed processes are visible near the mid-section of the bony nasal septum. Moving posteriorly in the coronal plane, these processes increase in length until they contact the lateral wall of the nasal fossa about 16 mm posterior to the nasal fossa to form a transverse bony septum. As in many extant strepsirrhines, the transverse bony septum of *Rooneyia* separates the olfactory recess superiorly from the nasopharyngeal meatus inferiorly. The olfactory recess is a mediolaterally compressed space about 5.9 mm in anteroposterior length and 4.4 mm wide at its anterior margin. The cribriform plate forms the roof of the olfactory recess along most of its length, and multiple turbinals are partly contained within the olfactory recess (see below).

Left nasal fossa As noted above, the anterior portion of the left nasal fossa is extensively damaged. The basal lamina of the left maxilloturbinal is preserved along most of its length, but the large portions of its medially directed scroll are missing. Only a small inferolateral portion of left ET I is identifiable, but this segment appears to have remained close to its original position by comparison with right ET I. Similarly, only small lateral and superior sections of the nasoturbinal remain intact. The left nasoturbinal is best preserved at its posterior margin where it contacts the cribriform plate. In contrast with these larger anterior turbinals, left ET II–IV, the left frontoturbinal, and the left interturbinal are somewhat better preserved. The anatomy of these smaller turbinals appears to closely mirror that of the corresponding turbinals in the right nasal fossa. Accordingly, the detailed descriptions of ET II–IV, the frontoturbinal, and the interturbinal are provided below.

Right nasal fossa The right nasal fossa of *Rooneyia* (Figs. 1 and 2) is approximately 21.9 mm in anteroposterior length, or about 41.5% of the cranial length (52.74 mm). It exhibits minor damage but appears to be largely free of distortion. Like the left nasal fossa, the right fossa contains one maxilloturbinal, four ethmoturbinals, one frontoturbinal, one interturbinal, and one nasoturbinal.

The anterior margin of the right maxilloturbinal is first visible about 1.4 mm posterior to the piriform aperture. Total length of the maxilloturbinal is about 13.5 mm (Figs. 1 and 2), but this measurement is probably an underestimate due to minor damage to its anterior and posterior margins. Anteriorly, the maxilloturbinal arises from a basal lamina that encloses the nasolacrimal canal and consists of a large inferomedially directed scroll. About 1.4 mm from the damaged anterior margin of the left maxilloturbinal, a smaller superiorly-directed scroll is also evident. Moving posteriorly in the coronal plane, the basal lamina of the maxilloturbinal slowly shifts from the lateral wall to the floor of the nasal fossa. Approximately 3.2 mm from its anterior margin, the smaller superior scroll of the maxilloturbinal is no longer evident, and the remainder of the maxilloturbinal is a single superomedially directed scroll.

The anterior-most portion of ET I is located about 6.9 mm posterior to the piriform aperture. ET I is well preserved (Fig. 1) and measures about 9.8 mm in length from its anterior margin to its posterior-most contact with the cribriform plate. The anterior margin of ET I forms an enclosed bulla that increases in volume for about 3 mm moving posteriorly in the coronal plane. Anterior to the nasoturbinal, ET I has a roughly triangular cross-section. However, where ET I lies medially adjacent to the nasoturbinal, it is mediolaterally compressed and has a superiorly directed lamina on its superior margin. This superior lamina of ET I is about 3.1 mm in total anteroposterior length. About 5.4 mm from the anterior margin of ET I, an inferolaterally directed scroll about 1 mm in anteroposterior length is visible within the bullar portion of ET I. The horizontal lamina is first evident 6.1 mm posterior to the anterior margin of ET I. Immediately posterior to this anterior margin of the horizontal lamina, the bullar anterior portion of ET I opens to the nasal cavity at its inferomedial margin. At this point, the horizontal lamina is horizontally oriented and ET I is connected to the horizontal lamina at a 90° angle by a superiorly oriented lamina. Arising from the superiorly oriented lamina are separate medially positioned and laterally positioned scrolls. The smaller laterally-directed scroll of ET I becomes indistinct about 1.4 mm posterior to its first appearance in coronal view, and the larger medially directed scroll comprises the remainder of ET I to its point of contact with the cribriform plate. Moving posteriorly in a coronal plane between the opening of the bullar portion of ET I and the anterior portion of ET III, the horizontal lamina gradually assumes a more superiorly directed, oblique orientation and the flexure between the horizontal lamina and ET I becomes less distinct.

ET II is approximately 3 mm in total anteroposterior length, and its anterior margin is located about 13.5 mm posterior to the piriform aperture. The main portion of ET II is a single scroll with a bullar anterior margin that is about 2.6 mm in length and located inferomedial to ET I. In coronal cross-section, ET II originates at the point of flexure between the horizontal lamina and ET I. Accordingly, the horizontal lamina forms a common basal lamina for both ET I and ET II in *Rooneyia*. However, the anterior-most portion of ET II has a complex cross-sectional geometry and contacts the lateral wall of the nasal fossa for a short distance (~0.5 mm) via an independent basal lamina located inferior to the horizontal lamina. This short independent inferior basal lamina of ET II is visible bilaterally. ET I and ET II also become indistinct from one another near their posterior contact with the cribriform plate. Although closely associated with ET I, ET II does not contact any other adjacent turbinals.

The anterior-most portion of ET III is located inferior to ET II and about 15.5 mm posterior to the piriform aperture. ET III is about 3.7 mm in total anteroposterior length, and appears to be bullar for the anterior-most 25% of its length (Fig. 1). About 0.6 mm anterior to the anterior margin of ET IV, the cross-sectional morphology of ET III shifts from a closed bulla to a superiorly directed scroll. Moving posteriorly, ET III loses this scrolled morphology and becomes and arcuate lamina near its point of contact with the cribriform plate.

The anterior-most portion of ET IV is located inferior to ET III and about 16 mm posterior to the piriform aperture. The total anteroposterior length of ET IV is about 3.1 mm. The anterior half of ET IV takes the form of a single scroll, whereas the posterior half is more laminar in cross-sectional morphology. Although the posterior portions of all ethmoturbinals and the interturbinal extend into the olfactory recess, ET IV is contained almost entirely within the olfactory recess (Fig. 1).

The anterior-most portion of the interturbinal is located in the gap between the horizontal lamina and the secondary independent basal lamina of ET II (see above). The posterior-most preserved segment of the interturbinal is located superior to the basal lamina of ET III. At 3.2 mm in anteroposterior length, the preserved

Table 3
Anatomical features of specimens in this study.[a]

Taxon	ET	IT	FT	NT	MT	NLC	OTSA (mm^2)	MTSA (mm^2)
Tupaia glis	4	1	2	P	DS	H	907.61	185.17
Tupaia belangeri	4	1	2	P	DS	H	918.41	333.23
Ptilocercus lowii	4	1	2	P	DS	H	459.44	164.8
Galeopterus variegatus	5	1	2	P	L	H	2233.34	221.46
Cynocephalus volans	5	1	2	P	L	H	1601.71	138.77
Mirza coquereli	4	0	2	P	S	O	961.95	365.63
Lepilemur mustelinus	5	2	1	P	S	O	600.46	260.36
Varecia rubra	4	1	2	P	S	O	3897.40	2134.40
Eulemur collaris	4	1	1	P	S	H	1713.84	1104.61
Hapalemur griseus	5	2	2	P	S	O	828.34	424.74
Avahi laniger	5	1	2	P	S	O	536.14[b]	197.47
Propithecus verreauxi	4	0	1	P	S	O	1266.90	878.78
Indri indri	5	1	1	P	S	O	2610.83	678.51
Daubentonia madagascariensis	4	4	6	P	S	V	5516.88	516.27
Otolemur crassicaudatus	4	1	2	P	S	O	1429.97	536.14
Euoticus elegantulus	4	1	1	P	S	O	447.12	163.92
Galago moholi	4	1	1	P	S	O	309.83	129.16
Galago senegalensis	4	1	1	P	S	O	625.91	282.18
Perodicticus potto	4	1	1	P	S	O	1258.80	366.35
Nycticebus coucang	4	1	1	P	S	O	691.47	221.74
Loris tardigradus	4	1	0	P	S	O	713.62	221.20
Carlito syrichta	2	0	0	P	S	V	119.46	23.77
Aotus griseimembra	2	0	0	P	S	V	418.29	144.1
Alouatta palliata	1	0	0	P	S	V	1217.09	283.93
Ateles geoffroyi	2	0	0	P	L	V	469.59	125.34
Callicebus discolor	1	0	0	P	S	V	205.24	177.97
Callithrix argentata	2	0	0	P	S	V	60.72	69.45
Saimiri oerstedii	1	0	0	P	L	V	158.90	80.43
Mandrillus leucophaeus	2 (DC)	0	0	A	L	O	1041.53	1267.43
Miopithecus talapoin	1 (DC)	0	0	A	S	V	156.77	134.83
Presbytis hosei	1 (DC)	0	0	A	S	V	133.29	126.75
Procolobus badius	2 (DC)	0	0	A	S	V	436.93	215.98
Hylobates lar	2 (DC)	0	0	A	L	V	214.81	610.63
Rooneyia viejaensis	4	1	1	P	S	O	408.31	145.42

Abbreviations: ET = ethmoturbinals; FT = frontoturbinals; IT = interturbinals; MT = maxilloturbinals; MTSA = maxilloturbinal surface area; NLC = nasolacrimal canal; NT = nasoturbinals; and OTSA = olfactory turbinal surface area.

[a] Definitions of descriptive turbinal shape terms used here: A = absent; DC = does not directly contact the cribriform plate; DS = double scrolled; H = horizontal; L = laminar in shape; O = oblique; P = present; S = scrolled; V = vertical.

[b] Note that the *Avahi* specimen included in this study has a broken ethmoturbinal I, so the olfactory turbinal surface area is an underestimate.

portions of the interturbinal are longer than both ET II and ET IV (Fig. 2). Nevertheless, the interturbinal has a small cross-sectional area that is restricted to the lateral half of the nasal fossa, making its surface area considerably smaller than any of the ethmoturbinals. The interturbinal appears to form a single scroll for most of its length, but it lacks a clear contact with the cribriform plate and may thus be broken posteriorly.

The nasoturbinal is a large structure about 5.9 mm in total anteroposterior length. The anterior-most 27% of the nasoturbinal has a laminar coronal cross-section, and is located lateral to ET I. This laminar anterior segment of the nasoturbinal contacts the lateral wall of the nasal fossa via three separate basal laminae. However, the inferior-most two basal laminae are short, and the posterior 4.5 mm of the nasoturbinal is connected to the lateral or superior wall of the nasal fossa via only the superior-most basal lamina. The middle 42% of the nasoturbinal takes the form of a mediolaterally compressed scroll. The posterior-most 31% of the nasoturbinal is more restricted in cross-sectional area and is confined to the superior portion of the nasal cavity, superior to ET I and superomedial to the frontoturbinal. This posterior segment of the nasoturbinal has a complex cross-sectional geometry and appears to form an enclosed tube for parts of its length as it approaches the cribriform plate.

The frontoturbinal is about 3.4 mm in total anteroposterior length, and appears to be intermediate in surface area between the more extensive nasoturbinal and the smaller interturbinal. Its anterior-most margin is located lateral to the scrolled midsection of the nasoturbinal. Although the anterior margin of the frontoturbinal basal lamina contacts the superior surface of the horizontal lamina, the majority of the frontoturbinal basal lamina has an independent contact with the lateral wall of the nasal fossa, superior to the horizontal lamina. Arcuate laminar portions of the frontoturbinal branch to run superiorly and inferiorly from the frontoturbinal basal lamina. It is not clear if the lack of scrolling of the inferior laminar segment of the frontoturbinal is an artifact of breakage. However, further posteriorly the superior surface of the frontoturbinal forms a mediolaterally compressed scroll.

The nasolacrimal canal in *Rooneyia* extends from the lacrimal fossa anterior to the orbit through the nasal and maxilla (Fig. 1). In lateral view, the nasolacrimal canal is oblique in orientation relative to the palate (Fig. 2). It opens into the nasal fossa just lateral and inferior to the maxilloturbinal.

3.2. Scandentia

The nasal fossa of scandentians contains one maxilloturbinal, four ethmoturbinals, one interturbinal, two frontoturbinals, one nasoturbinal, and an anterior accessory turbinal of uncertain homology (Figs. 3 and 4A–F). As in *Rooneyia*, the anterior margin of the maxilloturbinal has a basal lamina that originates from the

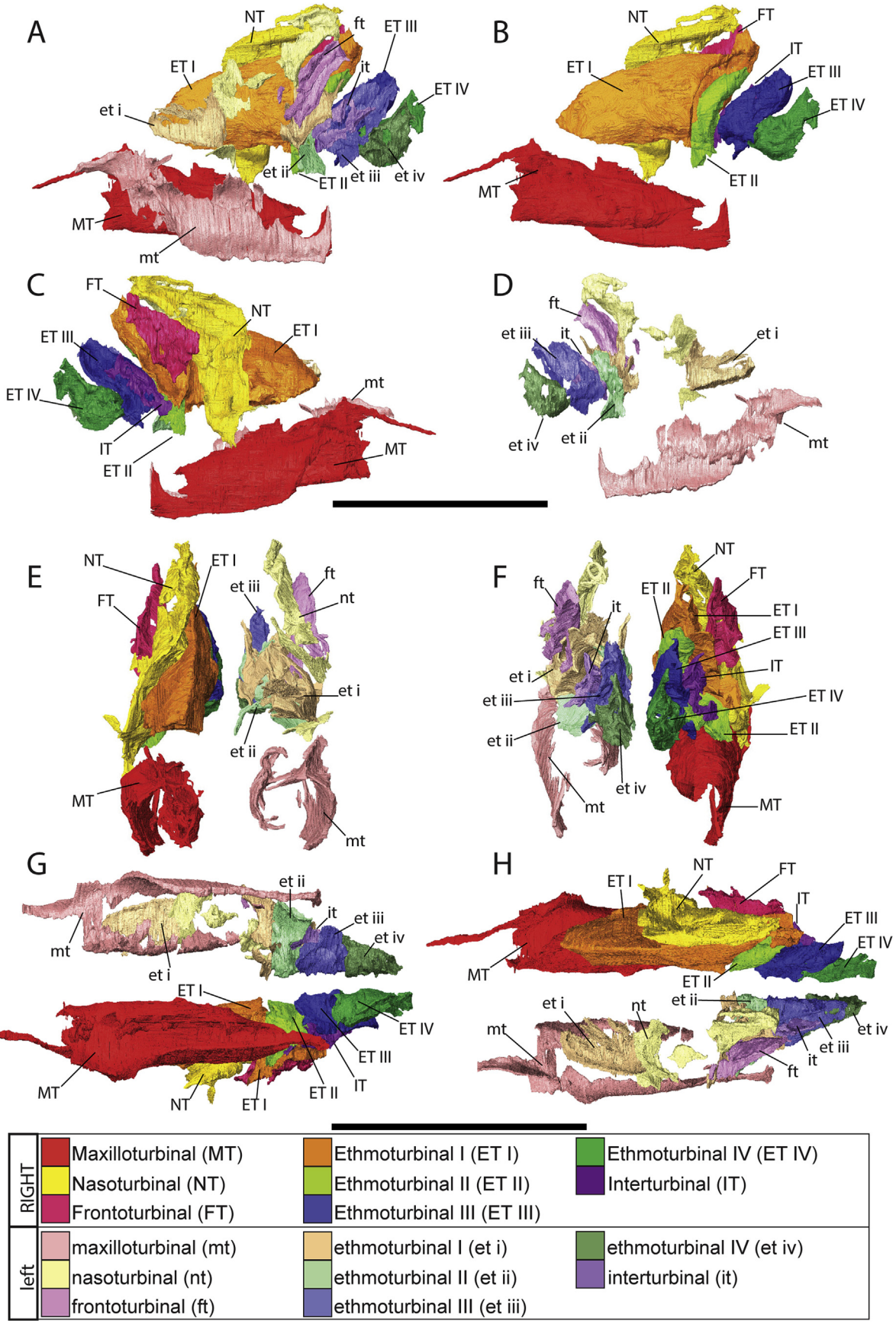

Figure 2. *Rooneyia* (TMM 40688-7) turbinal surface views: A) left lateral view; B) medial view of right nasal fossa turbinals; C) right lateral view; D) medial view of left nasal fossa turbinals; E–H) anterior (E), posterior (F), inferior (G), and superior (H) views of all turbinals. Right (uppercase abbreviations) and left (lowercase abbreviations) sides in surface view can be compared with cross-section views in Figure 1. Scale bars = 10 mm.

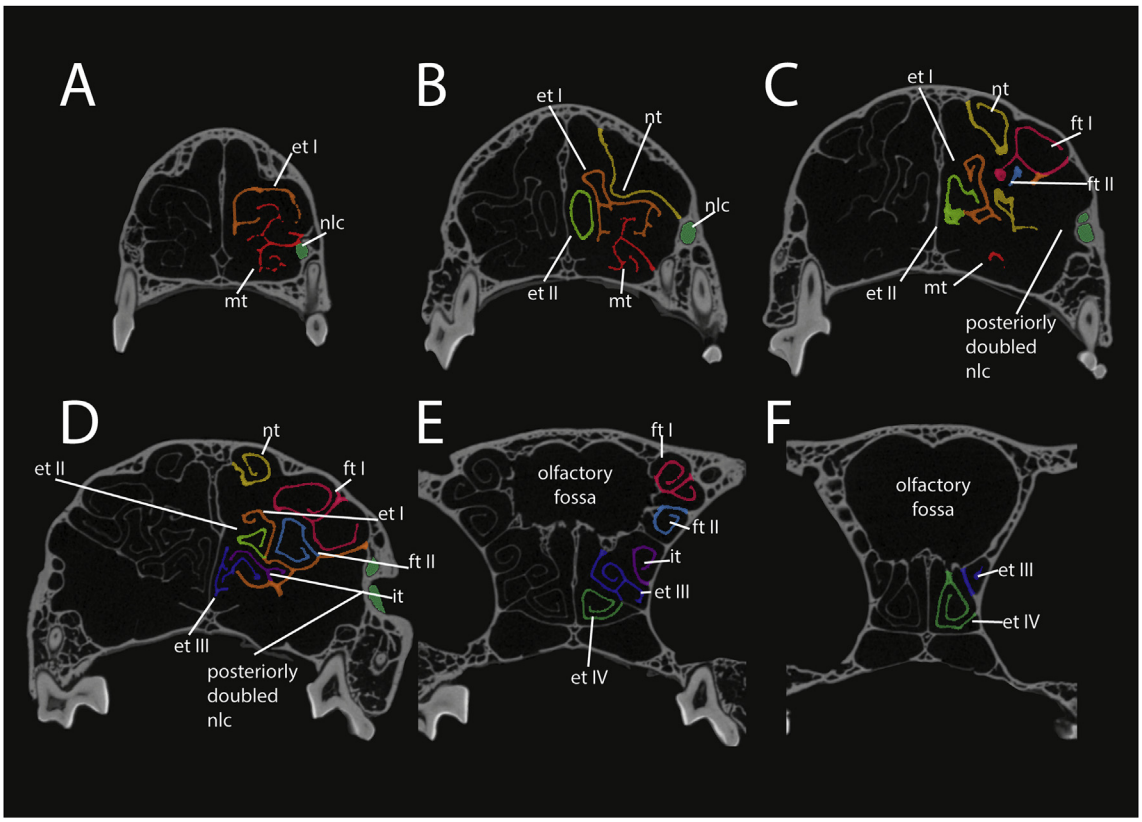

Figure 3. CT scan slices through the nasal fossa of *Tupaia glis* (TMM 2256) showing nasal fossa structures of Scandentia: 1547 (A), 1470 (B), 1412 (C), 1369 (D), 1290 (E) and 1247 (F) of 1872 total slices. Abbreviations: et I = ethmoturbinal I; et II = ethmoturbinal II; et III = ethmoturbinal III; et IV = ethmoturbinal IV; ft I = frontoturbinal I; ft II = frontoturbinal II; it = interturbinal; mt = maxilloturbinal; nlc = nasolacrimal canal; and nt = nasoturbinal.

lateral wall of the nasal fossa and a medial portion consisting of a single inferiorly directed scroll. However, moving posteriorly in the nasal fossa, the maxilloturbinal quickly assumes a more complex, arborized cross-sectional geometry. Near the region of the outlet of the nasolacrimal canal, two major branches of the maxilloturbinal arise from the basal lamina, each of which further branches into multiple subdivisions, some of which acquire a scrolled morphology. Moving further posteriorly from the outlet of the nasolacrimal canal, the maxilloturbinal basal lamina migrates from the lateral wall to the floor of the nasal fossa and the body of the maxilloturbinal again assumes a single-scrolled cross-section.

Closely associated with the maxilloturbinal in the anterior portion of the nasal fossa is an accessory turbinal of uncertain homology.[4] In *Tupaia*, this accessory turbinal has laminar cross-sectional morphology across its length, and extends approximately as far into the nasal fossa as the basal lamina of the maxilloturbinal. At its anterior end, the accessory turbinal arises from the inferior surface of the nasal bone and projects inferiorly and laterally into the space superior to the maxilloturbinal. Moving posteriorly in the nasal fossa, the origin of the accessory turbinal progressively migrates laterally and inferiorly onto the maxilla, where it projects first inferiorly and ultimately medially. At its posterior end, the accessory turbinal merges with the superior surface of the maxilloturbinal basal lamina adjacent to the outlet of the nasolacrimal canal. The anatomy of the anterior accessory turbinal is similar in *Ptilocercus*, although its cross-sectional anatomy assumes an L-shape near the anterior margin of ET I. Additionally, rather than merging with the maxilloturbinal basal lamina and becoming indistinct as in *Tupaia*, the posterior portion of the accessory turbinal in *Ptilocercus* migrates onto the superior surface of the maxilloturbinal basal lamina for a short distance. Accordingly, although the anterior accessory turbinal of scandentians has been identified as part of the nasoturbinal by previous authors (Le Gros Clark, 1926; Wible, 2011; Ruf, 2014; Ruf et al., 2015), it may be terminologically and functionally more appropriate to consider it as a distinct branch of the maxilloturbinal.

Unlike *Rooneyia*, in which the anterior surface of ET I has a bullar morphology and is located superior to the maxilloturbinal, the anterior portion of ET I in scandentians is a broadly curved lamina that surrounds the medial and lateral portions of the superior maxilloturbinal. In all three scandentian taxa examined here, a small bulla is formed in the superior portion of ET I near the anterior margin of ET II (Fig. 3). As ET I extends posteriorly from this point, it acquires an arborized cross-sectional morphology and forms the site of origin of both ET II and the anterior portion of the interturbinal. The anterior surfaces of ETs II–IV form a bulla in all scandentians (Fig. 4A–F). ET II anteriorly parallels the posterior surface of ET I. ET III is scrolled posteriorly with small lateral projections that do not contact the lateral wall of the nasal fossa. ET IV is bullar with laminar extensions

[4] Ruf (2014) identified this structure as the 'nasoturbinal', and further identified the structure here called the nasoturbinal as the 'lamina semicircularis'. By comparison, Le Gros Clark (1926) and Wible (2011) identified the anterior accessory turbinal of scandentians as the anterior end of the nasoturbinal. Our identification and description of nasoturbinals was chosen to be consistent with most prior accounts of nasal fossa morphology in primates (Smith et al., 2007c, 2016). In the scandentian sample considered here, the nasoturbinal and anterior accessory turbinal are separate distinct bony structures with the bulk of ET I intervening between them. If the terminology employed by Ruf (2014) were applied to primates, no primate species would possess a nasoturbinal, but strepsirrhines, platyrrhines, and *Rooneyia* would all possess a 'lamina semicircularis'.

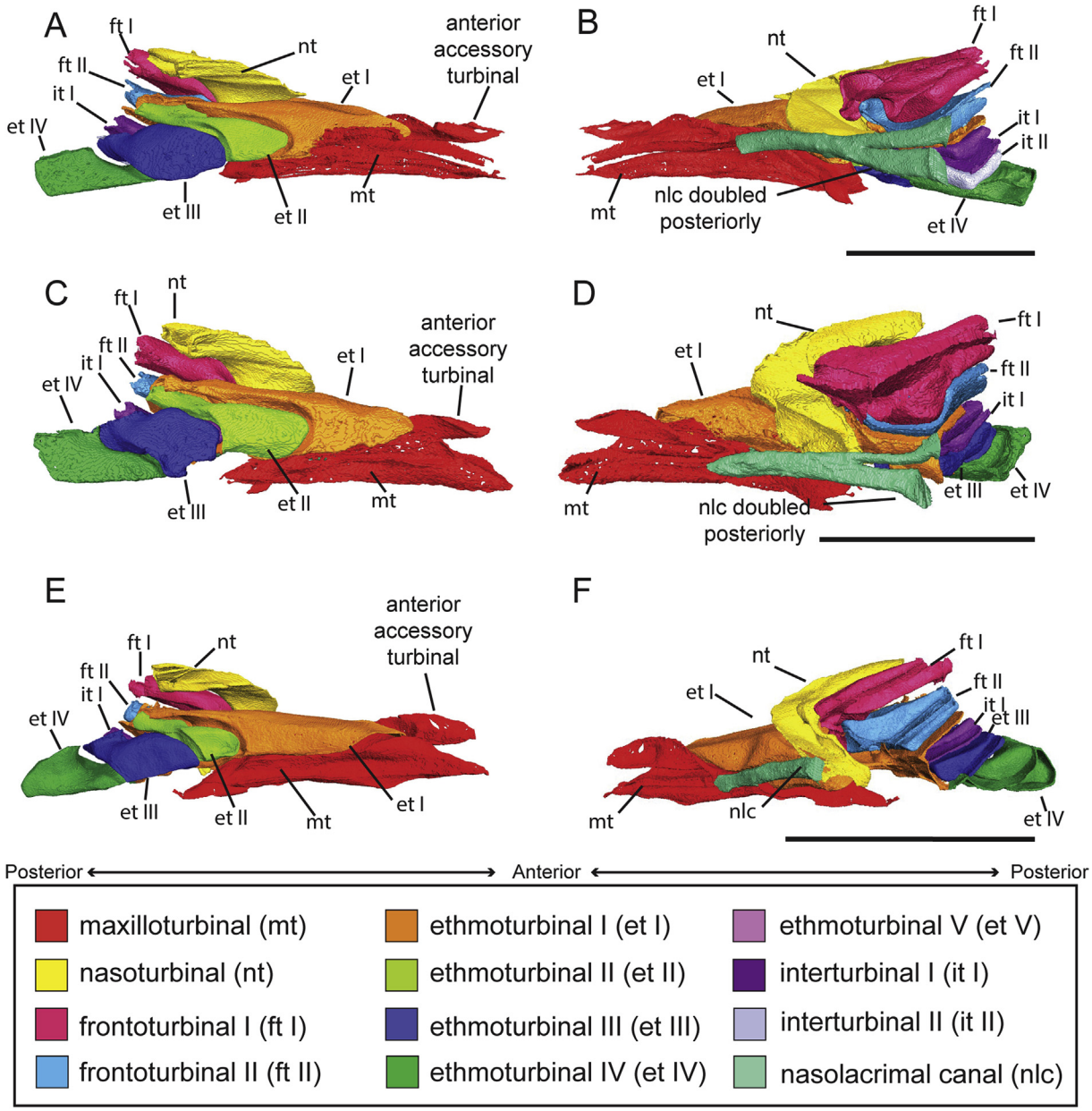

Figure 4. Scandentian turbinals and nasolacrimal canals: A, B) *Tupaia belangeri* (USNM-320680), in medial (A) and lateral (B) views; C, D) *Tupaia glis* (TMM 2256), in medial (C) and lateral (D) views; E, F) *Ptilocercus lowii* (USNM-481107), in medial (E) and lateral (F) views. Scale bars = 10 mm.

contacting the lateral wall of the nasal fossa. The interturbinal is located between ET I and ET III (*Tu. glis* and *Ptilocercus*) or between ET I and interturbinal II (*Tu. belangeri*). The frontoturbinals are immediately posterior to the nasoturbinal, with frontoturbinal I more anteriorly situated than frontoturbinal II. In *Tupaia*, frontoturbinal I is double-scrolled along its entire length. Frontoturbinal II has a single posterior scroll contacting the cribriform plate. In *Ptilocercus*, this condition is reversed, with frontoturbinal I having a single posterior scroll and frontoturbinal II being double-scrolled along its entire length. The nasoturbinal is anteriorly laminar and forms a scroll posteriorly as it approaches the cribriform plate. The nasolacrimal canal in all scandentians is horizontal in orientation relative to the palate (Fig. 4A–F). The nasolacrimal canals in both *Tu. belangeri* and *Tu. glis* have two orbital inlets. These inlets are nearly equal in size in *Tu. belangeri* but in *Tu. glis* the dorsal inlet is approximately 40% the size of the ventral canal.

3.3. Dermoptera

The dermopteran nasal fossa contains a maxilloturbinal, five ethmoturbinals, one interturbinal, two frontoturbinals, and one nasoturbinal (Figs. 5 and 6). Although the maxilloturbinal is greater in anteroposterior length than ET I, the maxilloturbinals of both *Cynocephalus* and *Galeopterus* are noteworthy for their diminutive coronal cross-sectional area. For most of its length, the maxilloturbinal in both species forms a single small scroll with 1–2 small osseous ridges located on its superior surface. ET I, by comparison, has a much greater coronal cross-sectional area. This characteristic dermopteran morphology in which ET I is very large and the maxilloturbinal is very small stands in contrast to scandentians and most strepsirrhines, in which ET I and the maxilloturbinal are more comparable in size. There is no evidence of an anterior accessory turbinal comparable to that seen in scandentians. Dermopteran ET I–V are bullar anteriorly and scrolled at their

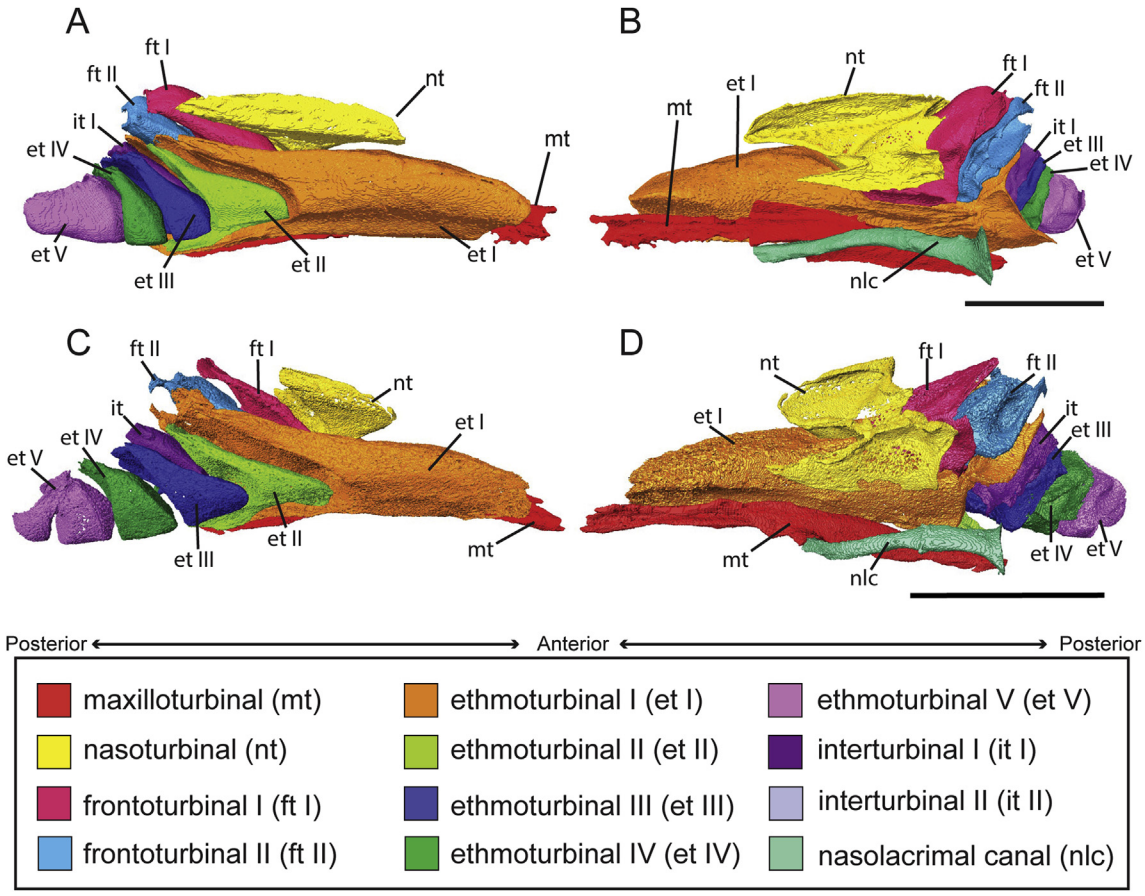

Figure 5. Dermopteran turbinals and nasolacrimal canals: A, B) *Galeopterus variegatus* (E.C. Kirk private specimen), in medial (A) and lateral (B) views; C, D) *Cynocephalus volans* (AMNH-M-187861), in medial (C) and lateral (D) views. Scale bars = 10 mm.

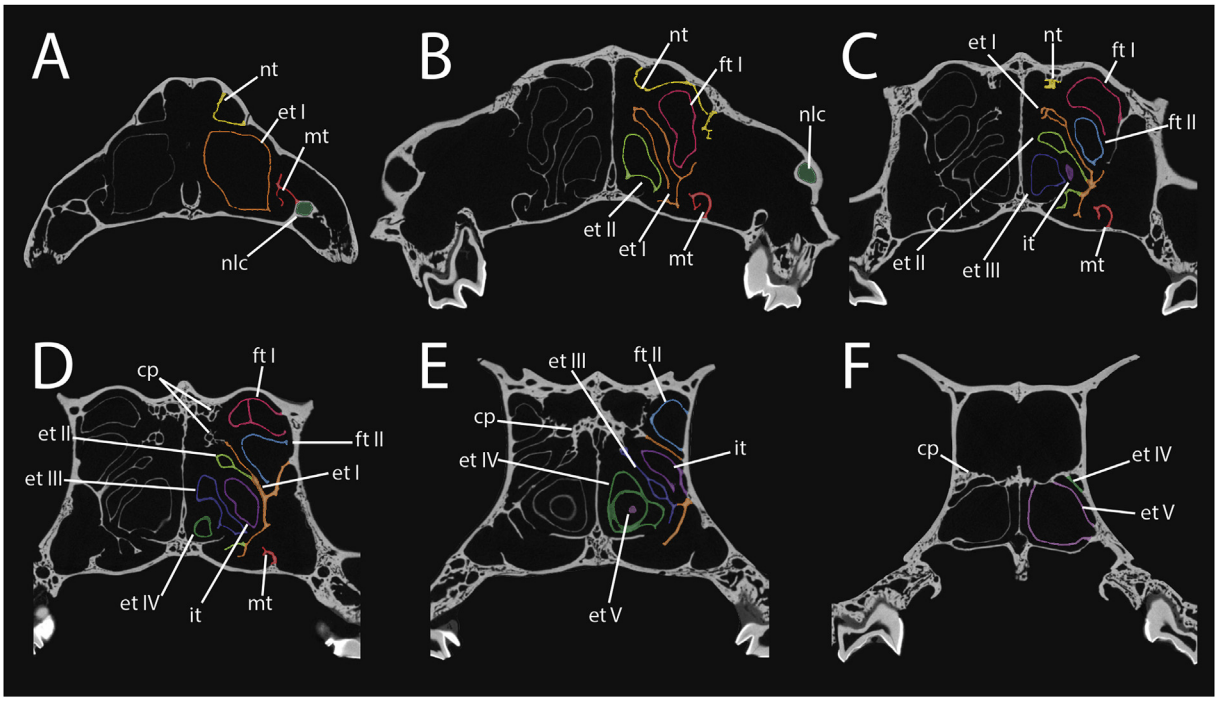

Figure 6. CT scan slices through the nasal fossa of *Galeopterus variegatus* (E.C. Kirk private specimen) showing nasal fossa structures of Dermoptera: 513 (A), 726 (B), 782 (C), 822 (D), 878 (E) and 952 (F) of 1872 total slices. Abbreviations: cp = cribriform plate; et I = ethmoturbinal I; et II = ethmoturbinal II; et III = ethmoturbinal III; et IV = ethmoturbinal IV; ft I = frontoturbinal I; ft II = frontoturbinal II; it = interturbinal; mt = maxilloturbinal; nlc = nasolacrimal canal; and nt = nasoturbinal.

posterior attachments with the cribriform plate (Fig. 5). ET I is nearly equal in length to the maxilloturbinal and appears just after the initial anterior appearance of the maxilloturbinal. The interturbinal is scrolled and has attachments to the cribriform plate and lateral wall of the nasal fossa that are independent of the ethmoturbinals. Frontoturbinals I and II are large and form closed bullae for much of their lengths. In coronal cross-section, the nasoturbinal forms a curved lamina that is fused at both its medial and lateral ends to the inferior surface of the broad nasal bone. This morphology sequesters a small space between the nasoturbinal and nasal bone from the superior nasal fossa. The nasoturbinal also has a small inferiorly directed lamina at its lateral margin, superior to the maxilloturbinal. The dermopteran nasolacrimal canal is horizontal relative to the palate (Fig. 5).

3.4. Strepsirrhini

The nasal fossae of strepsirrhines typically house a maxilloturbinal, four or five ETs, one or two interturbinals, one or two frontoturbinals, and one nasoturbinal (Figs. 7–16). The maxilloturbinal is either a single or double scroll that terminates posteriorly in the nasopharyngeal meatus inferior to the transverse lamina. In most taxa, the maxilloturbinal parallels the inferior surface of ET I. *Propithecus* is noteworthy among primates in exhibiting a particularly large maxilloturbinal (Fig. 9). However, the maxilloturbinal of *Daubentonia* (Figs. 7 and 8) has a morphology and orientation that is unique among the taxa examined here. The maxilloturbinal is double scrolled for most of its length, and its anterior portion is oriented anteroposteriorly as in other strepsirrhines. The anterior maxilloturbinal basal lamina is directed superomedially into the nasal fossa, and originates from the superior surface of the large incisor alveolus, which bulges medially into the nasal fossa. Moving posteriorly, the maxilloturbinal basal lamina of *Daubentonia* gradually shifts from the lateral wall to the floor of the nasal fossa as in other strepsirrhines, but in doing so the basal lamina runs inferiorly to traverse the medial surface of the large incisor alveolus. As a result, the middle portion of the maxilloturbinal is oriented superoinferiorly and is nearly orthogonal to the anterior portion of the maxilloturbinal. After traversing the incisor alveolus and reaching the floor of the nasal fossa, the posterior maxilloturbinal assumes a single-scrolled morphology and returns to a more conventional anteroposterior orientation. As a result, the maxilloturbinal of *Daubentonia* has two unique flexures (one on either side of the incisor alveolus) and assumes a characteristic sigmoidal shape when viewed laterally (Fig. 7). It seems plausible that this derived maxilloturbinal morphology is tied to the facial foreshortening and hypertrophy of the hypselodont maxillary incisors that are also characteristic of *Daubentonia* (Cartmill, 1974).

In all strepsirrhines, ET I is the largest ethmoturbinal. *Indri* (Fig. 9E, F), *Avahi* (Fig. 9A, B), *Hapalemur* (Fig. 11C, D), *Lepilemur* (Fig. 13), and *Daubentonia* (Figs. 7 and 8) all have five ethmoturbinals, while all other strepsirrhines examined here have four ethmoturbinals. In *Daubentonia*, the posterior portion of ET I has an unusually complex cross-sectional anatomy, consisting of at least 5 separate scrolls. *Daubentonia* is also notable in having an ET II that is not bullar on its anterior surface, and in having ET II–V, the frontoturbinals, and the interturbinals stacked in a superoinferior (rather than anteroposterior) array.

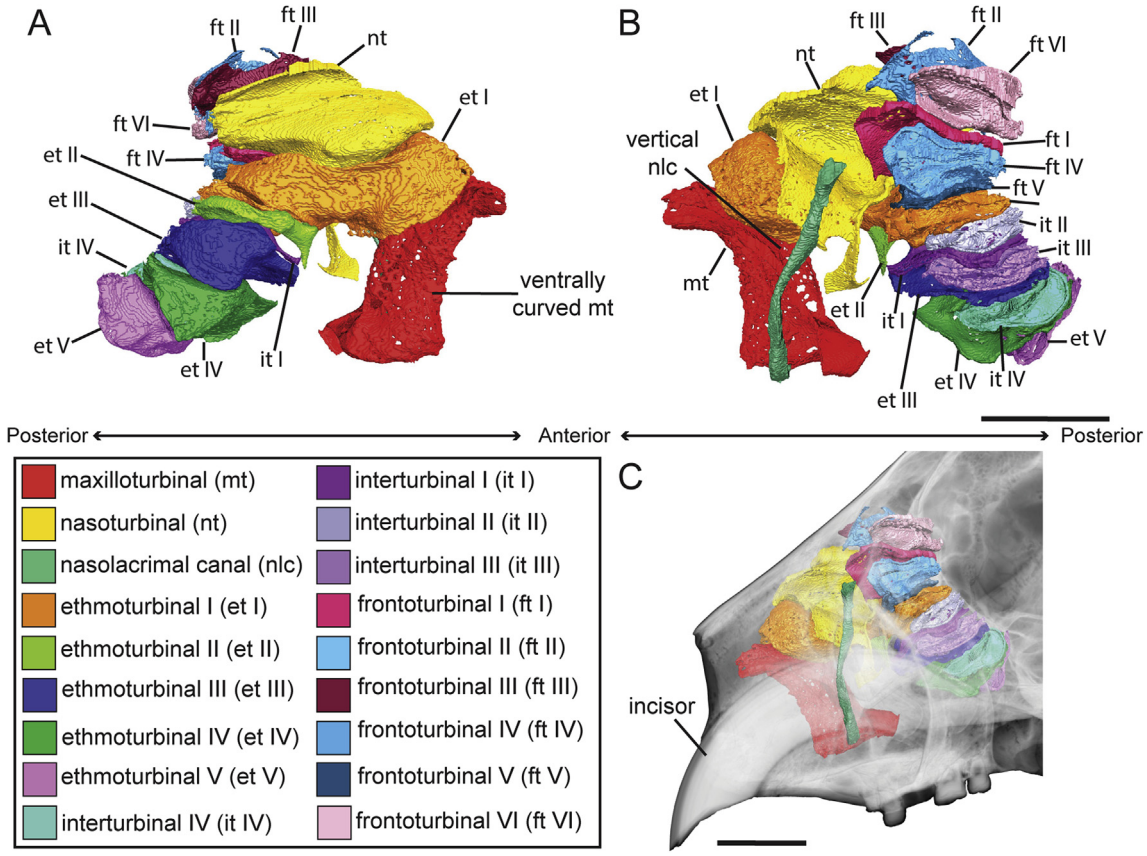

Figure 7. Daubenontiid turbinals and nasolacrimal canal: A–C) *Daubentonia madagascariensis* (AMNH-M-100632), in medial (A) and lateral (B), and lateral view showing turbinals in relation to incisor (C). Scale bar = 10 mm.

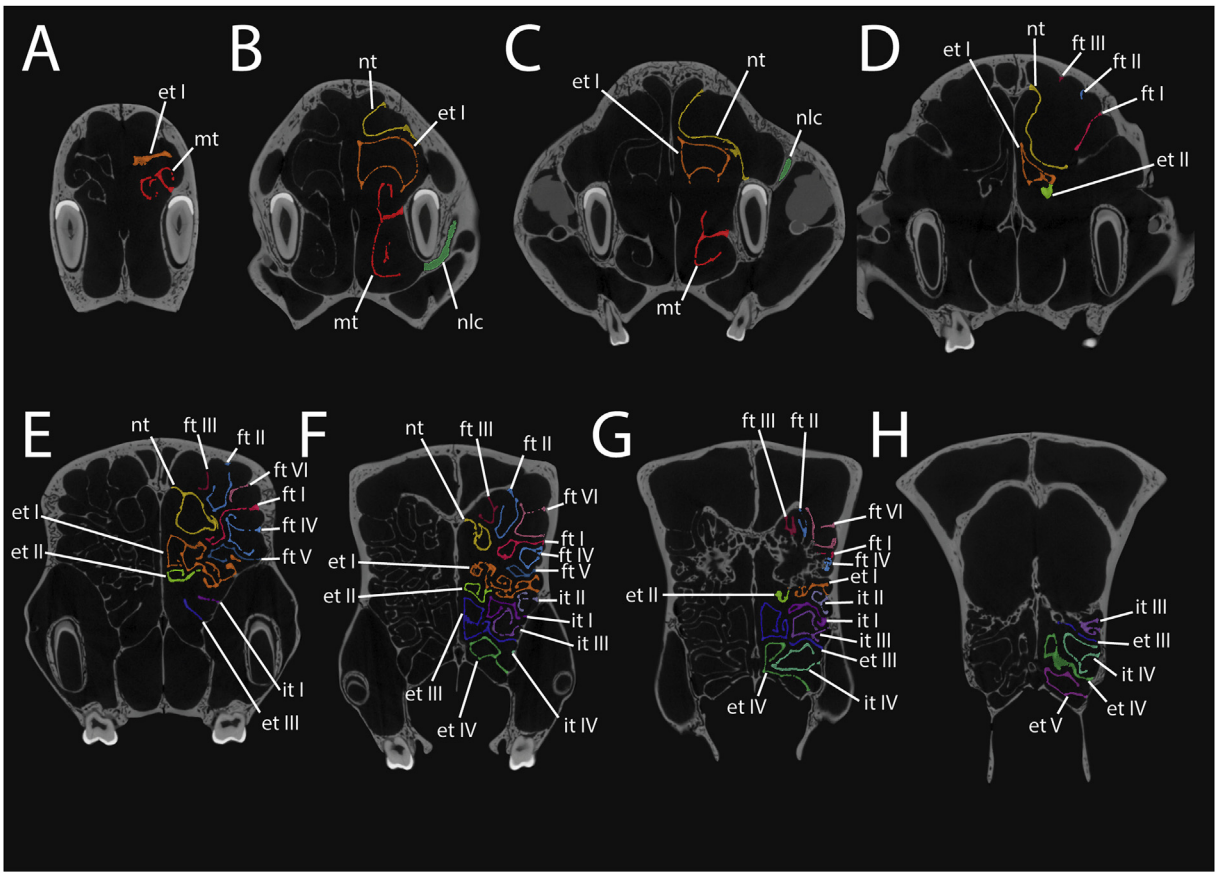

Figure 8. CT scan slices through the nasal fossa of *Daubentonia* (AMNH-M-100632) showing nasal fossa and nasolacrimal canal orientation: 240 (A), 307 (B), 340 (C), 399 (D), 433 (E), 481 (F), 511 (G), and 555 (H) of 1264 total slices. Abbreviations: et I = ethmoturbinal I; et II = ethmoturbinal II; et III = ethmoturbinal III; et IV = ethmoturbinal IV; et V = ethmoturbinal V; ft I = frontoturbinal I; ft II = frontoturbinal II; ft III = frontoturbinal III; ft IV = frontoturbinal IV; ft V = frontoturbinal V; ft VI = frontoturbinal VI; it I = interturbinal I; it II = interturbinal II; it III = interturbinal III; it IV = interturbinal IV; mt = maxilloturbinal; nlc = nasolacrimal canal; and nt = nasoturbinal.

With the exception of *Loris*, all lorisiform strepsirrhines (Figs. 14–16) have one interturbinal located in the space between the basal laminae of ET II and ET III (e.g., Fig. 15F, G). Lemuriform strepsirrhines are more variable in interturbinal numbers. Most lemuriforms examined here have one interturbinal located between the shared lateral wall contact of ET I/ET II (i.e., the horizontal lamina) and the basal lamina of ET III. However, both *Lepilemur* and *Hapalemur* have two interturbinals and *Daubentonia* has four interturbinals, while *Propithecus* has none (Table 3).

Frontoturbinals are the most variable turbinal group in strepsirrhines. *Daubentonia* has six frontoturbinals while most other lemuriforms have one (*Lepilemur, Eulemur, Propithecus, Indri*) or two (*Mirza, Varecia, Hapalemur, Avahi*). Most lorisiforms examined here have one frontoturbinal except for *Otolemur*, which has two frontoturbinals, and *Loris*, which has none.

Across strepsirrhine primates, the nasoturbinal extends posteriorly along the lateral wall of the nasal fossa toward the cribriform plate. In every strepsirrhine except *Loris*, the nasoturbinal is scrolled posteriorly. In *Loris*, by contrast, a thin and posteriorly directed lamina of the nasoturbinal contacts the cribriform plate.

Like scandentians (Fig. 3) and dermopterans (Fig. 6), all strepsirrhines possess a large olfactory recess that contains the posterior ethmoturbinals and is separated from the nasopharyngeal meatus by the transverse lamina. Our comparative sample reveals considerable variation in the disposition of the transverse lamina relative to the horizontal lamina. The latter structure provides the site of attachment for a variable number of ethmoturbinals, and in most taxa is distinct from the transverse lamina flooring the olfactory recess (e.g., Fig. 15). However, in adult *Eulemur* the horizontal and transverse laminae comprise a continuous horizontally oriented sheet of bone (Fig. 10). The basal laminae of all ethmoturbinals arise mainly from the superior surface of this combined bony sheet rather than from the lateral wall of the nasal cavity (Fig. 10D–H). In *Daubentonia* the horizontal lamina is also continuous with the transverse lamina, but unlike *Eulemur* the horizontal lamina is more vertically oriented (Fig. 8). As a result, the horizontal lamina meets the transverse lamina at approximately a 90° angle in *Daubentonia* (Fig. 8E-H).

The nasolacrimal canals of nearly all strepsirrhines may be characterized as horizontal or oblique in orientation (Table 3). This range of variation encompasses taxa such as *Eulemur* (Fig. 11B) and *Varecia* (Fig. 11F), in which the nasolacrimal canal is nearly parallel to the hard palate, and *Loris* (Fig. 16D), in which the angle between the nasolacrimal canal and hard palate is greater than 45°. In contrast to all other strepsirrhines examined here, *Daubentonia* has a vertically-oriented nasolacrimal canal (Fig. 7). The nasolacrimal canal of *Daubentonia* extends under the root of the maxillary incisor to terminate in the nasal fossa beneath the maxilloturbinal (Figs. 7C and 8B, C). While all examined strepsirrhine taxa have a single nasolacrimal canal inlet bilaterally, the specimen of *Galago senegalensis* exmained here has a double nasolacrimal canal inlet in the orbit on one side.

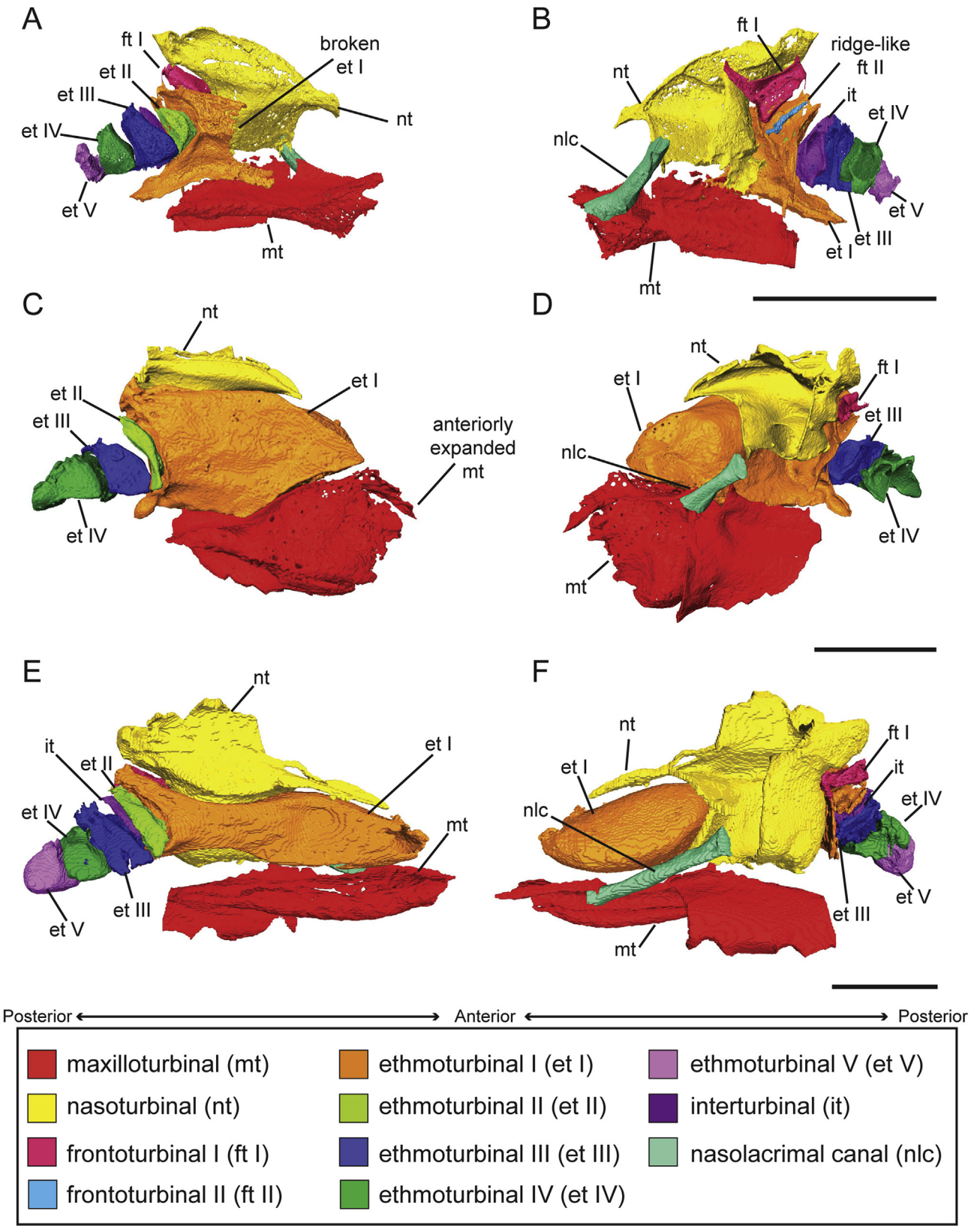

Figure 9. Indriid turbinals and nasolacrimal canals: A, B) *Avahi laniger* (MCZ-44879), in medial (A) and lateral (B) views, note the broken ET I; C, D) *Propithecus verreauxi* (MCZ-16375), in medial (C) and lateral (D) views; E, F) *Indri indri* (AMNH-M-100506), in medial (E) and lateral (F) views. Scale bars = 10 mm.

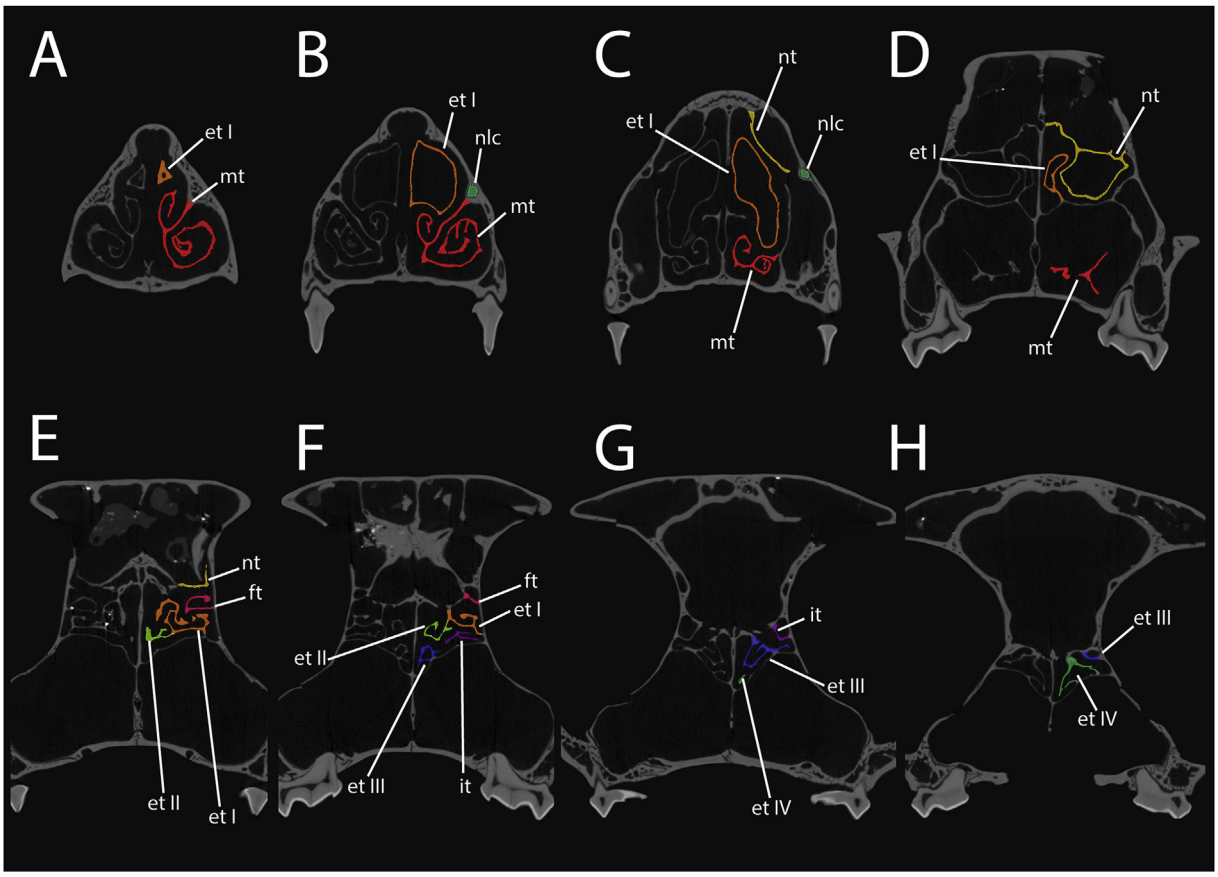

Figure 10. CT scan slices through the nasal fossa of *Eulemur* (MCZ-44896) showing nasal fossa structures of Lemuriformes: 1540 (A), 1447 (B), 1330 (C), 1190 (D), 1124 (E), 1080 (F), 1019 (G), and 972 (H) of 1799 total slices. Abbreviations: et I = ethmoturbinal I; et II = ethmoturbinal II; et III = ethmoturbinal III; et IV = ethmoturbinal IV; ft = frontoturbinal; it = interturbinal; mt = maxilloturbinal; nlc = nasolacrimal canal; and nt = nasoturbinal.

3.5. Haplorhini

Each nasal fossa in haplorhines contains a maxilloturbinal and either one or two ethmoturbinals, but lacks interturbinals and frontoturbinals. The ethmoturbinals of all haplorhines in our sample except *Aotus* are morphologically distinct from those of non-haplorhine euarchontans in lacking direct posterior contact with the cribriform plate. The nasoturbinal is either small or absent (Table 3; Figs. 17–24). All of the haplorhines included in this study had maxilloturbinals that were either scrolled or laminar. No haplorhines examined here had a capacious olfactory recess like those of non-haplorhine euarchontans, although some haplorhines exhibit a small space in the posterosuperior nasal fossa that is homologous with the olfactory recess (Rossie, 2006; see below).

Carlito syrichta has a maxilloturbinal, two ethmoturbinals, and a nasoturbinal (Figs. 17 and 18). ET I and ET II in *Carlito* are both bullar anteriorly (Fig. 18). The nasoturbinal in *Carlito* is laminar and extends inferiorly down the lateral wall of the nasal fossa to approach the basal lamina of the maxilloturbinal. The nasolacrimal canal in *Carlito* is vertical and opens directly into the nasal fossa from the orbit. The bullar anterior portion of ET II initially contacts the lateral wall of the nasal fossa via a single lamina, but moving posteriorly ET II fuses at its superior and inferior margins with the lateral wall. Moving further posteriorly, a small inferiorly-directed lamina of ET II diverges from the bullar superior portion of ET II (Fig. 18F) and travels a short distance before merging with the lateral wall of the nasal fossa. Similarly, the bullar portion of ET II decreases in cross-sectional area as one moves posteriorly, until it ultimately forms a small laminar projection from the lateral wall of the nasal fossa, in the same coronal plane as the M^1 protocone (Fig. 18G). This small bony projection, continuous with posterior ET II, grows medially as one moves further posteriorly until it contacts the bony nasal septum. In DPC 045 (Figs. 18 and 19) this horizontally-oriented bony lamina sequesters a mediolaterally compressed space about 0.67 mm in anteroposterior length from the nasopharyngeal meatus inferiorly. The foramina of the cribriform plate open into the superior-most portion of this space. This space is accordingly similar to the strepsirrhine olfactory recess in both its anatomical relationships and bony morphology, although in *Carlito* no ethmoturbinals extend into this space. Smith, Rossie, and colleagues (Rossie, 2006; Smith and Rossie, 2006; Smith et al., 2007c, 2014a, 2014b) have documented similar spaces in the posterior nasal fossae of some platyrrhines (e.g., *Callithrix* and *Saguinus*), which they term a "cupular recess" and regard as a "vestige of the olfactory recess of ancestral primates" (Smith et al., 2014b:2202). A μCT scan of one specimen of *Cephalopachus bancanus* (USNM 488084) reveals a cupular recess about 1.25 mm in anteroposterior length with a morphology similar to that of *Carlito*, suggesting that this structure may be typical for tarsiers. In both *Carlito* and *Cephalopachus*, the cupular recess lies anterior to the extensive apical interorbital septum (Spatz, 1968; Cartmill, 1972).

Platyrrhines have a maxilloturbinal, one or two ethmoturbinals, and a nasoturbinal that is either small or absent (Table 3; Figs. 20–23). No platyrrhine has bullar ethmoturbinals. *Callithrix*, *Aotus*, and *Ateles* have two ethmoturbinals (Fig. 21), but in both *Callithrix* (Fig. 20) and *Ateles* ET II is only a small ridge along the lateral wall of the nasal fossa. *Alouatta, Callicebus,* and *Saimiri* have only one ethmoturbinal (Fig. 21). While most platyrrhines have

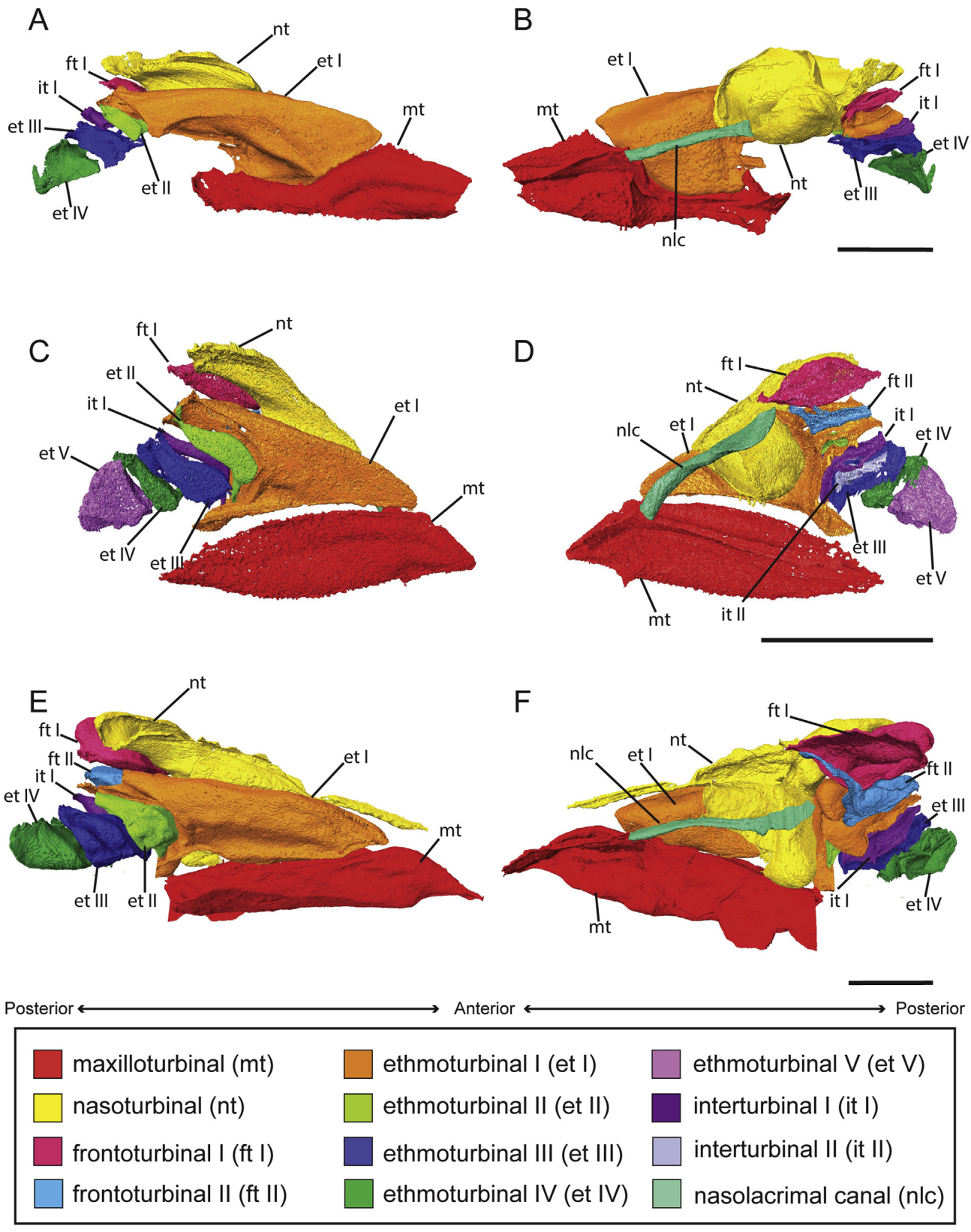

Figure 11. Lemurid turbinals and nasolacrimal canals: A, B) *Eulemur collaris* (MCZ-44896), in medial and lateral (B) views; C, D) *Hapalemur griseus* (MCZ-44913), in medial (C) and lateral (D) views; E, F) *Varecia rubra* (DPC-050), in medial (E) and lateral (F) views. Scale bars = 10 mm.

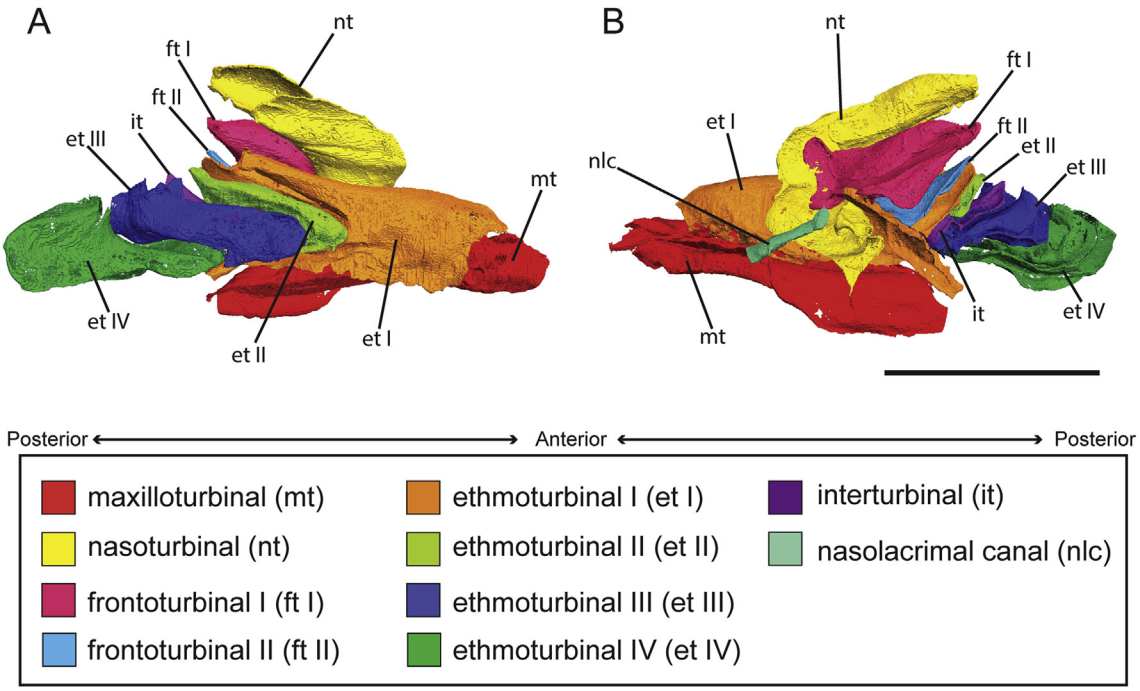

Figure 12. Cheirogaleid turbinals and nasolacrimal canal: A, B) *Mirza coquereli* (DPC-1139), in medial (A) and lateral (B) views. Scale bar = 10 mm.

fairly simple ethmoturbinals, *Aotus* and *Alouatta* have ethmoturbinals with more complex cross-sectional morphologies compared with those of other haplorhines (compare Fig. 20 with Figs. 22–23). The nasoturbinal in platyrrhines typically appears as an anterior ridge and extends posteriorly, either remaining as a simple ridge or expanding into a broader lamina in most taxa. The nasolacrimal canals in all platyrrhines are vertical in orientation (Fig. 21).

Unlike the other anthropoids that we examined, *Aotus* exhibits a large accessory pneumatic space that extends posteriorly from the superior portion of the nasal fossa adjacent to the cribriform plate (Fig. 19C). In MCZ 19802 (Fig. 22), this space is mediolaterally compressed, about 10.8 mm in anteroposterior length, and contains the posterior portions of ET II. At its anterior end, the space is floored by a transversely oriented lamina of bone, which in parasagittal cross-section runs obliquely relative to the horizontal plane

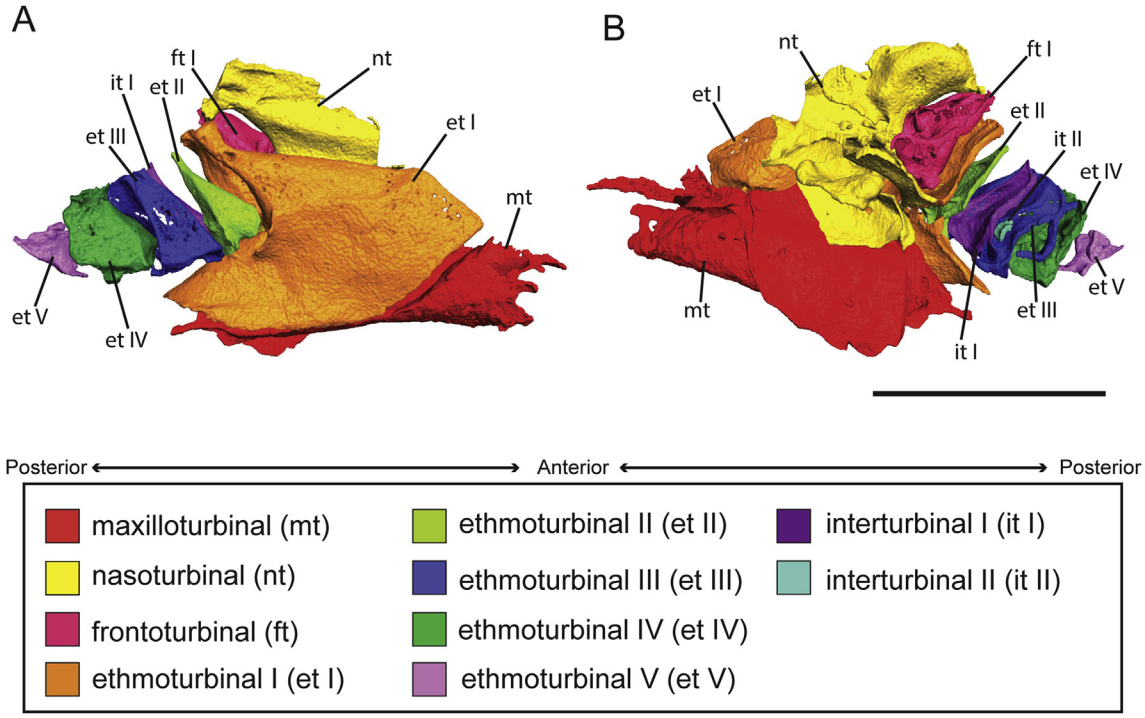

Figure 13. Lepilemurid turbinals: A, B) *Lepilemur mustelinus* (AMNH-M-170568) in medial (A) and lateral (B) views. Nasolacrimal canal is not shown (see Discussion). Scale bar = 10 mm.

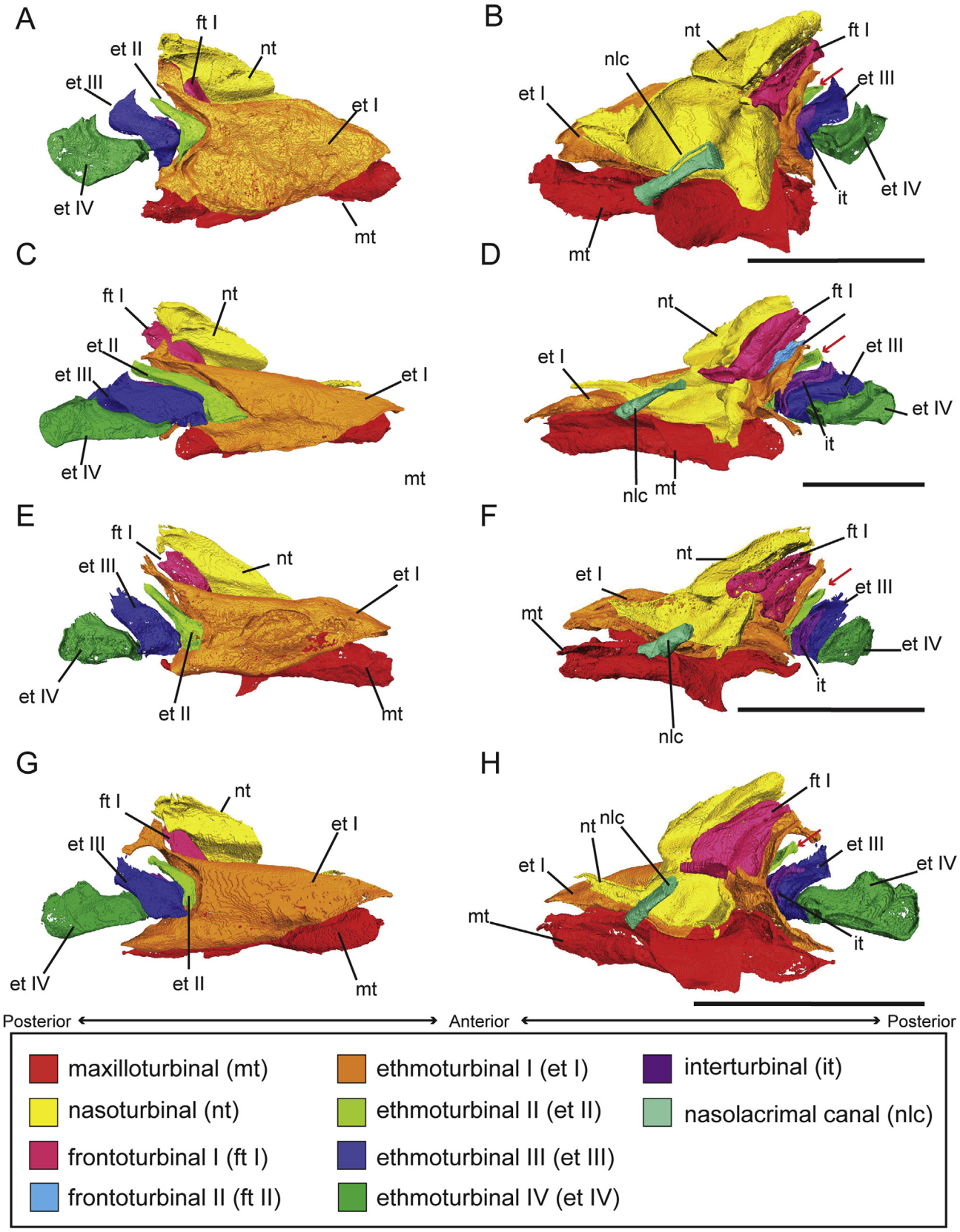

Figure 14. Galagid turbinals and nasolacrimal canals: A, B) *Galago senegalensis* (DPC-007), in medial (A) and lateral (B) views; C, D) *Otolemur crassicaudatus* (DPC-016), in medial (C) and lateral (D) views; E, F) *Euoticus elegantulus* (MCZ-14657), in medial (E) and lateral (F) views; G, H) *Galago moholi* (MCZ-44132) in medial (G) and lateral (H) views. Red arrow points to independent lateral wall contact of ethmoturbinal II. Scale bars = 10 mm.

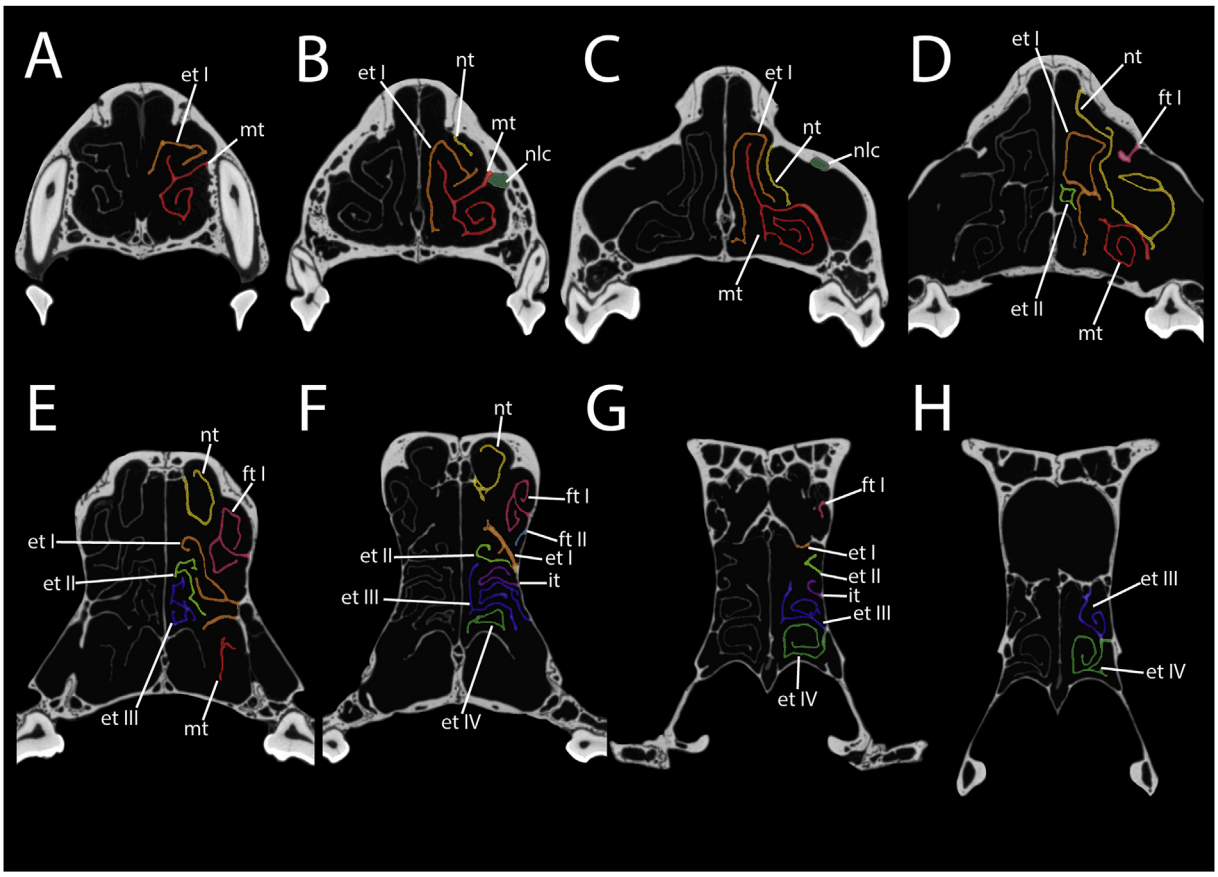

Figure 15. CT scan slices through the nasal fossa of *Otolemur* (DPC-016) showing nasal fossa structures of Lorisiformes: 1612 (A), 1484 (B), 1398 (C), 1278 (D), 1192 (E), 1129 (F), 1069 (G), and 1027 (H) of 1937 total slices. Abbreviations: et I = ethmoturbinal I; et II = ethmoturbinal II; et III = ethmoturbinal III; et IV = ethmoturbinal IV; ft I = frontoturbinal I; ft II = frontoturbinal II; it = interturbinal; mt = maxilloturbinal; nlc = nasolacrimal canal; and nt = nasoturbinal.

(Fig. 19C). Posteriorly the space extends well into the body of the sphenoid bone. Although in some respects this anatomy is superficially similar to the olfactory recesses of non-haplorhine euarchontans, this accessory space in *Aotus* is the product of secondary pneumatization of the much less extensive fetal cupular recess and is best termed a 'cupular sinus' (Rossie, 2006). Although the laminar anterior floor of the cupular sinus in MCZ 19802 is distinct from ET II, comparisons with CT scans of 2 additional *Ao. griseimembra* individuals (USNM 284777 and USNM 291971) demonstrate that this lamina may be continuous with the posterior portion of ET II. Narrow ostia connect the superior portions of the left and right cupular sinuses to the corresponding frontal sinuses (i.e., a 'Type 1' frontal sinus; Rossie, 2006).

Catarrhine primates have a maxilloturbinal, one or two ethmoturbinals, and no nasoturbinal (Table 3; Fig. 24). The ethmoturbinals of catarrhines are not bullar, and in most species the ethmoturbinals are simple laminar or arcuate bony projections from the lateral wall of the nasal fossa. Three catarrhine primates in our sample have two ethmoturbinals (*Procolobus, Mandrillus,* and *Hylobates*), while two catarrhines have one ethmoturbinal (*Miopithecus* and *Presbytis*). *Procolobus* has an ET II that appears only as a small lateral ridge, as in *Callithrix* and *Ateles*. In both *Mandrillus* and *Hylobates*, ET II is a medially projecting simple bony protuberance. *Mandrillus* (Fig. 24E, F) is distinctive among catarrhines in having an ET I that is elongated anteriorly. In most catarrhines, the nasolacrimal canal is a vertical bony canal, arising from the lacrimal on the medial edge of the orbit and extending inferiorly into the nasal fossa where it terminates under the maxilloturbinal. *Mandrillus* is the only exception to this pattern. In this taxon, the nasolacrimal canal is oblique in orientation. The oblique orientation of the nasolacrimal canal in *Mandrillus* differs from that of all other haplorhines examined here, but is very similar that of some strepsirrhines (e.g., *Hapalemur* and *Galago*; Figs. 11C, D and 13).

3.6. Turbinal surface area

Scaling of total olfactory turbinal surface area relative to cranial size is shown in Figure 25. Within both Strepsirrhini and Haplorhini, olfactory turbinal surface area is positively correlated with cranial size, with larger taxa tending to exhibit greater absolute turbinal surface areas. In this sample, the largest olfactory turbinal surface area is exhibited by *Daubentonia* (5516.88 mm^2) while the smallest olfactory turbinal surface area is found in *Callithrix* (60.72 mm^2). Extant strepsirrhines and haplorhines occupy non-overlapping regions of in this plot, with strepsirrhines transposed higher on the y-axis than haplorhines. These data demonstrate that haplorhines have smaller total olfactory turbinal surface area compared with strepsirrhines of comparable cranial size. Among extant haplorhines, nocturnal *Aotus* plots closest to the strepsirrhine distribution. Indeed, the relatively large olfactory turbinal surface area of *Aotus* (418.29 mm^2) is intermediate between that of *Nycticebus* (691.47 mm^2) and the similar-sized platyrrhines *Callicebus* (205.24 mm^2) and *Saimiri* (158.9 mm^2). *Carlito* plots near *Callithrix*, suggesting that extant tarsiiforms and anthropoids have broadly similar relative olfactory turbinal surface areas (Fig. 25). Extant non-primate euarchontans plot near or just above the upper

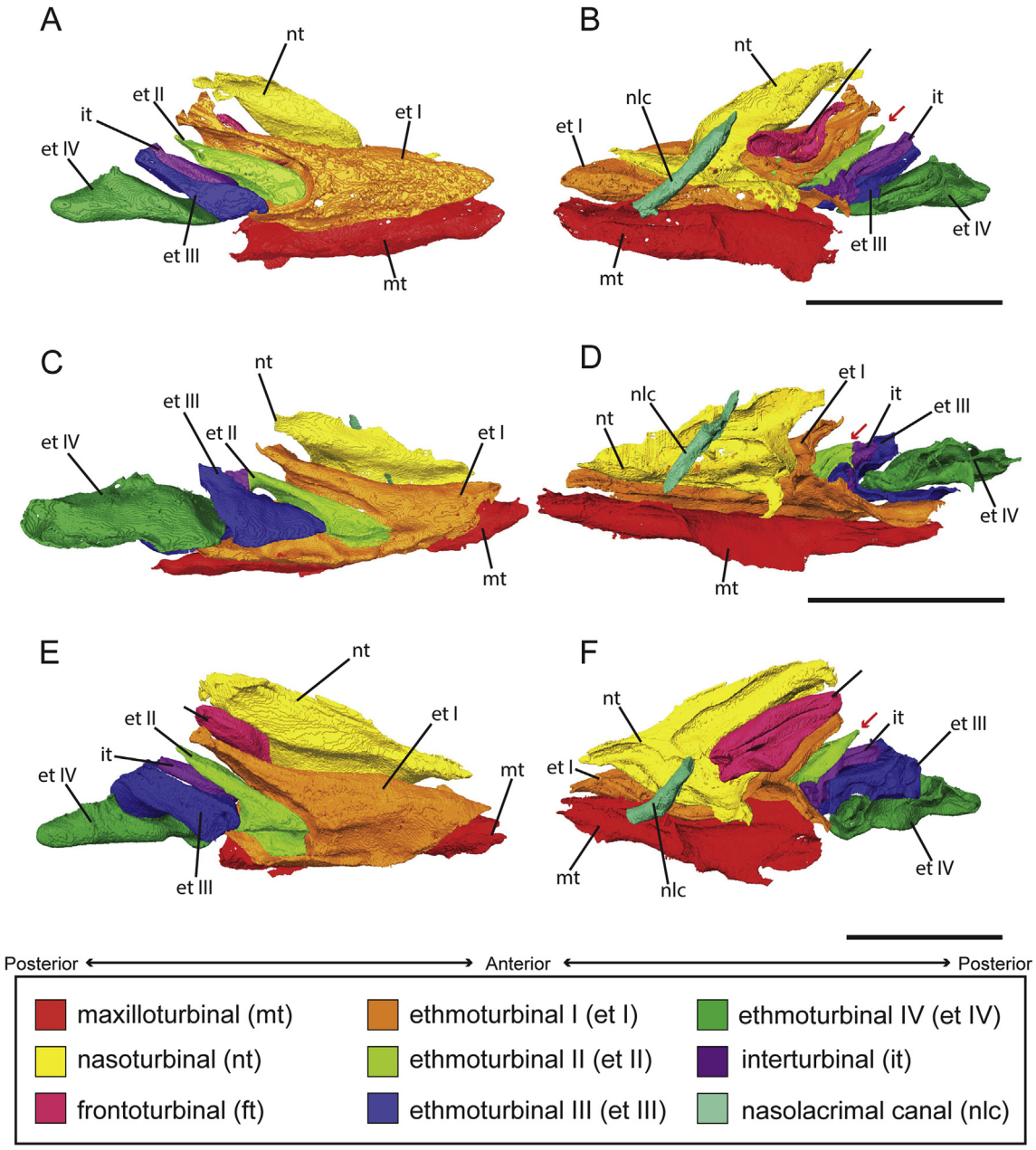

Figure 16. Lorisid turbinals and nasolacrimal canals: A, B) *Nycticebus coucang* (MCZ-BOM-5118), in medial (A) and lateral (B) views; C, D) *Loris tardigradus* (BAA-0006), in medial (C) and lateral (D) views; E, F) *Perodicticus potto* (MCZ-25831), in medial (E) and lateral (F) views. Red arrow points to independent lateral wall contact of ethmoturbinal II. Scale bars = 10 mm.

limit of the strepsirrhine distribution in Figure 25, suggesting that scandentians and dermopterans have larger olfactory turbinal surface areas for their cranial sizes than most extant primates. *Rooneyia* plots in the region between the extant strepsirrhine and haplorhine distributions in close proximity to *Aotus* (Fig. 25). Although *Rooneyia* may be slightly transposed downward on the y-axis due to damage to some olfactory turbinals (see above), the total surface area of the largely intact olfactory turbinals in *Rooneyia*'s right nasal fossa (408.31 mm^2) is substantially smaller than those of the similar-sized strepsirrhines *Lepilemur* (600.46 mm^2), *Nycticebus* (691.47 mm^2), and *Loris* (713.62 mm^2).

Figure 26 shows the relationship between maxilloturbinal surface area and cranial size in the comparative sample examined here. As with olfactory turbinal surface area, maxilloturbinal surface area tends to increase with increasing cranial size, and extant strepsirrhines and haplorhines demonstrate non-overlapping bivariate distributions. The smallest maxilloturbinal surface area is exhibited by *Carlito* (23.77 mm^2) and the largest are found in *Varecia* (2134.4 mm^2) and *Mandrillus* (1267.43 mm^2). At a given cranial size, strepsirrhines tend to have greater maxilloturbinal surface areas than haplorhines, but the magnitude of these differences is somewhat less than that observed for olfactory turbinal surface area (Fig. 25). Accordingly, *Callicebus* (177.97 mm^2) and *Hylobates* (610.63 mm^2) have maxilloturbinal surface areas that are very similar to those of *Nycticebus* (221.74 mm^2) and *Indri* (678.51 mm^2), respectively. When the anterior accessory turbinal of scandentians is included as a separate part of the maxilloturbinal, *Tupaia* and *Ptilocercus*

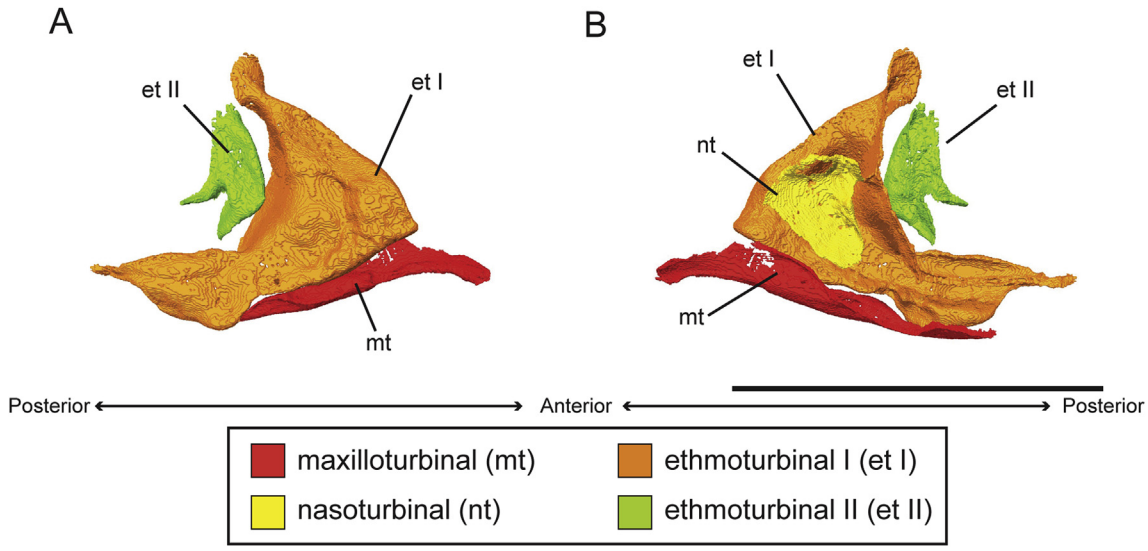

Figure 17. Tarsiiid turbinals: A, B) *Carlito syrichta* (DPC-045), in medial (A) and lateral (B) views. Nasolacrimal canal is too dorsoventrally short to be informative so is not shown (see Discussion). Scale bar = 10 mm.

plot near or just above the upper limit of the strepsirrhine distribution. By comparison, dermopterans plot below the strepsirrhine distribution in the upper limit of the haplorhine polygon. *Rooneyia* (145.42 mm^2) also plots near the upper limit of the haplorhine distribution in close proximity to both *Aotus* and *Callicebus*.

3.7. Ancestral state reconstruction

Figure 27 shows the parsimony-based ancestral state reconstructions and inferred character state changes among euarchontan lineages. The ancestral state reconstructed for crown Primates is 1 nasoturbinal, 4 or 5 ethmoturbinals, 1

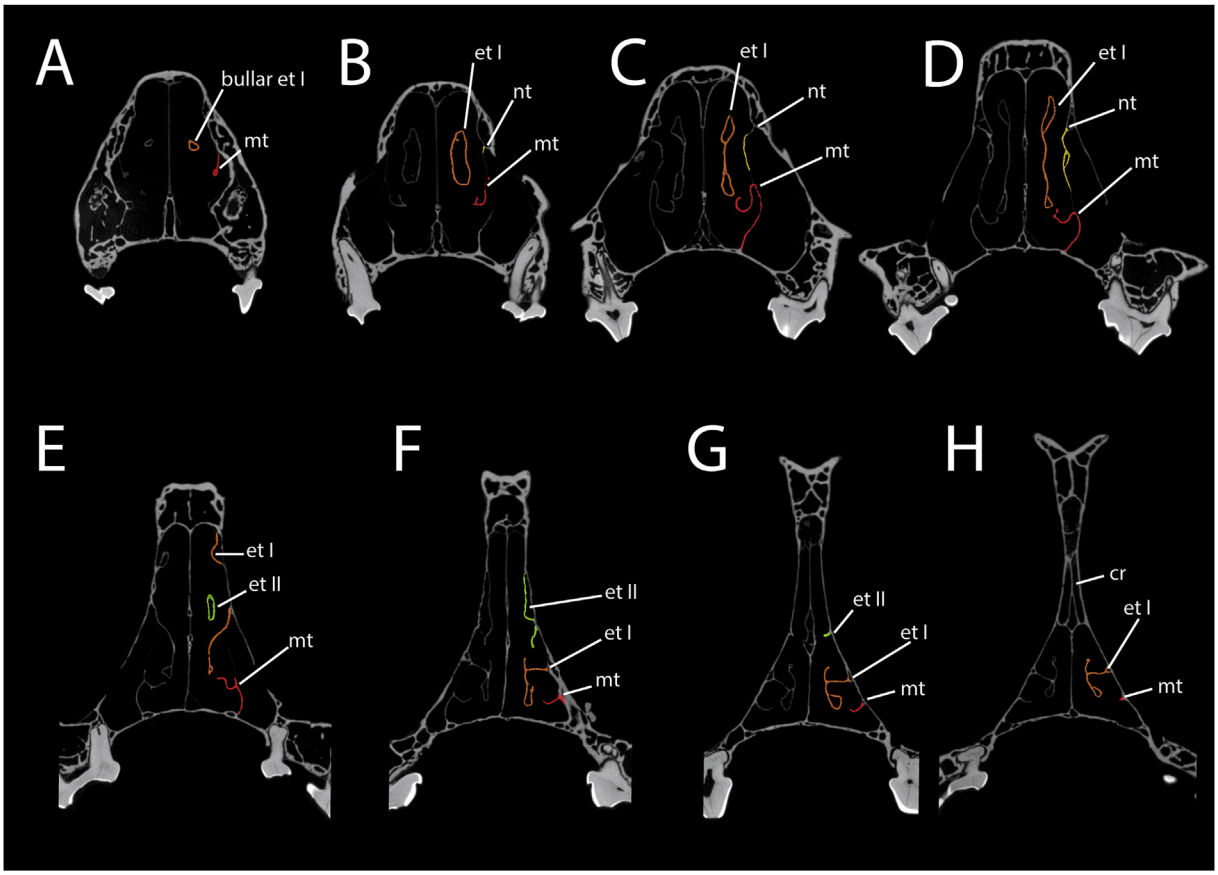

Figure 18. CT scan slices through the nasal fossa of *Carlito* (DPC-045) showing nasal fossa structures of tarsiids: 1598 (A), 1557 (B), 1519 (C), 1461 (D), 1420 (E), 1374 (F), 1333 (G), and 1299 (H) of 1826 total slices. Abbreviations: cr = cupular recess; et I = ethmoturbinal I; et II = ethmoturbinal II; mt = maxilloturbinal; and nt = nasoturbinal.

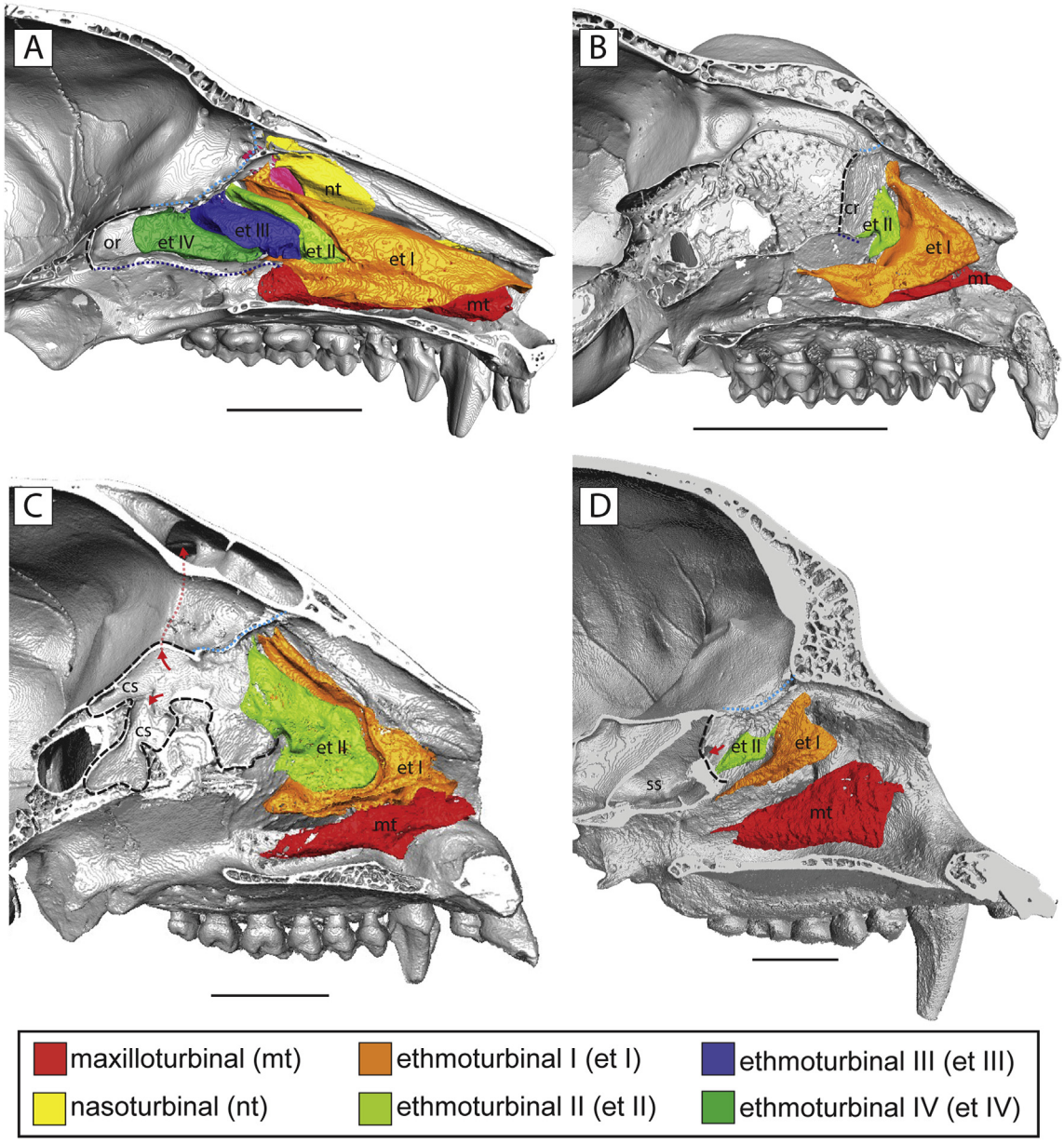

Figure 19. Digitally bisected volume renderings of skulls showing posterior nasal fossa anatomy in *Otolemur* (A), *Carlito* (B), *Aotus* (C), and *Hylobates* (D). The margins of the posterosuperior nasal fossa, cupular recess, and cupular sinus are identified by a dashed black line. The cribriform plate is identified by a light blue dotted line. The transverse bony lamina flooring the olfactory recess (A) or its likely homolog flooring the cupular recess (B) is identified by a dotted dark blue line. Ostia into sinuses are identified by the red arrows. Note the presence of a capacious olfactory recess in strepsirrhines (A), a well-defined cupular recess in tarsiids (B), and an extensive cupular sinus in *Aotus* (C). Abbreviations: cr = cupular recess; cs = cupular sinus; or = olfactory recess; ss = sphenoidal sinus. Scale bars = 10 mm.

interturbinal, and 2 frontoturbinals. This condition is the same as that reconstructed for crown Strepsirrhini. Either 1 frontoturbinal alone, or 1 frontoturbinal and 1 ethmoturbinal, are inferred to have been lost in the lorisiform lineage, depending on whether the crown primate last common ancestor possessed 4 or 5 ethmoturbinals. The ancestral state reconstructed for crown Lorisiformes is accordingly 1 nasoturbinal, 4 ethmoturbinals, 1 interturbinal, and 1 frontoturbinal. The lemuriform clade is more variable, with multiple losses and additions of interturbinals, frontoturbinals, and ethmoturbinals reconstructed along individual lineages (Fig. 27). *Hapalemur* and *Daubentonia* in particular are reconstructed as having substantially increased the number of olfactory turbinals compared to the primitive condition for crown strepsirrhines.

In stem haplorhines, 2 frontoturbinals, 1 interturbinal, and either 2 or 3 ethmoturbinals are reconstructed as having been lost (Fig. 27). The ancestral state reconstruction for crown-haplorhines is therefore 1 nasoturbinal and 2 ethmoturbinals. The bullar shape of the ethmoturbinals is lost in stem anthropoids, and the nasoturbinal is lost in stem catarrhines. The loss or addition of 1 ethmoturbinal seems to have occurred multiple times independently within crown Anthropoidea (Fig. 27).

4. Discussion

Prior authors have supported widely divergent hypotheses regarding the phylogenetic affinities of *Rooneyia* (Wilson, 1966; Szalay and Wilson, 1976; Kay et al., 2004b). Only two points of

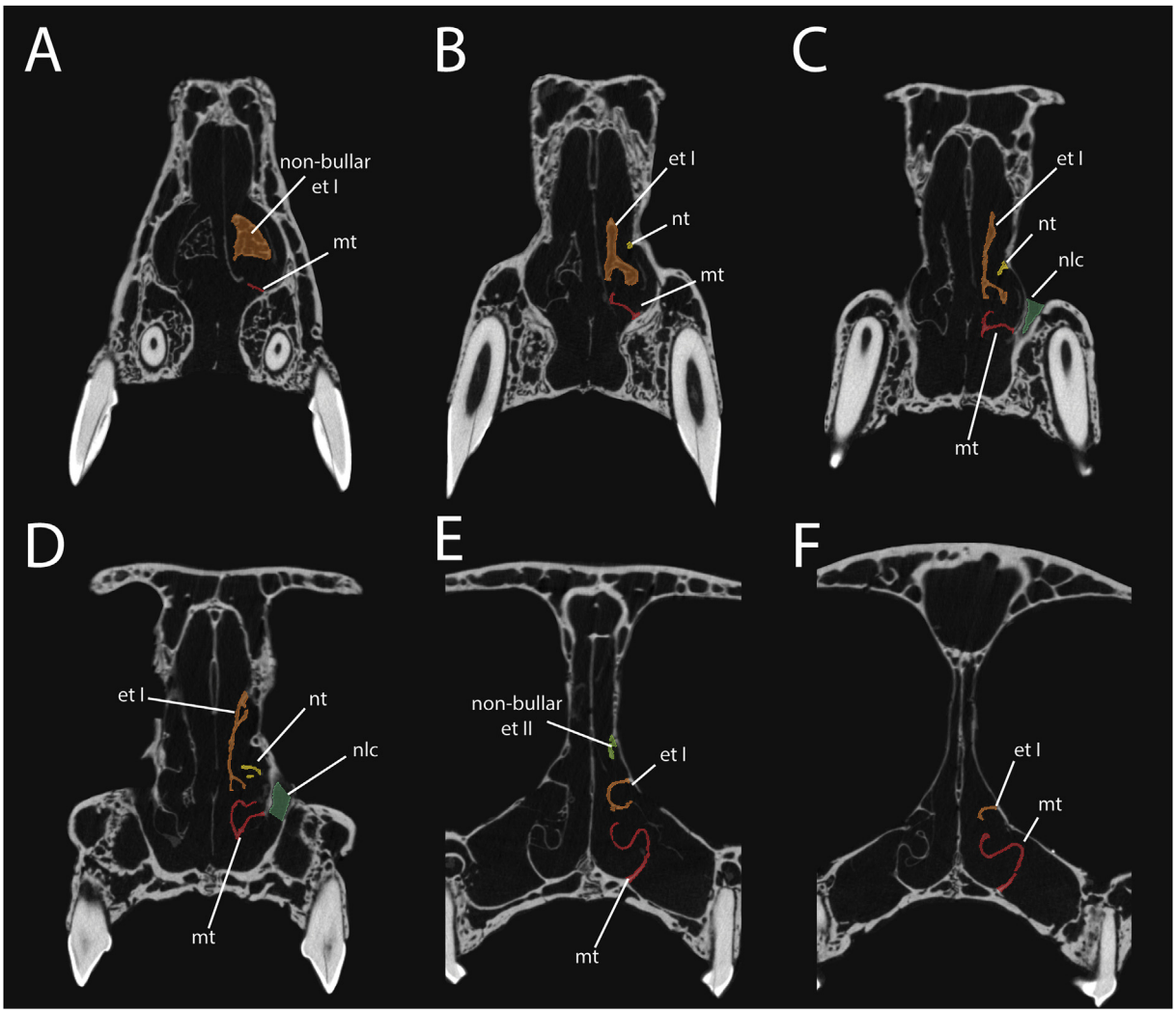

Figure 20. CT scan slices through the nasal fossa of *Callithrix* (MCZ-30582) showing nasal fossa structures: 986 (A), 960 (B), 945 (C), 926 (D), 893 (E), and 857 (F) out of 1106 total slices. Abbreviations: et I = ethmoturbinal I; et II = ethmoturbinal II; mt = maxilloturbinal; nlc = nasolacrimal canal; and nt = nasoturbinal.

consensus have emerged from the recent literature on this subject: (1) that *Rooneyia* is more closely related to crown primates than to dermopterans or scandentians; and (2) that *Rooneyia* is not a crown strepsirrhine. Given this diversity of viewpoints, a clear understanding of the morphological variation and character changes within extant Euarchonta is required to properly evaluate the phylogenetic implications of the nasal cavity morphology observed here for *Rooneyia*. Early comparative research on mammalian nasal cavity morphology emphasized the fact that some primate species exhibit reduced nasal fossa complexity compared with non-primate mammals (Paulli, 1900a; Dieulafé, 1906; Elliot Smith, 1927; Negus, 1956; Le Gros Clark, 1959). More recent anatomical studies have better clarified the interspecific variation in bony nasal cavity morphology in extant Mammalia (Maier, 1980, 2000; Van Valkenburgh et al., 2004, 2014a; Smith et al., 2007b,c, 2013, 2015, 2016; Smith and Rossie, 2008; Green et al., 2012; Eiting et al., 2014a; Maier and Ruf, 2014; Ruf, 2014; Ruf et al., 2015; Yee et al., 2016). As a group, these studies suggest that while haplorhine primates are indeed characterized by derived reductions in nasal cavity complexity, most strepsirrhine primates have nasal cavities that are largely plesiomorphic in their bony anatomy. Our observations here further reinforce these conclusions, and document additional variation within the major euarchontan clades.

4.1. Euarchonta, Primatomorpha, and Primates

Our findings support prior observations (e.g., Loo and Kanagasuntheram, 1971; Loo, 1973) that strepsirrhine primates and non-primate euarchontans share numerous anatomical features of the nasal cavity. Indeed, living scandentians, dermopterans, and strepsirrhines have complex nasal fossae with a maxilloturbinal, a nasoturbinal, and 4 or more ethmoturbinals. Most species possess at least one interturbinal and at least one frontoturbinal, and the ethmoturbinals typically have a bullar morphology. Furthermore, all scandentians, dermopterans, and strepsirrhines have an olfactory recess that contains the posterior-most olfactory turbinals, is roofed by the cribriform plate, and is separated from the nasopharyngeal meatus by a transverse bony lamina. The olfactory turbinals of these taxa are also anchored directly to the cribriform plate at their posterior margins. Most of the scandentians, dermopterans, and strepsirrhines we examined also possess a horizontally- or obliquely-oriented nasolacrimal canal.

Among taxa examined here, ethmoturbinal numbers are more variable within Strepsirrhini than they are within either Scandentia or Dermoptera. All of the lorisiforms and many of the lemuriforms that we examined exhibit 4 ethmoturbinals (Loo and Kanagasuntheram, 1971; Cave, 1973; Smith and Rossie, 2006), but

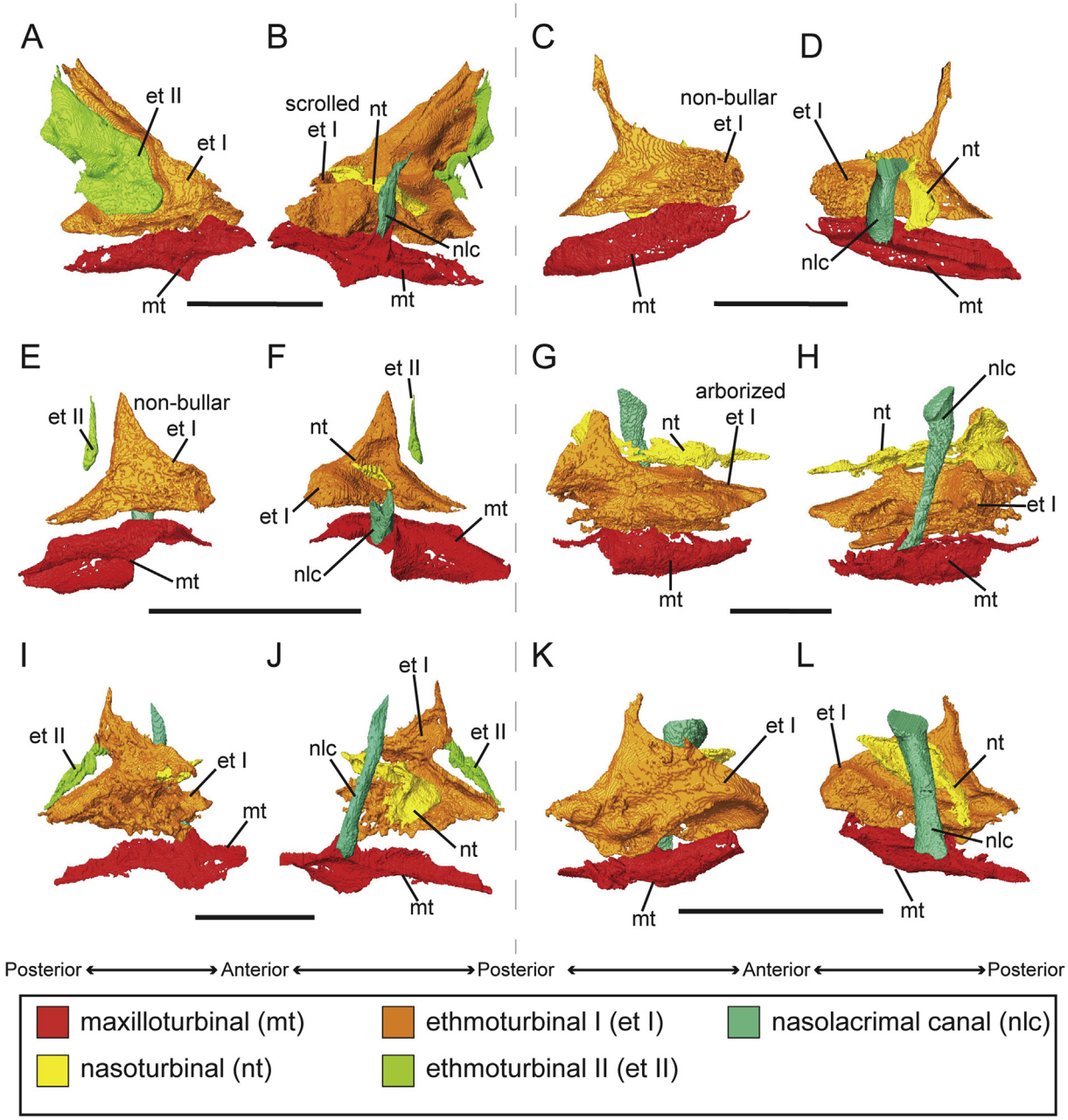

Figure 21. Platyrrhine turbinals and nasolacrimal canals: A, B) *Aotus trivirgatus* (MCZ-19802), in medial (A) and lateral (B) views; C, D) *Callicebus discolor* (MCZ-26922), in medial (C) and lateral (D) views; E, F) *Callithrix jacchus* (MCZ-30582) in medial (E) and lateral (F) views; G, H) *Alouatta palliata* (MCZ-BOM-5329) in medial (G) and lateral (H) views; I, J) *Ateles geoffroyi* (MCZ-BOM-5336), in medial (I) and lateral (J) views; K, L) *Saimiri oerstedii* (MCZ-10131) in medial (K) and lateral (L) views. Scale bars = 10 mm.

four lemuriform taxa (*Avahi*, *Hapalemur*, *Indri*, and *Lepilemur*) possess 5 ethmoturbinals (Table 3). By comparison, the scandentians *Tupaia* and *Ptilocercus* have 4 ethmoturbinals (Wible, 2011; Ruf et al., 2015) and the dermopterans *Cynocephalus* and *Galeopterus* have 5 ethmoturbinals (Table 3). Using parsimony as the criterion for ancestral state reconstruction, it is not possible to determine whether 4 or 5 ethmoturbinals represents the most probable ancestral condition for crown Primates (Fig. 27).

Tupaia belangeri was unique among scandentians in having 2 interturbinals, a condition shared with some lemuriform strepsirrhines. Scandentians, dermopterans, and all lemuriforms examined here except *Lepilemur* have an interturbinal positioned between the horizontal lamina and ET III. This condition has been noted previously in *Tupaia*, *Ptilocercus*, and lagomorphs[5] (Ruf, 2014; Ruf et al., 2015)[5]. These observations suggest that the presence of an interturbinal between the horizontal lamina and ET III may be plesiomorphic for crown Euarchonta, crown Primatomorpha, and crown Primates.

Our observations of 2 frontoturbinals in *Tupaia* and *Ptilocercus* agree with previous studies of scandentian turbinal morphology (Le Gros Clark, 1926; Ruf, 2014; Ruf et al., 2015). Dermopterans and many strepsirrhines also exhibit 2 frontoturbinals, suggesting that

[5] Both of these studies refer to ET III as ET II and do not distinguish between ETs I and II (Ruf, 2014; Ruf et al., 2015).

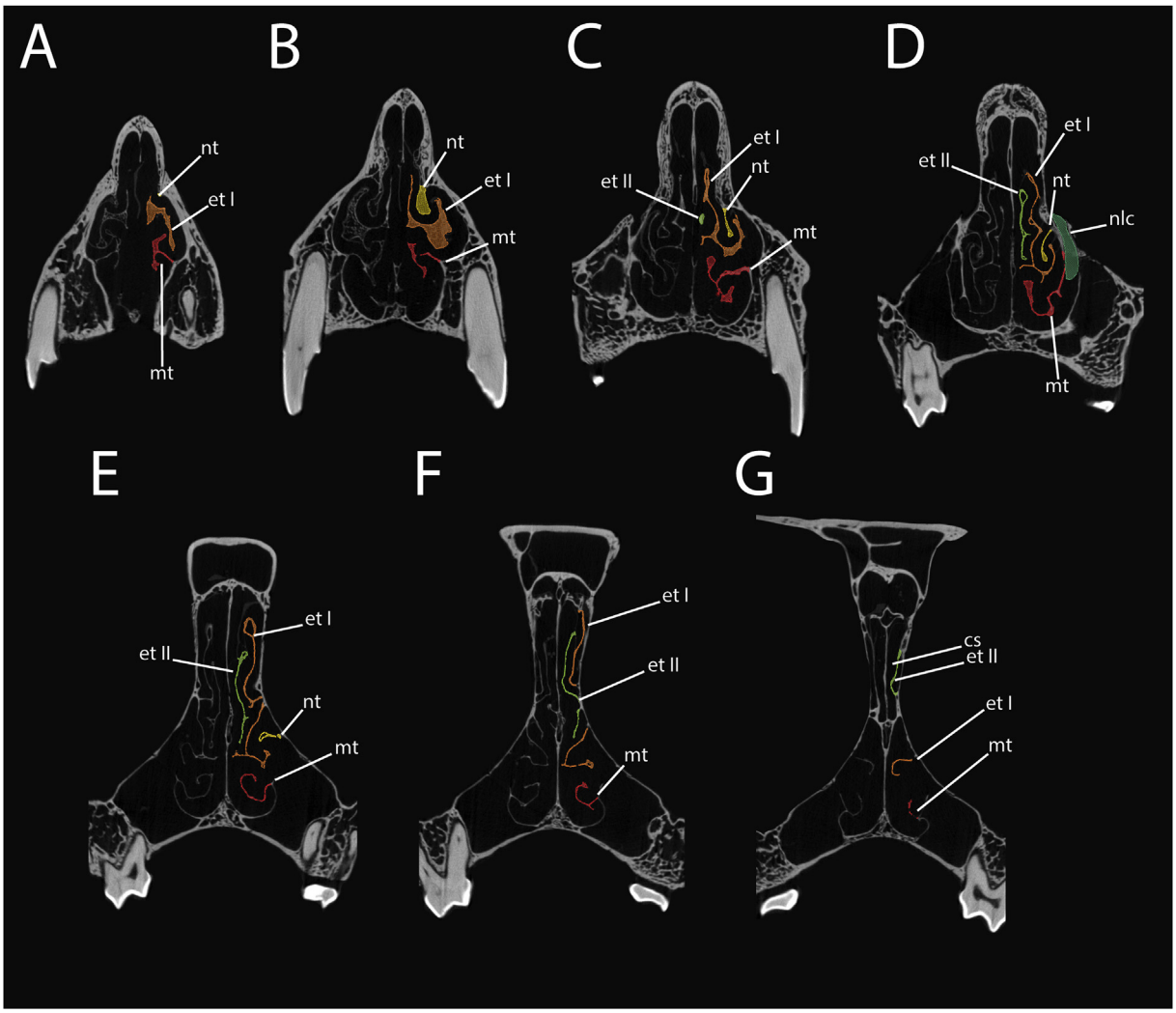

Figure 22. CT scan slices through the nasal fossa of *Aotus* showing nasal fossa structures: 1322 (A), 1286 (B), 1256 (C), 1229 (D), 1173 (E), 1134 (F), and 1100 (G) of 1506 total slices. Abbreviations: cs = cupular sinus; et I = ethmoturbinal I; et II = ethmoturbinal II; mt = maxilloturbinal; nlc = nasolacrimal canal; and nt = nasoturbinal.

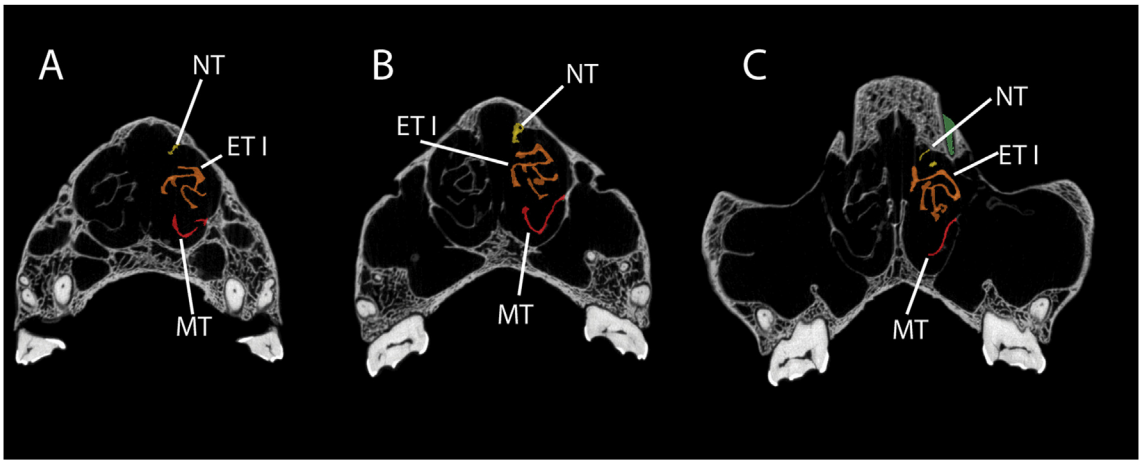

Figure 23. CT scan slices through the nasal fossa of *Alouatta* showing nasal fossa structures: 1095 (A), 1067 (B), and 983 (C) of 1413 total slices. Abbreviations: et I = ethmoturbinal I; mt = maxilloturbinal; nlc = nasolacrimal canal; and nt = nasoturbinal.

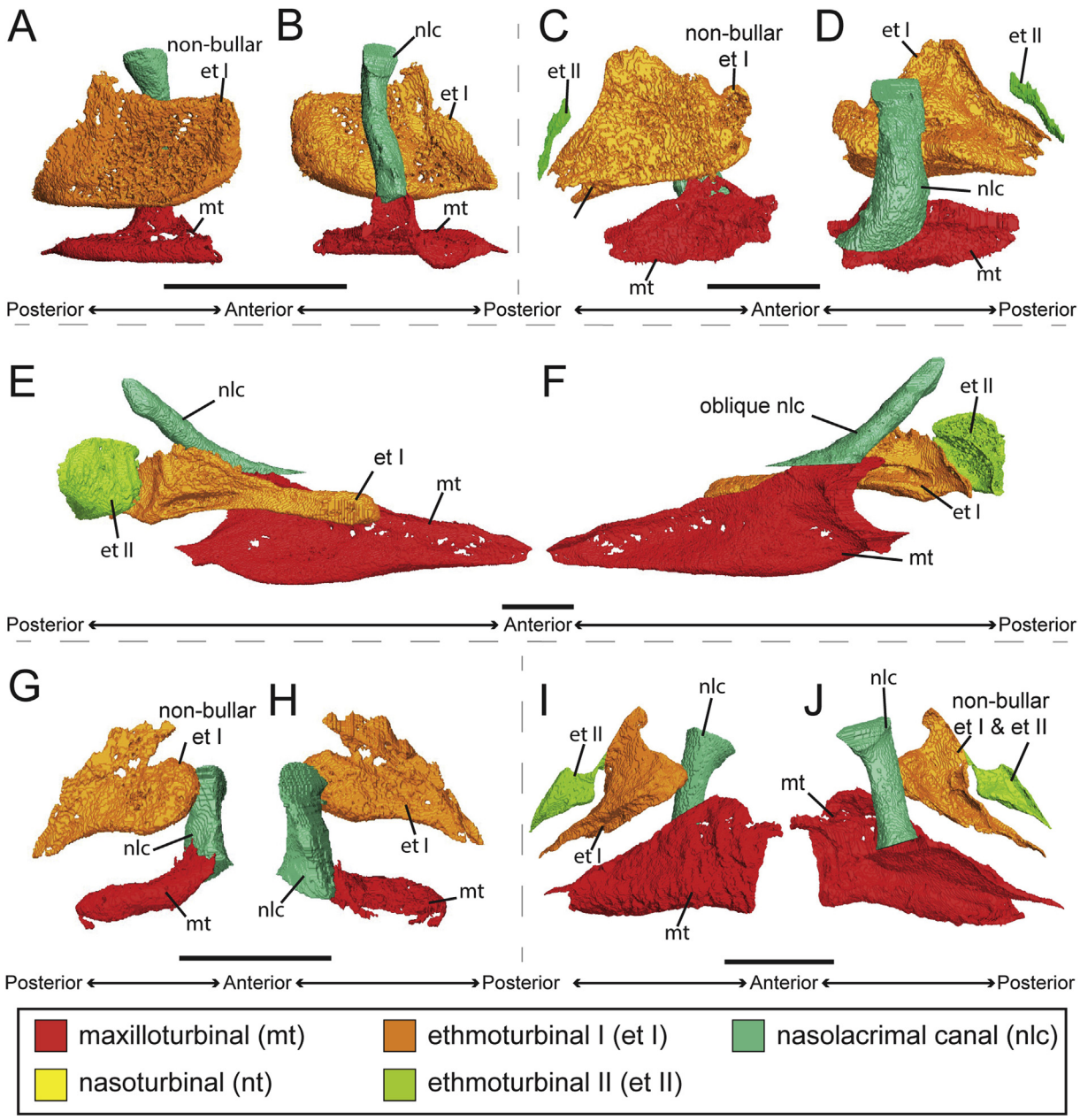

Figure 24. Catarrhine turbinals and nasolacrimal canals: A, B) *Miopithecus talapoin* (MCZ-23196), in medial (A) and lateral (B) views; C, D) *Procolobus badius* (MCZ-24080), in medial (C) and lateral (D) views; E, F) *Mandrillus leucophaeus* (MCZ-19986) in medial (E) and lateral (F) views; G, H), *Presbytis hosei* (MCZ-37371), in medial (G) and lateral (H) view; I, J) *Hylobates lar* (MCZ-41463), in medial (I) and lateral (J) views. Scale bars = 10 mm.

this condition may be plesiomorphic for crown Euarchonta, crown Primatomorpha, and crown Primates. Nevertheless, the number of frontoturbinals is variable within Strepsirrhini, and homoplastic losses and additions of frontoturbinals must have occurred in multiple strepsirrhine lineages (Fig. 27).

Despite the fact that scandentians are broadly similar to strepsirrhines in the total number of olfactory turbinals, scandentians typically have larger olfactory turbinal surface areas than strepsirrhines of similar skull size (Fig. 25). By comparison, dermopterans are more similar to strepsirrhines in relative olfactory turbinal surface area. Taken at face value, these results may indicate that a modest reduction in olfactory turbinal cross-sectional complexity occurred in the primatomorphan stem lineage. This presumptive decrease in the surface area of the bony substrate available to support OE could be linked to reduced numbers of functional olfactory receptor genes in primatomorphans (Mason et al., 2016; Niimura et al., 2018).

Notably, none of the strepsirrhines or dermopterans that we examined exhibit a structure resembling the anterior accessory turbinal associated with the maxilloturbinal in scandentians. Similarly, strepsirrhines and scandentians lack the reductions in maxilloturbinal cross-sectional size that make dermopterans resemble haplorhines in relative maxilloturbinal surface area (Fig. 26). In light of these comparative observations, the anterior accessory turbinal of scandentians and the reduced size and complexity of the dermopteran maxilloturbinal are both best interpreted as clade-specific autapomorphies.

With the exception of *Daubentonia* (see below), all of the strepsirrhines and non-primate euarchontans that we examined have horizontal or oblique nasolacrimal canals. This finding

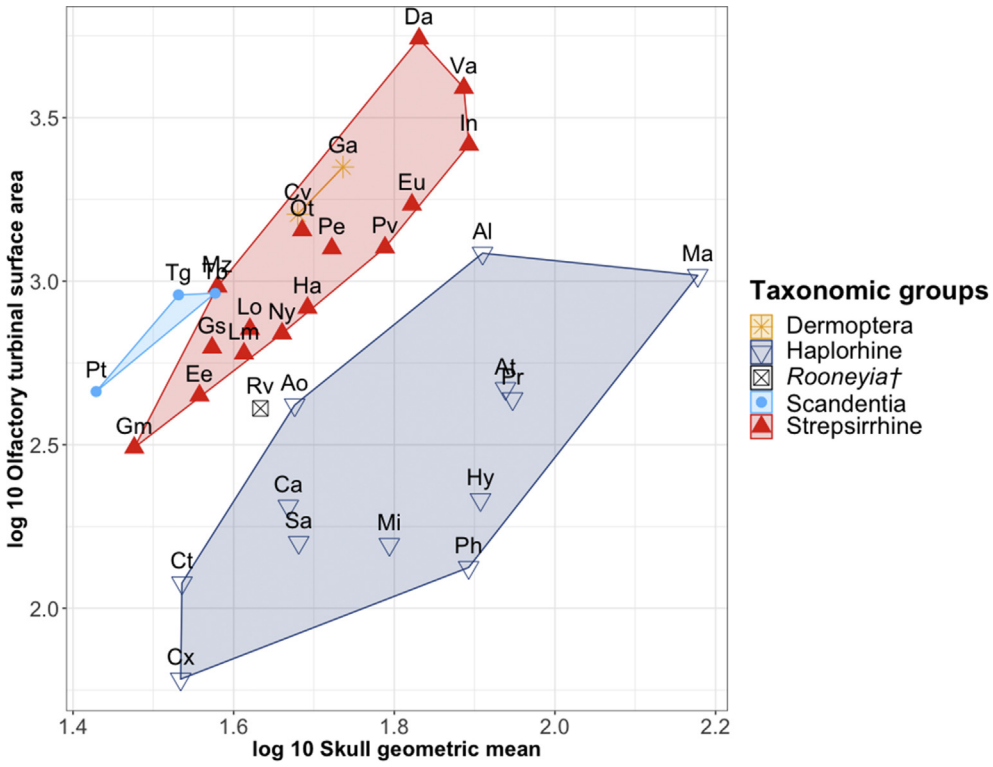

Figure 25. Biplot showing log-transformed olfactory turbinal surface area and log-transformed skull geometric mean. Taxon abbreviations: Al = *Alouatta*; Ao = *Aotus*; At = *Ateles*; Ca = *Callicebus*; Ct = *Carlito*; Cx = *Callithrix*; Cv = *Cynocephalus*; Da = *Daubentonia*; Ee = *Euoticus*; Eu = *Eulemur*; Gm = *Galago moholi*; Gs = *Galago senegalensis*; Ga = *Galeopterus*; Ha = *Hapalemur*; Hy = *Hylobates*; In = *Indri*; Lm = *Lepilemur*; Lo = *Loris*; Ma = *Mandrillus*; Mz = *Mirza*; Mi = *Miopithecus*; Ny = *Nycticebus*; Ot = *Otolemur*; Pe = *Perodicticus*; Ph = *Presbytis*; Pr = *Procolobus*; Pv = *Propithecus*; Pt = *Ptilocercus*; Rv = *Roonyeia*; Sa = *Saimiri*; Tb = *Tupaia belangeri*; Tg = *Tupaia glis*; and Va = *Varecia*.

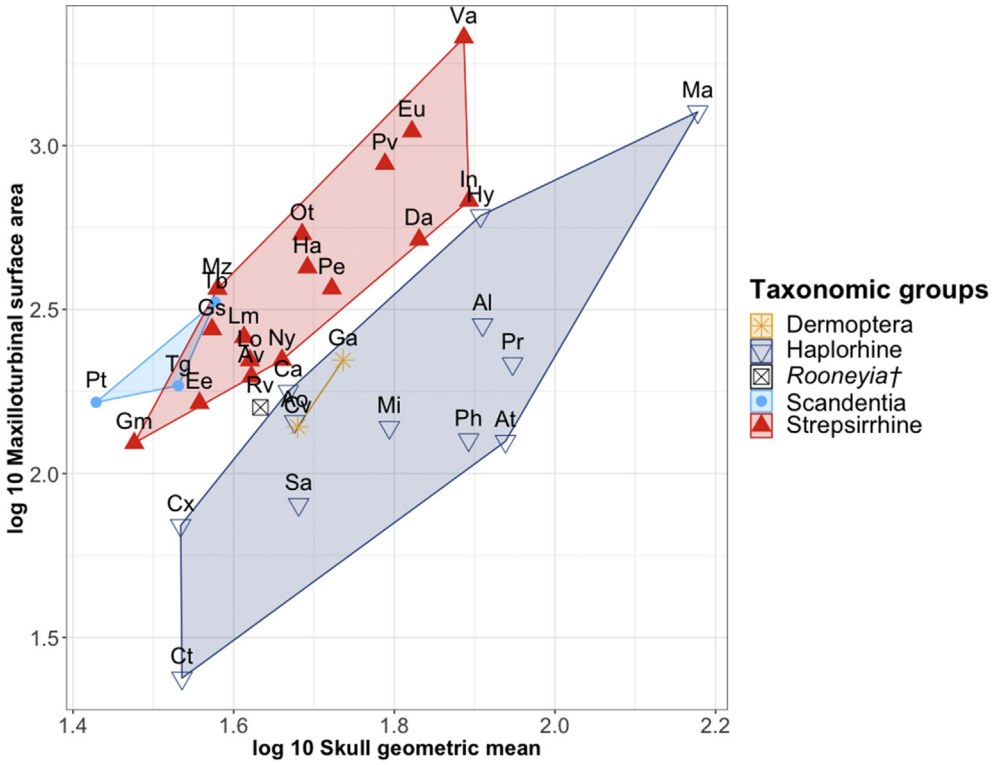

Figure 26. Biplot showing log-transformed maxilloturbinal surface area and log-transformed skull geometric mean. Taxon abbreviations: Av = *Avahi*; other abbreviations as in Figure 25.

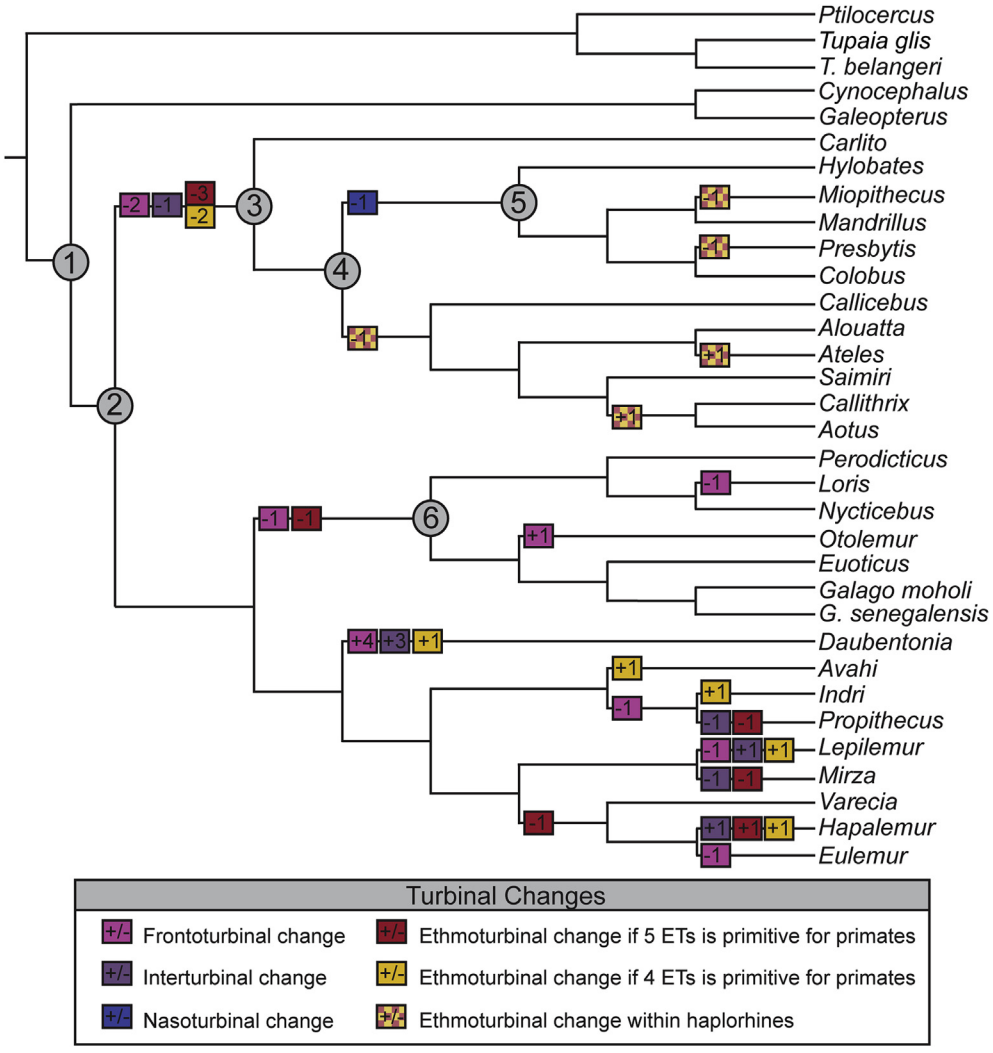

Figure 27. Molecular phylogeny of examined euarchontans from Perelman et al. (2011) and Mason et al. (2016). Gray circles show most parsimonious ancestral state condition at different euarchontan nodes: 1) crown-Primatomorpha: 1 nasoturbinal (NT), 4–5 ethmoturbinals (ET), 1 interturbinal (IT), 2 frontoturbinals (FT), horizontal nasolacrimal canal (NLC); 2) crown-Primates: 1 NT, 4–5 ETs, 1 IT, 2 FT, horizontal NLC; 3) crown-haplorhine: 1 NT, 2 ET, vertical NLC; 4) crown-anthropoids: 1 NT, 2 non-bullar ET, vertical NLC; 5) crown-catarrhines: 2 non-bullar ET, vertical NLC; 6) crown-lorisiforms: 1 NT, 4 ET, 1 IT, 1 FT; most parsimonious turbinal changes are shown in colored boxes; yellow boxes show changes in ethmoturbinal number if Scandentia represents the primitive condition for Primates; red boxes show changes in ethmoturbinal number if Dermoptera represents the primitive condition for Primates.

corroborates previous research on nasolacrimal canal orientation in primates (Rossie and Smith, 2007; Rossie et al., 2018). While the nasolacrimal canals of scandentians and dermopterans are horizontally oriented, the nasolacrimal canals of strepsirrhines tend to be more obliquely oriented. Despite these differences, the non-vertical orientation of the nasolacrimal canal in scandentians, dermopterans, and strepsirrhines is likely a plesiomorphic functional attribute of the accessory olfactory system, in which lachrymal fluid is transported by the nasolacrimal duct to irrigate the rhinarium and enhance odorant transport to the vomeronasal organ (Rossie and Smith, 2007). The posteriorly doubled nasolacrimal canals seen in *Tupaia* are unlike the condition seen in *Ptilocercus*, Dermoptera, and most strepsirrhine primates. The sole exception to this generalization was observed in a single specimen of *G. senegalensis* that possessed a unilaterally doubled orbital inlet to the nasolacrimal canal. It is currently unclear whether the doubled nasolacrimal canal inlet of *Tu. glis* and *Tu. belangeri* in our sample is a synapomorphy of tupaiid scandentians or the product of intraspecific variation.

These findings suggest that most living strepsirrhines retain nasal cavity morphologies that are generally plesiomorphic with respect to the last common ancestor of crown primates. The presence of a capacious olfactory recess lodging the posterior olfactory turbinals is almost certainly plesiomorphic for Primates. However, the precise numbers of olfactory turbinals are more difficult to ascertain based on the distribution of character states among extant euarchontan taxa. Previous studies have suggested that the last common ancestor of crown primates probably had 4 ethmoturbinals (Smith et al., 2007c; Kirk et al., 2014), but the current study indicates that it is equally parsimonious to conclude that 5 ethmoturbinals is plesiomorphic for crown primates (Fig. 27). Our parsimony analysis further suggests that the last common ancestor of crown primates had a nasal fossa with 1 nasoturbinal, 1 interturbinal, and 2 frontoturbinals, as in extant non-primate euarchontans (Fig. 27). Finally, the nasolacrimal canal in both non-primate euarchontans and strepsirrhines was either horizontal or oblique in orientation, suggesting that a non-vertical orientation of the nasolacrimal canal is primitive for crown primates.

4.2. Extant Strepsirrhini

While there are broad similarities in turbinal numbers across strepsirrhines, the present study also documents substantial interspecific variation in turbinal numbers within this clade (Table 3). The presence of a single nasoturbinal is constant among the strepsirrhines that we examined, but the numbers of ethmoturbinals, interturbinals and frontoturbinals are all variable between species. Although interturbinal variation (0–2) and frontoturbinal variation (0–6) have not been examined broadly across taxa within the same study, the morphology observed for each species here (Table 3) largely corroborates previous analyses that have examined closely related taxa (Cave, 1973; Smith et al., 2005, 2007c, 2011, 2014b, 2016; DeLeon et al., 2014; Eiting et al., 2014a).

Within Strepsirrhini, a salient difference in ET II basal lamina morphology and interturbinal position is observed between lemuriforms and lorisiforms. While non-primate euarchontans and lemuriforms (with the exception of *Lepilemur*) have an interturbinal located between the shared basal lamina of ET I/II (i.e., the horizontal lamina) and the basal lamina of ET III, none of the lorisiforms exhibit this configuration and instead have an interturbinal between ET II and ET III. The prevalence of this condition among lorisiforms suggests that it may be derived for the clade. This morphological difference in interturbinal location between lemuriforms and lorisiforms may reflect a change in the relationship between ET II and the horizontal lamina. In non-primate euarchontans and lemuriforms, ET II originates from ET I and/or the horizontal lamina and does not contact the lateral wall of the nasal fossa directly. Thus, the interturbinal, which sits lateral to the ethmoturbinals, is positioned between the horizontal lamina and ET III. In most lorisiforms, ET II contacts the lateral wall of the nasal fossa directly rather than via the horizontal lamina, so the interturbinal sits between the basal laminae of ET II and ET III. The anatomy of *Loris* is unique in having an interturbinal positioned between ET II and ET III like other lorisiforms, but in having contact between ET II and the horizontal lamina as in lemuriforms. The reason for this presumably derived morphology in most lorisiforms is unclear but could theoretically be related to the presence of large and convergent orbits in the last common ancestor of crown lorisiforms. In other words, if the breadth of the nasal cavity is mediolaterally restricted due to the presence of convergent and enlarged orbits, it may be more likely for ET II to develop an independent connection to the lateral wall of the nasal cavity. Similarly, reductions in the size and complexity of the haplorhine nasal fossa may be functionally linked to increases in orbit size and convergence (Cartmill, 1970; Smith et al., 2014b). If so, then strepsirrhines with substantially enlarged and convergent orbits might be expected to be subject to similar spatial constraints. Indeed, *Loris* has extremely large and convergent orbits (Cartmill, 1974; Kirk, 2006; Heesy, 2009) and exhibits a complete loss of one group of olfactory turbinals, the frontoturbinals.

Within lemuriforms, there is substantial variation in olfactory turbinal number, size, and morphology. While some of the lemuriform taxa examined here like *Eulemur* and *Indri* have four ethmoturbinals, others like *Hapalemur* and *Lepilemur* have five ethmoturbinals and additional interturbinals and frontoturbinals. The most parsimonious condition for crown lemuriforms is the same as in crown primates: 1 nasoturbinal, 4 or 5 ethmoturbinals, 1 interturbinal, and 2 frontoturbinals. Within lemuriforms, parsimony favors at least four changes in ethmoturbinal numbers, five changes in interturbinal number, and four changes in frontoturbinal number (Fig. 27). However, it is also important to note that most species in this analysis are represented by a single individual, and that turbinal numbers may be variable within species. For example, among the lemurids in our sample, we observed 4 ethmoturbinals in *Eulemur* and *Varecia* and 5 ethmoturbinals in *Hapalemur* (Table 3). These observations contrast with a previous developmental study of lemurids that noted the presence of only 4 ethmoturbinals in *Hapalemur* (Smith et al., 2016).[6] This same study reported the presence of ET V in one perinatal *Lemur catta*, while adults of the same species had 4 ethmoturbinals (Smith et al., 2016). This variation suggests that while 4 ethmoturbinals commonly occur in multiple lemurid species, the fifth ethmoturbinal may be more intraspecifically variable than other turbinals.

Among living strepsirrhines, *Daubentonia* stands out as having uniquely derived nasal fossa morphology (Figs. 7 and 8; Maier and Ruf, 2014). In terms of total turbinal numbers, *Daubentonia* has more distinct olfactory turbinals ($n = 15$) than any other strepsirrhine ($n = 6–10$; Table 3). It is particularly notable that *Daubentonia* has 6 frontoturbinals and 4 interturbinals,[7] while no other strepsirrhine has more than 2 of either turbinal type. This increase in turbinal number, combined with the greater cross-sectional complexity of ET I (see above), is probably responsible for the fact that *Daubentonia* has the greatest absolute and relative olfactory turbinal surface area of any taxon in our sample (Fig. 25). If we are correct in our assumption that a larger olfactory turbinal surface area reflects a greater total surface area of OE in the nasal cavity, then this morphology would be consistent with aye-ayes having highly acute and/or sensitive olfactory abilities compared to other primates. Such a conclusion is further supported by the fact that *Daubentonia* has the largest olfactory bulb (685 mm^3) recorded for any living primate (Stephan et al., 1981), which in turn presumably indicates the presence of larger or more numerous olfactory bulb glomeruli and an expansion of the functional olfactory gene repertoire (Kirk, 2018a). Enhanced olfactory abilities may be tied to the unique foraging strategies of aye-ayes, which depend on olfactory, auditory, and tactile cues to detect and recover hidden food items (Erickson et al., 1998).

Daubentonia is also unique among the taxa examined here in having a maxilloturbinal with a sigmoidal lateral profile and a vertically oriented midsection, and in having most posterior olfactory turbinals stacked in a nearly vertical array (Fig. 7A). Similarly, *Daubentonia* is the only known non-haplorhine euarchontan that exhibits a vertically-oriented nasolacrimal canal (Fig. 7B, C; see Rossie and Smith, 2007; Rossie et al., 2018). All of these features are plausibly linked to the derived suite of cranial features that characterize aye-ayes, including a shortened rostrum, marked klinorhynchy, and hypselodont incisors (Cartmill, 1974). These observations indicate that although reorganization of the cranium had a major impact on nasal fossa morphology in *Daubentonia*, shortening of the rostrum was achieved concurrently with an expansion in both olfactory turbinal number and olfactory turbinal surface area. Furthermore, *Daubentonia* indicates that having a vertically-oriented nasolacrimal canal is not always associated with the absence of the rhinarium in primates.

While most euarchontans have fully-enclosed, bony nasolacrimal canals (Rossie and Beard, 2004; Rossie and Smith, 2007), observations of multiple specimens reveal that *Lepilemur* is unique

[6] Smith et al. (2016) used comparable ethmoturbinal definitions to those used here.

[7] Maier and Ruf (2014) also observed comparable morphology in *Daubentonia* but were inconsistent in their application of the terms 'frontoturbinal' and 'interturbinal'.

among our sample in possessing an unossified nasolacrimal canal. These *Lepilemur* specimens exhibit a lacrimal foramen in the orbit, which leads to a shallow groove on the inner surface of the maxilla that presumably contained the nasolacrimal duct. This finding suggests that the absence of a bony nasolacrimal canal does not necessarily indicate the absence of a nasolacrimal duct and rhinarium.

4.3. Extant Haplorhini

Our results support prior conclusions that multiple bony structures of the nasal fossa were lost in the haplorhine stem lineage (Negus, 1956; Maier, 1980; Smith and Rossie, 2006). The extant haplorhines in our sample lack interturbinals and frontoturbinals entirely, and no species has more than 2 ethmoturbinals. *Carlito* retains a small simple nasoturbinal (Smith and Rossie, 2006), and the nasoturbinal in platyrrhines is further reduced to a ridge or small lamina. No nasoturbinals were observed in catarrhines, suggesting that this structure was retained in the crown anthropoid last common ancestor but was lost in catarrhines (Fig. 27). Accordingly, if the last common ancestor of crown primates had a nasal fossa with 4 or 5 ethmoturbinals, 1 interturbinal, 2 frontoturbinals, and 1 nasoturbinal (Fig. 27), then crown Haplorhini are characterized by a derived loss of either 5 or 6 olfactory turbinals. This precipitous reduction in olfactory turbinal number partly explains the fact that living haplorhines exhibit much smaller olfactory turbinal surface areas than non-haplorhine euarchontans of similar cranial size (Fig. 25). Maxilloturbinal surface area is also smaller in haplorhines compared with strepsirrhines of similar cranial size (Fig. 26). The function of this reduction in maxilloturbinal surface area is not clear, but could be developmentally linked to the observed reductions in olfactory turbinal surface area if common genetic mechanisms influence turbinal size and morphology more generally.

Our observation that the haplorhines in our sample have either 1 or 2 ethmoturbinals agrees with other studies that have examined ethmoturbinal numbers in these taxa (Cave, 1967; Maier, 1980; Rossie, 2006; Smith and Rossie, 2006; Smith et al., 2007c), although ET III has been noted in some platyrrhine species (Cave, 1967). While *Carlito* retains the primitive bullar shape of the ethmoturbinals (Figs. 17 and 18), no anthropoids have this morphology (Figs. 20–24), suggesting that bullar ethmoturbinal morphology was lost in stem anthropoids (Fig. 27). Haplorhines except *Aotus* are also distinctive in having ethmoturbinals that do not directly contact the cribriform plate of the ethmoid. By comparison, in scandentians, dermopterans, and strepsirrhines, the posterior margin of each ethmoturbinal is directly anchored to the cribriform plate. Because the ethmoturbinals are covered to varying degrees by OE (Smith and Bhatnagar, 2004; Smith et al., 2007b; Van Valkenburgh et al., 2014b), ethmoturbinal-cribriform plate contact in non-haplorhine euarchontans presumably provides a direct route for olfactory receptor neuron axons to reach the olfactory foramina and pass into the olfactory bulb. The possible functional implications of this loss of direct contact between the ethmoturbinals and cribriform plate in haplorhines are unclear, although it seems possible that lack of contact could be the byproduct of reductions in olfactory turbinal surface area (Fig. 25).

These reductions in olfactory turbinal number and the loss of contact between the ethmoturbinals and cribriform plate may relate to the fact that haplorhines lack an olfactory recess (Rossie, 2005, 2006; Smith and Rossie, 2006). In strepsirrhines, dermopterans, and scandentians, ET III–V occur partly or entirely within the olfactory recess, while in extant haplorhines these ethmoturbinals and an olfactory recess are both absent. Similarly, the cribriform plate of non-haplorhine euarchontans forms the roof of the olfactory recess, so the contacts between the ethmoturbinals and cribriform plate are primarily contained within the olfactory recess. In most living haplorhines, the cribriform plate forms the posterosuperior roof of the nasal fossa proper and is spatially removed from the remaining olfactory turbinals. These changes represent a fundamental reorganization of the nasal cavity in crown haplorhines, which differ from other mammals in lacking a substantial portion of the nasal cavity that is sequestered from the main airway to increase the residence time of odorant molecules (Craven et al., 2010; Eiting et al., 2014a,b).

Nevertheless, our comparative observations support the conclusions of Rossie, Smith, and colleagues (Rossie, 2006; Smith and Rossie, 2006; Smith et al., 2007c, 2014a, 2014b) that some living haplorhines retain a vestigial remnant of the olfactory recess. Such cupular recesses have been documented in a variety of fetal and adult platyrrhines, and may be lined with OE (Rossie, 2006; Smith and Rossie, 2006; Smith et al., 2007c, 2014a, 2014b). Like the olfactory recesses of non-haplorhine euarchontans, cupular recesses develop from the posterior-most primary pneumatic space of the fetal nasal capsule without additional (i.e., secondary) pneumatization (Rossie, 2006; Smith and Rossie, 2006). However, cupular recesses in haplorhines may be distinguished from the olfactory recesses of strepsirrhines, dermopterans, and scandentians by their small size, by the fact that they do not contain olfactory turbinals, and by the lack of a transverse bony lamina separating the cupular recess from the nasopharyngeal meatus (Smith and Rossie, 2006; Smith et al., 2014a,b). Here we note the presence of a small but well-defined cupular recess in two tarsier genera: *Carlito* and *Cephalopachus*. As in platyrrhines that retain a cupular recess, the cupular recesses of tarsiers are small, roofed by the cribriform plate, and do not contain olfactory turbinals (Fig. 19). The tarsier cupular recess is also floored by a very short, horizontally oriented bony lamina that is presumably homologous with the much larger transverse bony lamina that forms the floor of the olfactory recess in non-haplorhine euarchontans. These comparative observations are consistent with the hypothesis that a capacious olfactory recess containing the posterior ethmoturbinals is plesiomorphic for both Euarchonta and Primates, but that only a tiny remnant of this structure (i.e., a cupular recess) was retained in the last common ancestor of Haplorhini.

Aotus is unique among the extant haplorhines in our sample in possessing a large cupular sinus that is broadly confluent with the posterosuperior nasal fossa and occupies a position analogous to that of the strepsirrhine olfactory recess (Fig. 19). Rossie (2006) has shown that similar sinuses are present in a variety of platyrrhine taxa and are formed via secondary pneumatization of the recessus cupularis during development. Accordingly, the cupular sinuses seen in some platyrrhines are not homologous with the olfactory recesses of non-haplorhine euarchontans. It is also currently unclear to what extent cupular sinuses may play a role in olfaction. Some role for olfaction in *Aotus* is suggested by the fact that (1) the cribriform plate forms the anterior roof of the cupular sinus and (2) the cupular sinus contains the posterior portion of ET II, as well as the point of direct contact between ET II and the cribriform plate. Nevertheless, the cupular sinus of *Aotus* is mediolaterally much narrower than the olfactory recesses of non-haplorhine euarchontans, and is largely devoid of ethmoturbinals. These factors indicate that the area of OE in the cupular sinus of *Aotus* is probably much less than that in the olfactory recesses of a similar-sized strepsirrhine (e.g., *Nycticebus* and *Otolemur*).

The fact that *Aotus* has one of the largest relative eye sizes of any living primate (Kirk, 2006) indicates that having very large and medially approximated eyes is not incompatible with also possessing extensive (though mediolaterally compressed) pneumatic spaces in the interorbital region (Cartmill, 1974). This conclusion is

reinforced by the presence of a well-defined cupular recess in tarsiers, which also exhibit greatly enlarged eyes relative to head size (Kirk, 2006). Although approximation of the eyes and orbits may constrain the volumes of primary and secondary pneumatic spaces in the interorbital region (Cartmill, 1970; Maier, 1993, 2000; Rossie, 2006; Smith and Rossie, 2008; Smith et al., 2014a,b), the anatomy observed here for *Aotus*, *Carlito*, and *Cephalopachus* indicates the potential for pneumatic spaces containing OE to persist in species with very large eyes and high degrees of orbital convergence, frontation, and approximation (Cartmill, 1974; Ross, 1994; Kirk, 2006). In the case of *Aotus*, it is intriguing to note that a taxon with a relatively large olfactory turbinal surface area compared to other haplorhines also possesses a large secondary pneumatic space that is broadly confluent with the posterosuperior nasal cavity and forms the substrate for an unknown amount of OE.

In addition to *Aotus*, several other anthropoid taxa appear to have independently evolved increased olfactory turbinal surface areas, which may indicate an increased surface area of OE (Pihlström, 2012; Bird et al., 2014). *Alouatta* lacks ET II, but nevertheless resembles *Aotus* in possessing one of the largest olfactory turbinal surface areas relative to head size of any living haplorhine (Fig. 25). In *Alouatta*, this increase in olfactory turbinal surface area appears to have been achieved partly through an increase in turbinal cross-sectional complexity. The nasoturbinal of *Alouatta* is not laminar or ridge-like as in other platyrrhines, but instead has an arborized cross-section and is widened posteriorly. ET I in *Alouatta* is also arborized, with major branches extending both inferiorly and superiorly (Fig. 23). *Ateles* also exhibits small branches extending from ET I, suggesting that this feature might be shared among atelids. However, *Ateles* has a total olfactory turbinal surface area that is much smaller than that of *Alouatta* (Fig. 25).

Mandrillus[8] has the largest absolute olfactory turbinal surface area among anthropoids, and exhibits both an unusually elongate ET I and a relatively large ET II (Fig. 24E). *Mandrillus* is also unique among the haplorhines we examined in having an obliquely orientated nasolacrimal canal rather than a vertical nasolacrimal canal as in all other haplorhines (Fig. 24; Rossie and Smith, 2007; Tabuce et al., 2009; Rossie et al., 2018). It is not clear at present whether this derived orientation is the result of derived elongation of the rostrum in *Mandrillus*, but such a link is plausible since the only known strepsirrhine with a vertical nasolacrimal canal (*Daubentonia*) also possesses a foreshortened rostrum (Cartmill, 1974). Both observations may indicate that nasolacrimal canal orientation in primates could be influenced by selection acting on facial architecture. Moreover, just as the presence of a vertical nasolacrimal canal in *Daubentonia* does not indicate the absence of a rhinarium, our findings for *Mandrillus* indicate that an obliquely oriented nasolacrimal canal is not always associated with the presence of a rhinarium in primates.

The observed distribution of character states in Euarchonta suggests that a fundamental reorganization of nasal cavity morphology occurred in the stem haplorhine lineage (Negus, 1958; Cave, 1973; Rossie, 2005; Smith et al., 2014b). This change in haplorhine nasal bauplan includes the loss of numerous olfactory turbinals, reductions in turbinal cross-sectional complexity, and corresponding decreases in turbinal surface area (Figs. 25 and 26). Although the last common ancestor of living haplorhines may have possessed a small cupular recess like those of extant tarsiers, it almost certainly lacked a large and complex olfactory recess like those of living scandentians, dermopterans, and strepsirrhines. While it is always theoretically possible that the many derived features of nasal cavity morphology shared by tarsiers and anthropoids evolved in parallel, the close resemblance in nasal cavity morphology between tarsiers like *Carlito* (Fig. 17) and small platyrrhines like *Callithrix* (Fig. 20E, F) is striking. In this context, it is worth emphasizing that the degree of nasal cavity reduction observed for haplorhines is highly unusual among mammals generally, with cetaceans perhaps being the only major mammalian clade to exhibit greater reductions in olfactory structures (Pihlström, 2012; Van Valkenburgh et al., 2014b). Functionally, reductions in olfactory turbinal number, size, and complexity lead haplorhines to have nasal cavities with much smaller areas of OE compared with strepsirrhines (Smith et al., 2007c, 2014a; Maier and Ruf, 2014). Such reductions in the size of the OE provide a diminished mucosal surface area in which volatile odorants can bind with olfactory receptor neurons and initiate a transduction cascade. This anatomy in turn may cause haplorhines to have reduced olfactory sensitivity compared with strepsirrhines (Pihlström, 2012).

4.4. *Implications for* Rooneyia

Perhaps the most salient feature of the nasal cavity in *Rooneyia* is its persistently primitive morphology. With 4 ethmoturbinals, a large nasoturbinal, 1 interturbinal, and 1 frontoturbinal in each nasal fossa, *Rooneyia* does not differ substantially from the condition inferred for the last common ancestors of Euarchonta, Primatomorpha, and Primates. The only likely reductions in turbinal number in *Rooneyia* are the loss of 1 frontoturbinal and, if the presence of 5 ethmoturbinals is primitive for Primates, the loss of ET V. Accordingly, in total olfactory turbinal count, *Rooneyia* is identical to *Eulemur collaris* and most living lorisiforms (Table 3). *Rooneyia* further resembles extant strepsirrhines and the inferred ancestral condition for Primates in having bullar ethmoturbinals that directly contact the cribriform plate and are partly contained within a capacious olfactory recess. *Rooneyia* notably lacks any of the derived features of the nasal cavity that characterize crown haplorhines.

In total olfactory turbinal surface area, *Rooneyia* differs from both extant strepsirrhines and haplorhines in possessing intermediate values relative to cranial size (Fig. 25). *Rooneyia* thus has an olfactory turbinal surface area that is smaller than similar-sized strepsirrhines *Lepilemur* and *Loris*, but larger than similar-sized haplorhines like *Callicebus* and *Saguinus*. In this regard, *Rooneyia* is perhaps most similar to *Aotus*, which demonstrates secondary increases in the size and complexity of olfactory structures compared with other anthropoids. It is also possible that *Rooneyia*'s position in Figure 25 is the result of underestimation of turbinal surface areas due to breakage. However, these findings are consistent with those of Kirk et al. (2014), who reported that *Rooneyia* is also intermediate between extant strepsirrhines and haplorhines in terms of olfactory bulb size relative to brain size. These data suggest that *Rooneyia* may exhibit derived modest reductions in both olfactory turbinal surface area and relative olfactory bulb size. *Rooneyia* also exhibits relatively small values for maxilloturbinal surface area (Fig. 26), but we are less confident in this result due to possible breakage of the anterior and posterior margins of the maxilloturbinal in *Rooneyia*'s left nasal fossa (Fig. 2).

The largely primitive morphology of *Rooneyia*'s nasal cavity is most consistent with three possible phylogenetic scenarios—that *Rooneyia* is either an advanced stem primate, a stem strepsirrhine (Kay et al., 2004b), or a stem haplorhine (Ross, 1994; Ross et al., 1998). However, the notable absence of any of the various nasal synapomorphies shared by living tarsiers and anthropoids provides further evidence that *Rooneyia* is not a crown haplorhine (Kirk

[8] The only specimen of *Mandrillus* that we examined is an adult male (Table 2), so the potential influence of sexual dimorphism on our observations is currently unknown (Singleton, 2013).

et al., 2014). In order for *Rooneyia* to be either a stem tarsiiform (Szalay and Delson, 1979; Seiffert et al., 2010; Ni et al., 2013, 2016) or stem anthropoid (Rosenberger, 2006; Rosenberger et al., 2008), tarsiers and anthropoids would have to have lost in parallel their olfactory recess, interturbinal, frontoturbinals, and all but 2 ethmoturbinals. Alternatively, *Rooneyia* would have to have regained all of these structures after their loss in the haplorhine stem lineage. While both of the latter scenarios are certainly possible, we regard them as less plausible than the more parsimonious possibility that *Rooneyia* is not a crown haplorhine. This conclusion is further reinforced by the fact that *Rooneyia* lacks other crown haplorhine synapomorphies, such as a postorbital septum with zygomatic-alisphenoid contact and subdivision of the middle ear space to form an anterior accessory cavity and a perbullar course for the internal carotid artery (MacPhee and Cartmill, 1986; Ross, 1994; Kirk et al., 2014). Given the large number of phylogenetic analyses favoring haplorhine affinities for *Rooneyia* (Ross, 1994; Ross et al., 1998; Seiffert et al., 2010; Ni et al., 2013, 2016), we believe the hypothesis that *Rooneyia* is a stem haplorhine is the best supported by the currently available evidence.

The anatomy of *Rooneyia*'s nasal cavity further suggests that this taxon resembled living strepsirrhines and many other mammals in relying on olfactory cues to meet a variety of socioecological needs (Charles-Dominique, 1977; Bolen and Green, 1997; Bicca-Marques and Garber, 2004; Nekaris, 2005; Barton, 2006). Although *Rooneyia* probably had a somewhat diminished area of OE compared to the primitive condition for crown primates, the observable features of its main olfactory system favor the conclusion that *Rooneyia* nevertheless possessed a keen sense of smell, perhaps most comparable to extant taxa like *Aotus* and *Lepilemur* (Fig. 25). Furthermore, the nasolacrimal canal in *Rooneyia* is similar in its oblique orientation to the nasolacrimal canals seen in extant strepsirrhines, suggesting the presence of a rhinarium irrigated by the nasolacrimal duct (Rossie and Smith, 2007; Rossie et al., 2018). *Rooneyia* also exhibits a vomeronasal groove, which in vivo houses the cartilage encapsulating the vomeronasal organ (Garrett, 2015). In combination the nasolacrimal canal orientation and the vomeronasal groove indicate that *Rooneyia* likely had a functional accessory olfactory system as in extant strepsirrhines, tarsiers, and platyrrhines. Therefore, the presence of a functional accessory olfactory organ in *Rooneyia* suggests that olfactory sociosexual cues may have been important in the behavioral repertoire of this taxon, as in many extant strepsirrhines (Scordato and Drea, 2007; Delbarco-Trillo et al., 2011; Sacha et al., 2012).

5. Conclusions

Our analysis of nasal cavity morphology in living euarchontans suggests that crown strepsirrhines exhibit nasal cavities that are not fundamentally different from those of the last common ancestors of Euarchonta, Primatomorpha, and Primates. Within Strepsirrhini, there is nevertheless substantial variation in the numbers of frontoturbinals and interturbinals, with a considerable expansion in olfactory turbinal number and surface area evident in *Daubentonia*. Haplorhines, by contrast, are characterized by a suite of derived nasal features, including (1) loss of 5–6 olfactory turbinals, (2) loss of direct contact between the ethmoturbinals and cribriform plate, (3) loss of a capacious olfactory recess containing the posterior olfactory turbinals, (4) a precipitous reduction in the relative olfactory turbinal surface area that in vivo supports olfactory epithelium, (5) a reduction of maxilloturbinal surface area, and (6) reorientation of the nasolacrimal canal. Although several extant haplorhines appear to have independently evolved character states that superfically resemble the ancestral condition for primates (e.g., direct contact between the ethmoturbinals and cribriform plate in *Aotus* and an obliquely oriented nasolacrimal canal in *Mandrillus*), this nasal fossa morphology was likely present in the last common ancestor of crown Haplorhini. Subsequent to this radical change in haplorhine nasal fossa bauplan, bullar ethmoturbinal morphology was evidently lost in the anthropoid stem lineage and nasoturbinals were lost in the catarrhine stem lineage.

High resolution μCT scans of *R. viejaensis* demonstrate that this late middle Eocene primate had a nasal fossa with 4 ethmoturbinals, 1 nasoturbinal, 1 interturbinal, 1 frontoturbinal, and an obliquely oriented nasolacrimal canal. This anatomy is very similar to that inferred for the last common ancestor of primates, although *Rooneyia* appears to have lost 1 frontoturbinal and to have modestly reduced the total surface area of its olfactory turbinals. *Rooneyia* lacks the fundamental reorganization of the nasal cavity shared by all living haplorhines, and is therefore unlikely to have been a stem tarsiiform (Szalay and Delson, 1979; Seiffert et al., 2010; Ni et al., 2013, 2016) or stem anthropoid (Rosenberger, 2006; Rosenberger et al., 2008). If we are correct in our conclusion that *Rooneyia* is a stem haplorhine (Ross, 1994; Ross et al., 1998), then this taxon may provide a window into the sensory ecology of the haplorhine stem lineage prior to the evolution of the greatly enhanced visual functionality and diminished olfactory functionality that characterizes crown members of the lineage (Kirk, 2018a,b; Kirk and Kay, 2004; Ross and Kirk, 2007; Williams et al., 2010). Based on its optic foramen quotient, *Rooneyia* did not exhibit the very high visual acuity that is the sensory hallmark of diurnal anthropoids, but may have had higher visual acuity than living strepsirrhines and nocturnal haplorhines (Kirk and Kay, 2004; Veilleux and Kirk, 2014). Similarly, with a total olfactory turbinal surface area and an olfactory bulb volume that are both intermediate between extant haplorhines and strepsirrhines (Kirk et al., 2014), *Rooneyia*'s olfactory sensitivity and/or ability to discriminate between odorants may have been greater than most living haplorhines but somewhat diminished compared to living strepsirrhines. If these phylogenetic and functional inferences are correct, then *Rooneyia* may document an important early step in the sensory evolution of Haplorhini. Some stem haplorhines like *Rooneyia* may have exhibited only modest reductions in olfaction and enhancements in vision compared to the living representatives of this lineage. The shifts inferred for *Rooneyia*'s sensory ecology could therefore anticipate additional changes in more derived haplorhines due to persistent selection for increased visual acuity and relaxed selection on the main olfactory system. Given the mosaic or stepwise nature of many macroevolutionary processes (Carroll, 2008), it is to be expected that some stem haplorhines would exhibit character states that are intermediate between the inferred ancestral condition for primates and the derived condition observed in extant Haplorhini.

Acknowledgments

We thank David Alba, James Rossie, Addison Kemp, Amy Atwater, Liza Shapiro, two anonymous reviewers, and an associate editor at the Journal of Human Evolution for providing feedback on an earlier version of this manuscript. We also thank Matt Colbert, Rich Ketcham, Jessie Maisano, and the staff of the UT High-Resolution X-ray Computed Tomography Facility for assistance with CT scanning. We are indebted to Doug Boyer and the many colleagues at Duke University who have worked to maintain Morphosource.org. We also thank Kari Allen, Eric Delson, Doug Boyer, Lynn Copes, Eva Garrett, Rich Kay, and Lynn Lucas for making data available on Morphosource. The MCZ specimen data used here was supported by NSF (#DDIG-0925793) and a Wenner-Gren Dissertation Grant (#8102; both to L. Copes). AMNH and USNM comparative data used here was supported by NSF (#BCS-1552848 and #BCS-1304045; both to D.M. Boyer), AMNH, and NYCEP grants

(to E. Delson). Duke Division of Fossil Primates specimens scanning was supported by Leakey foundation (#181951) and NSF (#BCS-1232534; to K. Allen and R. Kay). Matt Brown, Chris Sagebiel, and the staff of the Jackson School Museum of Earth History provided assistance with access to the *Rooneyia* holotype. Finally, we are grateful for the late John A. Wilson for his discovery and initial description of the *Rooneyia* holotype.

Supplementary Online Material

Supplementary online material to this article can be found online at https://doi.org/10.1016/j.jhevol.2019.04.009.

References

Adipietro, K.A., Mainland, J.D., Matsunami, H., 2012. Functional evolution of mammalian odorant receptors. PLoS Genetics 8, e1002821.
Allen, H., 1882. On a revision of the ethmoid bone in Mammalia, with special reference to the description of this bone in and of the sense of smell in Chiroptera. Bulletin of the Museum of Comparative Zoology, Harvard 10, 135–164.
Baron, G., Frahm, H.D., Bhatnagar, K.P., Stephan, H., 1983. Comparison of brain structure volumes in insectivora and primates. III. Main olfactory bulb (MOB). Journal für Hirnforschung 24, 551–568.
Barton, R.A., Purvis, A., Harvey, P.H., 1995. Evolutionary radiation of visual and olfactory brain systems in primates, bats and insectivores. Philosophical Transactions of the Royal Society of London B 348, 381–392.
Barton, R.A., 2006. Olfactory evolution and behavioral ecology in primates. American Journal of Primatology 68, 545–558.
Beard, K.C., 1988. The phylogenetic significance of strepsirhinism in Paleogene primates. International Journal of Primatology 9, 83–96.
Bicca-Marques, J.C., Garber, P.A., 2004. Use of spatial, visual, and olfactory information during foraging in wild nocturnal and diurnal anthropoids: A field experiment comparing *Aotus, Callicebus*, and *Saguinus*. American Journal of Primatology 62, 171–187.
Bird, D.J., Amirkhanian, A., Pang, B., Van Valkenburgh, B., 2014. Quantifying the cribriform plate: influences of allometry, function, and phylogeny in Carnivora. The Anatomical Record 297, 2080–2092.
Bolen, R.H., Green, S.M., 1997. Use of olfactory cues in foraging by owl monkeys (*Aotus nancymai*) and capuchin monkeys (*Cebus apella*). Journal of Comparative Psychology 111, 152–158.
Buck, L., Axel, R., 1991. A novel multigene family may encode odorant receptors: a molecular basis for odor recognition. Cell 65, 175–187.
Carroll, S.B., 2008. Evo-devo and an expanding evolutionary synthesis: A genetic theory of morphological evolution. Cell 134, 25–36.
Cartmill, M., 1970. The orbits of arboreal mammals: A reassessment of the arboreal theory of primate evolution. Ph.D. Dissertation, University of Chicago.
Cartmill, M., 1972. Arboreal adaptations and the origin of the order Primates. In: Tuttle, R. (Ed.), The Functional and Evolutionary Biology of Primates. Aldine, Chicago, pp. 97–122.
Cartmill, M., 1974. Daubentonia, Dactylopsila, woodpeckers and klinorhynchy. In: Martin, R.D., Doyle, G.A., Walker, A.C. (Eds.), Prosimian Biology. Duckworth, London, pp. 655–670.
Cave, A.J.E., 1967. Observations on the platyrrhine nasal fossa. American Journal of Physical Anthropology 26, 277–288.
Cave, A.J.E., 1973. The primate nasal fossa. Biological Journal of the Linnean Society 5, 377–387.
Charles-Dominique, P., 1977. Ecology and Behaviour of Nocturnal Primates. Duckworth, London.
Craven, B. a., Neuberger, T., Paterson, E.G., Webb, A.G., Josephson, E.M., Morrison, E.E., Settles, G.S., 2007. Reconstruction and morphometric analysis of the nasal airway of the dog (*Canis familiaris*) and implications regarding olfactory airflow. Anatomical Record 290, 1325–1340.
Craven, B.A., Paterson, E.G., Settles, G.S., 2010. The fluid dynamics of canine olfaction: unique nasal airflow patterns as an explanation of macrosomia. Journal of the Royal Society 7, 933–943.
de Beer, G.R., 1937. The Development of the Vertebrate Skull. Chicago University Press, Chicago.
Delbarco-Trillo, J., Burkert, B.A., Goodwin, T.E., Drea, C.M., 2011. Night and day: the comparative study of strepsirrhine primates reveals socioecological and phylogenetic patterns in olfactory signals. Journal of Evolutionary Biology 24, 82–98.
DeLeon, V.B., Smith, T.D., De Leon, V.B., Smith, T.D., 2014. Mapping the nasal airways: using histology to enhance CT-based three-dimensional reconstruction in *Nycticebus*. The Anatomical Record 297, 2113–2120.
Dieulafé, L., 1906. Morphology and embryology of the nasal fossae of vertebrates. Annals of Otology, Rhinology & Laryngology 15, 1–584.
Eiting, T.P., Smith, T.D., Dumont, E.R., 2014a. Olfactory epithelium in the olfactory recess: A case study in New World leaf-nosed bats. Anatomical Record 297, 2105–2112.
Eiting, T.P., Smith, T.D., Perot, J.B., Dumont, E.R., 2014b. The role of the olfactory recess in olfactory airflow. The Journal of Experimental Biology 217, 1799–1803.
Elliot Smith, G., 1927. The Evolution of Man. Oxford University Press, London.
Erickson, C.J., Nowicki, S., Dollar, L., Goehring, N., 1998. Percussive foraging: Stimuli for prey location by aye-ayes (*Daubentonia madagascariensis*). International Journal of Primatology 19, 111–122.
Garrett, E.C., 2015. Was there a sensory trade-off in primate evolution? The vomeronasal groove as a means of understanding the vomeronasal system in the fossil record. Ph.D. Dissertation, City University of New York.
Garrett, E.C., Dennis, J.C., Bhatnagar, K.P., Durham, E.L., Burrows, A.M., Bonar, C.J., Steckler, N.K., Morrison, E.E., Smith, T.D., 2013. The vomeronasal complex of nocturnal strepsirhines and implications for the ancestral condition in primates. Anatomical Record 296, 1881–1894.
Green, P.A., Van Valkenburgh, B., Pang, B., Bird, D.J., Rowe, T.B., Curtis, A., 2012. Respiratory and olfactory turbinal size in canid and arctoid carnivorans. Journal of Anatomy 221, 609–621.
Heesy, C.P., 2009. Seeing in stereo: the ecology and evolution of primate binocular vision and stereopsis. Evolutionary Anthropology 18, 21–35.
Heritage, S., 2014. Modeling olfactory bulb evolution through primate phylogeny. PLoS One 9, e113904.
Hill, W.C.O., 1953. Primates, Comparative Anatomy and Taxonomy. I. Strepsirrhini. Edinburgh University Press, Edinburgh.
Hiramatsu, C., Melin, A.D., Aureli, F., Schaffner, C.M., Vorobyev, M., Kawamura, S., 2009. Interplay of olfaction and vision in fruit foraging of spider monkeys. Animal Behaviour 77, 1421–1426.
Hofer, H.O., Wilson, J.A., 1967. An endocranial cast of an early Oligocene primate. Folia Primatologica 5, 148–152.
Irwin, M.T., Raharison, F.J.L., Rakotoarimanana, H., Razanadrakoto, E., Ranaivoson, E., Rakotofanala, J., Randrianarimanana, C., 2007. Diademed sifakas (*Propithecus diadema*) use olfaction to forage for the inflorescences of subterranean parasitic plants (Balanophoraceae: *Langsdorffia* sp., and Cytinaceae: *Cytinus* sp.). American Journal of Primatology 69, 471–476.
Kappel, P., Hohenbrink, S., Radespiel, U., 2011. Experimental evidence for olfactory predator recognition in wild mouse lemurs. American Journal of Primatology 73, 928–938.
Kay, R.F., Campbell, V.M., Rossie, J.B., Colbert, M.W., Rowe, T.B., 2004a. Olfactory fossa of *Tremacebus harringtoni* (Platyrrhini, early Miocene, Sacanana, Argentina): Implications for activity pattern. The Anatomical Record. Part A, Discoveries in Molecular, Cellular, and Evolutionary Biology 281, 1157–1172.
Kay, R.F., Williams, B.A., Ross, C.F., Takai, M., Shigehara, N., 2004b. Anthropoid origins: A phylogenetic analysis. In: Ross, C.F., Kay, R.F. (Eds.), Anthropoid Origins. Springer US, Boston, pp. 91–135.
Keverne, E.B., 1999. The vomeronasal organ. Science 286, 716–720.
Kirk, E.C., Kay, R.F., 2004. The evolution of high visual acuity in the Anthropoidea. In: Ross, C.F., Kay, R.F. (Eds.), Anthropoid Origins. Springer US, Boston, pp. 539–602.
Kirk, E.C., 2006. Effects of activity pattern on eye size and orbital aperture size in primates. Journal of Human Evolution 51, 159–170.
Kirk, E.C., Daghighi, P., Macrini, T.E., Bhullar, B.A.S., Rowe, T.B., 2014. Cranial anatomy of the Duchesnean primate *Rooneyia viejaensis*: New insights from high resolution computed tomography. Journal of Human Evolution 74, 82–95.
Kirk, E.C., 2018a. Sensory ecology: olfaction. In: Trevathan, W. (Ed.), The International Encyclopedia of Biological Anthropology. John Wiley & Sons, Hoboken. https://doi.org/10.1002/9781118584538.ieba0562.
Kirk, E.C., 2018b. Sensory ecology: vision. In: Trevathan, W. (Ed.), The International Encyclopedia of Biological Anthropology. John Wiley & Sons, Hoboken. https://doi.org/10.1002/9781118584538.ieba0440.
Kollmann, M., Papin, L., 1925. Etudes sur lémuriens. Anatomie compareé des fosses nasales et de leurs annexes. Archives de Morphologie Génerale et Experimentale 22, 1–60.
Lancet, D., Greer, C.A., Kauer, J.S., Shepherd, G.M., 1982. Mapping of odor-related neuronal activity in the olfactory bulb by high-resolution 2-deoxyglucose autoradiography. Proceedings of the National Academy of Sciences USA 79, 670–674.
Le Gros Clark, W.E., 1926. On the anatomy of the pen-tailed tree-shrew (*Ptilocercus lowii*). Proceedings of the Zoological Society of London 96, 1179–1309.
Le Gros Clark, W.E., 1959. The Antecedents of Man. Edinburgh University Press, Edinburgh.
Lewis, R.J., 2005. Sex differences in scent-marking in sifaka: Mating conflict or male services? American Journal of Physical Anthropology 128, 389–398.
Loo, S.K., Kanagasuntheram, K., 1971. The nasal fossa of *Tupaia glis* and *Nycticebus coucang*. Folia Primatologica 16, 74–84.
Loo, S.K., 1973. A comparative study of the nasal fossa of four nonhuman primates. Folia Primatologica 20, 410–422.
Macrini, T.E., 2014. Development of the ethmoid in *Caluromys philander* (Didelphidae, Marsupialia) with a discussion on the homology of the turbinal elements in marsupials. The Anatomical Record 297, 2007–2017.
MacPhee, R.D.E., Cartmill, M., 1986. Basicranial structures and primate systematics. In: Swindler, D.R., Erwin, J. (Eds.), Comparative Primate Biology, Vol. 1. Systematics, Evolution, and Anatomy, pp. 219–275. Alan R. Liss, New York.
Maddison, W.P., Maddison, D.R., 2017. Mesquite: A Modular System for Evolutionary Analysis. Version 3.2. http://www.mesquiteproject.org.
Maier, W., 1980. Nasal structures in Old and New World Primates. In: Ciochon, R.L., Chiarelli, A.B. (Eds.), Evolutionary Biology of the New World Monkeys and Continental Drift. Academic Press, London, pp. 219–241.

Maier, W., 1993. Zur evolutiven und funktionellen Morphologie des Gesichtsschädels der Primaten. Zeitschrift fur Morphologie und Anthropologie 79, 279–299.
Maier, W., Ruf, I., 2014. Morphology of the nasal capsule of primates-with special reference to *Daubentonia* and *Homo*. The Anatomical Record 297, 1985–2006.
Maier, W., 2000. Ontogeny of the nasal capsule in cercopithecoids: a contribution to the comparative and evolutionary morphology of catarrhines. In: Whitehead, P.F., Jolly, C.J. (Eds.), Old World Monkeys. Cambridge University Press, Cambridge, pp. 99–132.
Mason, V.C., Li, G., Minx, P., Schmitz, J., Churakov, G., Doronina, L., Melin, A.D., Dominy, N.J., Lim, N.T.-L., Springer, M.S., Wilson, R.K., Warren, W.C., Helgen, K.M., Murphy, W.J., 2016. Genomic analysis reveals hidden biodiversity within colugos, the sister group to primates. Science Advances 2, e1600633.
Martin, R.D., 1990. Primate Origins and Evolution. A Phylogenetic Reconstruction. Princeton University Press, Princeton.
Martin, C., 2017. ggConvexHull: Add a Convex Hull Geom to ggplot2. R package v. 010. http://github.com/cmartin/ggConvexHull.
Moore, W.J., 1981. The Mammalian Skull. Cambridge University Press, London.
Morelli, T.L., Hayes, R.A., Nahrung, H.F., Goodwin, T.E., Harelimana, I.H., MacDonald, L.J., Wright, P.C., 2013. Relatedness communicated in lemur scent. Naturwissenschaften 100, 769–777.
Muchlinski, M.N., 2010. A comparative analysis of vibrissa count and infraorbital foramen area in primates and other mammals. Journal of Human Evolution 58, 447–473.
Negus, V.E., 1956. The air-conditioning mechanism of the nose. British Medical Journal 1, 367–371.
Negus, V.E., 1958. The Comparative Anatomy and Physiology of the Nose and Paranasal Sinuses. Edinburgh University Press, Edinburgh.
Nei, M., Niimura, Y., Nozawa, M., 2008. The evolution of animal chemosensory receptor gene repertoires: roles of chance and necessity. Nature Reviews Genetics 9, 951–963.
Nekaris, K.A.-I., 2005. Foraging behaviour of the slender loris (*Loris lydekkerianus lydekkerianus*): Implications for theories of primate origins. Journal of Human Evolution 49, 289–300.
Ni, X., Gebo, D.L., Dagosto, M., Meng, J., Tafforeau, P., Flynn, J.J., Beard, K.C., 2013. The oldest known primate skeleton and early haplorhine evolution. Nature 498, 60–64.
Ni, X., Li, Q., Li, L., Beard, K.C., 2016. Oligocene primates from China reveal divergence between African and Asian primate evolution. Science 352, 673–677.
Niimura, Y., 2012. Olfactory receptor multigene family in vertebrates: from the viewpoint of evolutionary genomics. Current Genomics 13, 103–114.
Niimura, Y., Matsui, A., Touhara, K., 2018. Acceleration of olfactory receptor gene loss in primate evolution: Possible link to anatomical change in sensory systems and dietary transition. Molecular Biology and Evolution 35, 1437–1450.
International Committee on Veterinary Gross Anatomical Nomenclature (ICVGAN), 2017. Nomina Anatomica Veterinaria. World Association of Veterinary Anatomists, Columbia, Missouri, USA.
Paulli, S., 1900a. Über die Pneumaticität des Schädels bei den Säugetieren. I. Über die Morphologie des Siebbeins und die Pneumaticität bei den Monotrematen und den Marsupialliern. Gegenbaurs Morphologisches Jahrbuch 28, 147–178.
Paulli, S., 1900b. Über die Pneumaticität des Schädels bei den Säugethieren. II. Über die Morphologie des Siebbeins der Pneumaticität bei den Ungulaten und Proboscіden. Gegenbaurs Morphologisches Jahrbuch 28, 179–251.
Paulli, S., 1900c. Über die Pneumaticität des Schadels bei den Säugerthieren. III. Über die Morphologie des Siebbeins und die Pneumaticität bei den Insectivoren, Hyracoideen, Chiropteren, Carnivoren, Pinnipedien, Edentaten, Rodentiern, Prosimien und Primaten. Gegenbaurs Morphologisches Jahrbuch 28, 483–564.
Pedziwiatr, Z.F., 1972. Das Siebbeinlabyrinth. II. Diferenzierung and Systematik der Hauptmuschel bein einigen Gattungen der Säugetiere. Anatomischer Anzeiger 131, 378–390.
Perelman, P., Johnson, W.E., Roos, C., Seuánez, H.N., Horvath, J.E., Moreira, M.A.M., Kessing, B., Pontius, J., Roelke, M., Rumpler, Y., Schneider, M.P.C., Silva, A., O'Brien, S.J., Pecon-Slattery, J., 2011. A molecular phylogeny of living primates. PLoS Genetics 7, e1001342.
Persuy, M.-A., Sanz, G., Tromelin, A., Thomas-Danguin, T., Gibrat, J.-F., Pajot-Augy, E., 2015. Mammalian olfactory receptors: Molecular mechanisms of odorant detection, 3D-modeling, and structure-activity relationships. Progress in Molecular Biology and Translational Science 130, 1–36.
Pihlström, H., 2012. The size of major mammalian sensory organs as measured from cranial characters, and their relation to the biology and evolution of mammals. Ph.D. Dissertation, University of Helsinki.
Purves, D., Augustin, G.J., Fitzpatrick, D., Katz, L.C., La Mantia, A.S., McNamara, J.O., Williams, S.M. (Eds.), 2001. Neuroscience. Sinauer Associates, Sunderland, pp. 317–344.
Robinson, P., Gunnell, G.F., Walsh, S.L., Clyde, W.C., Storer, J.E., Stucky, R.K., Froehlich, D.J., Ferrusquia-Villafranca, I., McKenna, M.C., 2004. Wasatchian through Duchesnean biochronology. In: Woodburne, M.O. (Ed.), Late Cretaceous and Cenozoic Mammals of North America. Columbia University Press, New York, pp. 106–157.
Rosenberger, A.L., 2006. Protoanthropoidea (Primates, Simiiformes): a new primate higher taxon and a solution to the *Rooneyia* problem. Journal of Mammalian Evolution 13, 139–146.
Rosenberger, A.L., Hogg, R., Wong, S.M., 2008. *Rooneyia*, postorbital closure, and the beginnings of the age of Anthropoidea. In: Sargis, E.J., Dagosto, M. (Eds.), Mammalian Evolutionary Morphology. Springer, Dordecht, pp. 325–346.
Ross, C.F., 1994. The craniofacial evidence for anthropoid and tarsier relationships. In: Fleagle, J.G., Kay, R.F. (Eds.), Anthropoid Origins. Plenum Press, New York, pp. 469–547.
Ross, C.F., Kirk, E.C., 2007. Evolution of eye size and shape in primates. Journal of Human Evolution 52, 294–313.
Ross, C.F., Williams, B.A., Kay, R.F., 1998. Phylogenetic analysis of anthropoid relationships. Journal of Human Evolution 35, 221–306.
Rossie, J.B., Beard, K.C., 2004. Intracranial anatomy of Shoshonius cooperi (Tarsiiformes, primates) as revealed by high-resolution computed tomography. Journal of Vertebrate Paleontology 24, 106A.
Rossie, J.B., 2005. Anatomy of the nasal cavity and paranasal sinuses in *Aegyptopithecus* and early miocene African catarrhines. American Journal of Physical Anthropology 126, 250–267.
Rossie, J.B., 2006. Ontogeny and homology of the paranasal sinuses in Platyrrhini (Mammalia: Primates). Journal of Morphology 267, 1–40.
Rossie, J.B., Ni, X., Beard, K.C., 2006. Cranial remains of an Eocene tarsier. Proceedings of the National Academy USA 103, 4381–4385.
Rossie, J.B., Smith, T.D., 2007. Ontogeny of the nasolacrimal duct in primates: Functional and phylogenetic implications. Journal of Anatomy 210, 195–208.
Rossie, J.B., Smith, T.D., Beard, K.C., Godinot, M., Rowe, T.B., 2018. Nasolacrimal anatomy and haplorhine origins. Journal of Human Evolution 114, 176–183.
Rowe, T.B., Eiting, T.P., Macrini, T.E., Ketcham, R.A., 2005. Organization of the olfactory and respiratory skeleton in the nose of the gray short-tailed opossum *Monodelphis domestica*. Journal of Mammalian Evolution 12, 303–336.
RStudio Team, 2015. RStudio: integrated development for R. Rstudio, Inc., Boston.
Ruf, I., 2014. Comparative anatomy and systematic implications of the turbinal skeleton in Lagomorpha (Mammalia). The Anatomical Record 297, 2031–2046.
Ruf, I., Janßen, S., Zeller, U., 2015. The ethmoidal region of the skull of *Ptilocercus lowii* (Ptilocercidae, Scandentia, Mammalia). Primate Biology 2, 89–110.
Sacha, C.R., Dubay, G.R., Drea, C.M., 2012. *Eulemur*, me lemur: the evolution of scent-signal complexity in a primate clade. Philosophical Transactions of the Royal Society of London B 367, 1909–1922.
Schoppa, N.E., Westbrook, G.L., 2001. Glomerulus-specific synchronization of mitral cells in the olfactory bulb. Neuron 31, 639–651.
Scordato, E.S., Drea, C.M., 2007. Scents and sensibility: information content of olfactory signals in the ringtailed lemur, *Lemur catta*. Animal Behaviour 73, 301–314.
Seiffert, E.R., Kappelman, J., Ryan, T.M., 1999. The nasal fossa of *Rooneyia viejaensis* as revealed by high-resolution X-ray computed tomography. American Journal of Physical Anthropology 108 S28, 247–248.
Seiffert, E.R., Simons, E.L., Boyer, D.M., Perry, J.M., Ryan, T.M., Sallam, H.M., 2010. A fossil primate of uncertain affinities from the earliest late Eocene of Egypt. Proceedings of the National Academy of Sciences USA 107, 9712–9717.
Shepherd, G.M., 1972. Synaptic organization of the mammalian olfactory bulb. Physiological Reviews 52, 864–917.
Silcox, M.T., Dalmyn, C.K., Bloch, J.I., 2009. Virtual endocast of *Ignacius graybullianus* (Paromomyidae, Primates) and brain evolution in early primates. Proceedings of the National Academy of Sciences USA 106, 10987–10992.
Silcox, M.T., Benham, A.E., Bloch, J.I., 2010. Endocasts of *Microsyops* (Microsyopidae, Primates) and the evolution of the brain in primitive primates. Journal of Human Evolution 58, 505–521.
Singleton, M., 2013. Primate cranial diversity. Nature Education Knowledge 2, 1.
Smith, T.D., Bhatnagar, K.P., 2004. Microsmatic primates: reconsidering how and when size matters. The Anatomical Record. Part B, New Anatomist 279, 24–31.
Smith, T.D., Rossie, J.B., 2006. Primate olfaction: anatomy and evolution. In: Brewer, W.J., Castle, D., Pantelis, C. (Eds.), Olfaction and the Brain. Cambridge University Press, Cambridge, pp. 135–166.
Smith, T.D., Rossie, J.B., 2008. Nasal fossa of mouse and dwarf lemurs (Primates, Cheirogaleidae). The Anatomical Record 291, 895–915.
Smith, T.D., Bhatnagar, K.P., Burrows, A.M., Shimp, K.L., Dennis, J.C., Smith, M.A., Maico-Tan, L., Morrison, E.E., 2005. The vomeronasal organ of greater bushbabies (*Otolemur* spp.): Species, sex, and age differences. Journal of Neurocytology 34, 135–147.
Smith, T.D., Alport, L.J., Burrows, A.M., Bhatnagar, K.P., Dennis, J.C., Tuladhar, P., Morrison, E.E., 2007a. Perinatal size and maturation of the olfactory and vomeronasal neuroepithelia in lorisoids and lemuroids. American Journal of Primatology 69, 74–85.
Smith, T.D., Bhatnagar, K.P., Rossie, J.B., Docherty, B.A., Burrows, A.M., Cooper, G.M., Mooney, M.P., Siegel, M.I., 2007b. Scaling of the first ethmoturbinal in nocturnal strepsirrhines: Olfactory and respiratory surfaces. The Anatomical Record 290, 215–237.
Smith, T.D., Rossie, J.B., Bhatnagar, K.P., 2007c. Evolution of the nose and nasal skeleton in primates. Evolutionary Anthropology 16, 132–146.
Smith, T.D., Eiting, T.P., Rossie, J.B., 2011. Distribution of olfactory and nonolfactory surface area in the nasal fossa of *Microcebus murinus*: Implications for micro-computed tomography and airflow studies. The Anatomical Record 294, 1217–1225.
Smith, T.D., Alport, L.J., Burrows, A.M., 2013. Size of olfactory structures in strepsirrhines: Ontogenetic and ecological factors. In: Masters, J., Gamba, M., Génin, F. (Eds.), Leaping Ahead: Advances in Prosimian Biology. Springer Science, New York, pp. 247–255.

Smith, T.D., Eiting, T.P., Bonar, C.J., Craven, B.A., 2014a. Nasal morphometry in marmosets: loss and redistribution of olfactory surface area. The Anatomical Record 297, 2093–2104.
Smith, T.D., Laitman, J.T., Bhatnagar, K.P., 2014b. The shrinking anthropoid nose, the human vomeronasal organ, and the language of anatomical reduction. The Anatomical Record 297, 2196–2204.
Smith, T.D., Eiting, T.P., Bhatnagar, K.P., 2015. Anatomy of the nasal passages in mammals. In: Doty, R.L. (Ed.), Handbook of Olfaction and Gustation. John Wiley & Sons, Hoboken, pp. 39–61.
Smith, T.D., Martell, M.C., Rossie, J.B., Bonar, C.J., De Leon, V.B., 2016. Ontogeny and microanatomy of the nasal turbinals in Lemuriformes. The Anatomical Record 299, 1492–1510.
Spatz, W.B.V., 1968. Die bedeutung der augen für die sagittale Gestaltung des schädels von Tarsius (Prosimiae, Tarsiiformes). Folia Primatologica 9, 22–40.
Stephan, H., Frahm, H.D., Baron, G., 1981. New and revised data on volumes of brain structures in insectivores and primates. Folia Primatologica 35, 1–29.
Szalay, F.S., Delson, E., 1979. Evolutionary History of the Primates. Academic Press, San Diego.
Szalay, F.S., Wilson, J.A., 1976. Basicranial morphology of the early tertiary tarsiiform *Rooneyia* from Texas. Folia Primatologica 25, 288–293.
Tabuce, R., Marivaux, L., Lebrun, R., Adaci, M., Bensalah, M., Fabre, P.-H., Fara, E., Gomes Rodrigues, H., Hautier, L., Jaeger, J.-J., Lazzari, V., Mebrouk, F., Peigné, S., Sudre, J., Tafforeau, P., Valentin, X., Mahboubi, M., 2009. Anthropoid versus strepsirhine status of the African Eocene primates *Algeripithecus* and *Azibius*: craniodental evidence. Proceedings of the Royal Society of London B 276, 4087–4094.
Tegoni, M., Pelosi, P., Vincent, F., Spinelli, S., Campanacci, V., Grolli, S., Ramoni, R., Cambillau, C., 2000. Mammalian odorant binding proteins. Biochimica et Biophysica Acta 1482, 229–240.
Valenta, K., Burke, R.J., Styler, S.A., Jackson, D.A., Melin, A.D., Lehman, S.M., 2013. Colour and odour drive fruit selection and seed dispersal by mouse lemurs. Scientific Reports 3, 2424.
Van Valkenburgh, B., Theodor, J., Friscia, A., Pollack, A., Rowe, T.B., 2004. Respiratory turbinates of canids and felids: A quantitative comparison. Journal of Zoology 264, 281–293.
Van Valkenburgh, B., Pang, B., Bird, D.J., Curtis, A., Yee, K., Wysocki, C., Craven, B.A., 2014a. Respiratory and olfactory turbinals in feliform and caniform carnivorans: The influence of snout length. The Anatomical Record 297, 2065–2079.
Van Valkenburgh, B., Smith, T.D., Craven, B.A., 2014b. Tour of a labyrinth: exploring the vertebrate nose. The Anatomical Record 297, 1975–1984.
Veilleux, C.C., Kirk, E.C., 2014. Visual acuity in mammals: effects of eye size and ecology. Brain, Behavior & Evolution 83, 43–53.
Von Haller, A., 1756. Icones Anatomicae. A. Vandenhoeck, Gottingen.
Wible, J.R., 2011. On the treeshrew skull (Mammalia, Placentalia, Scandentia). Annals of Carnegie Museum 79, 149–230.
Williams, B.A., Kay, R.F., Kirk, E.C., 2010. New perspectives on anthropoid origins. Proceedings of the National Academy of Sciences USA 107, 4797–4804.
Wilson, J.A., 1966. A new primate from the earliest Oligocene, West Texas, preliminary report. Folia Primatologica 4, 227–248.
Wilson, J.A., 1986. Stratigraphic occurence and correlation of Early Tertiary vertebrate faunas, trans-pecos Texas: Agua Fria-Green Valley areas. Journal of Vertebrate Paleontology 6, 350–373.
Yee, K.K., Craven, B.A., Wysocki, C.J., Van Valkenburgh, B., 2016. Comparative morphology and histology of the nasal fossa in four mammals: Gray squirrel, bobcat, coyote, and white-tailed deer. The Anatomical Record 299, 840–852.